Molecular Models of Hydration in Methanol-Water Mixtures

Sanhita Dixit

Thesis submitted for the degree of Doctor of Philosophy

Department of Physics and Astronomy

University of Edinburgh

2002

Abstract

The self-assembly of amphiphilic macromolecules into exotic structures like micelles and bilayers in aqueous media is a fascinating phenomenon. Intermolecular interactions responsible for the formation of such structures include hydrophobic, electrostatic and hydrogen bond interactions. At molecular length scales, the relative importance of each is still being actively investigated.

The work presented in this thesis addresses the issue of hydration of a simple amphiphile-like molecule; methanol. High-resolution Raman spectroscopy is used to study methanol-water mixtures over the whole concentration range. A highly non-linear dependence of the carbon-oxygen and carbon-hydrogen stretching frequencies with composition is observed. The data suggest the first global picture of the progressive hydration of methanol: water first breaks up the molecular chains which exist in pure methanol, and then completely hydrates the hydroxyl groups before solvating the hydrophobic methyl groups.

In order to corroborate this proposed picture, neutron diffraction experiments using hydrogen/deuterium substitution were performed on a concentrated methanol in water mixture (70 mole% methanol : 30 mole% water) and a dilute methanol in water mixture (5 mole% methanol : 95 mole% water). The diffraction data were modelled using the Empirical Potential Structural Refinement technique.

In the concentrated mixture, although there is insufficient water for the classical hydrophobic mechanism to operate, the structural effects observed are consistent with those that might be expected in a hydrophobically driven system. An

unexpected reduction is found in the methyl-methyl contact distance compared to pure methanol, which corresponds to an overall compressive effect apparently driven by hydrogen bonding of the added water to the alcohol hydroxyl groups. Surprisingly, the water structure is largely preserved in this mixture.

In the dilute mixture a significant association of the methanol molecules via their methyl groups is observed. This is driven by the hydrophobic interaction. However, water hydrates the methyl groups and this solvent layer restricts the methyl groups from forming direct contact configurations. The water structure is found to be perturbed by the presence of the methanol molecules. The perturbation is qualitatively similar to that observed due to the application of external hydrostatic pressure to water or the dissolution of ionic solutes in water.

The results obtained provide unambiguous evidence for the preferential interaction of the methanol hydroxyl group with water and suggest that hydrogen bonding interactions between water and polar groups of amphiphilic molecules may be more important than previously thought.

Acknowledgements

First and foremost, I would like to thank my supervisors, Dr. Jason Crain and Prof. Wilson Poon for their constant support and enthusiasm towards this project. I would also like to thank the Committee of Vice-Chancellors and Principals (CVCP) for the ORS award and Edinburgh University for the Chalmers Scholarship.

This project would not have reached fruition without the help, advice and support of Prof. John Finney and Prof. Alan Soper. I would also like to thank Dr. Daniel Bowron for his help in clarifying a lot of concepts on neutron diffraction from pulsed sources. Prof. Alan Soper spent a lot of time with me to explain to me the ideas behind the development of the EPSR data modelling algorithm. I would like to thank him for allowing me to use this algorithm to analyse the data collected from the neutron scattering experiments performed at the pulsed neutron source, ISIS, at the Rutherford Appleton Laboratory. Thank you to all staff at ISIS for helping me at various levels, right from technical to computing help. Technical assistance from Hugh Vass while performing the spectroscopic measurements is greatly appreciated.

I would like to thank all my colleagues here, in the Physics department for their support and help, especially in computing. I would also like to thank Dr. Stefan Egelhaaf for useful discussions.

Lastly, none of this would have been possible without the love and encouragement from my family and close friends. A big thank you to all of them.

Contents

Chapter 1

Introduction

1.1 Hydration in Aqueous Solutions

The physical properties of aqueous solutions are determined to a large extent by the chemical nature of solutes [1, 2]. Hydrophilic or *water loving* solutes can form hydrogen bonds with water and dissolve in water easily. On the other hand hydrophobic or *water fearing* solutes cannot form hydrogen bonds with water and are only slightly soluble in water. The most interesting types of solutes, referred to as amphiphilic solutes have a mixture of hydrophilic and hydrophobic chemical groups. Amphiphilic molecules spontaneously self assemble in aqueous solutions to form super structures [3]. This self-assembly is driven by the two extreme responses that hydrophilic and hydrophobic groups have to the presence of water.

Nonpolar molecules and headgroups attract each other and tend to form aggregates in aqueous solutions. The driving force behind this attraction is called the hydrophobic interaction. Traditional views attributed the molecular origins of these interactions, which occur in dilute aqueous solutions, to the expulsion of structured water surrounding nonpolar groups of molecules [4]. This interpretation was based on the widely held view that the poor solubility of nonpolar

molecules in water was due to the structural order imposed by these solutes on the surrounding water rendering the process entropically unfavourable [5]. The magnitude of the hydrophobic interaction is a function of temperature and pressure since these thermodynamic parameters affect the structure of water [6, 7]. Ions in aqueous solution also affect the structure of water [8] and the Hofmeister series is often used to indicate whether a specific type of ion will promote hydrophobic associations. In the case of large amphiphilic molecules, hydrophobic interactions result in the formation of complex structures such as micelles and bilayers [3]. The importance of hydrophobic interactions in the biological context is manifested in their influence over the folding and stability of proteins and in the formation of cell membranes.

Investigations over the past three decades have questioned certain aspects of these traditional interpretations. Several systems which include aqueous solutions of argon, methane and simple amphiphilic solutes like alcohols have been under intense study [6]. There has been little experimental evidence confirming the traditional hypothesis directly.

Water-alcohol mixtures have long been used to develop a molecular level understanding of the phenomenon of hydrophobic interactions. Alcohols have a polar (-OH) group and a hydrophobic alkyl group. Thus they are amphiphilic in nature and are relatively simple molecules to study. The solubility of alcohols in water is governed by the length and branching of the alkyl headgroup [3]. Linear higher alcohols (n-butanol and beyond) show significant immiscibility regions as a function of the alcohol concentration. It has been widely accepted that since simple alcohols (methanol, ethanol) are completely miscible in water, they must be homogeneously mixed. Recent investigations have revealed that there is reason to believe that ethanol and water do not mix homogeneously [9] while no evidence was found in methanol-water mixtures regarding microhetrogeneity at the molecular level [10]. The spirit of such investigations has been largely fuelled by the belief that hydrophobic interactions dominate the structure of aqueous alcohol solutions.

With the advent of pulsed lasers and sophisticated diffraction techniques it is now possible to determine the structure of aqueous solutions in detail. It is hoped that such structural studies will resolve longstanding issues regarding the nature of the hydrophobic interaction by investigating simple systems.

Methanol is the simplest alcohol. The small size of its alkyl group means it will not show conventional self-assembly behaviour. However, its amphiphilic nature implies that it can act as the starting point for a fundamental understanding of the hydration of amphiphiles. In the present thesis, the methanol-water system has been investigated in detail. High-resolution Raman spectroscopy is used to determine how hydration of methanol molecules changes with increasing concentration of water. Two key concentrations which involve extreme ends of the composition scale are determined from this analysis. Neutron diffraction is then used to interpret the structure of these aqueous mixtures in atomic detail. The results are then placed in context with current literature to determine the relative importance of specific intermolecular interactions in this system.

1.2 Thesis Layout

- The methanol-water system is introduced along with several other systems which have been under investigation over the past several years to understand at a microscopic level the origin of hydrophobic interactions in aqueous media. This introduction is in the form of a summary of work done primarily over the past decade and comprises all of chapter 2.

- The thesis then addresses the specific case of the methanol-water system and describes a detailed investigation of the hydration of methanol using high-resolution Raman spectroscopy in chapter 3.

- The theory behind neutron diffraction and introduction to current data modelling techniques is provided in chapter 4.

- The main results in this thesis are presented in chapters 5 and 6. These are

from neutron diffraction studies of two methanol-water mixtures which are at extreme compositions.

- The conclusions and directions for future work are summarised in chapter 7.

Chapter 2

Molecular Interactions in Aqueous Media

2.1 Water - A Unique Solvent

One can confidently say that water holds the unique status of being the most widely studied liquid. The structure of water is characterised by a tetrahedral network which is held together via hydrogen bonds between the water molecules. A hydrogen bond forms between two water molecules because the electron associated with the hydrogen atom is involved in a covalent O-H bond which descreens the hydrogen atom. This gives rise to a dipole with positive charge at the hydrogen end of the O-H covalent bond. This dipole interacts via the coulomb interaction with the electro-negative oxygen atom from a neighbouring water molecule. The net result is a hydrogen bond. Its origin lies in the strong bond moment of the O-H bond in the water molecule [11]. Water has exceptionally high melting and boiling points compared to other liquids. Thus intermolecular interactions between water molecules are quite strong. The strength of most hydrogen bonds lie between 10 - 40 $kJmol^{-1}$. All atoms and molecules also interact via forces of attraction called van der Waals forces which are not a result of any chemical bonds or simple ionic interactions but are weak interactions experienced

due to dipole-dipole forces. When the strength of a hydrogen bond is compared to the strength of a typical van der Waals bond which is around 1 $kJmol^{-1}$ it is at once clear that the interaction between water molecules is stronger than the interaction between the molecules of a hydrocarbon liquid like n-hexane which interact via the van der Waals interaction [11]. This highly structured and cohesive nature of water makes it a rather unusual and interesting solvent. To cite an everyday example, consider what happens when vinegar is mixed with olive oil to make a salad dressing. The two appear to mix initially, but after some time has elapsed the oil forms a layer on top of the vinegar/water mixture. What really is happening here is that vinegar (which is made from acetic acid) is soluble in water and forms a clear liquid where as oil does not dissolve in water. Molecules of vinegar have chemical sites which are capable of forming hydrogen bonds with water and hence the water molecules do not mind if these molecules intrude into the water network. On the other hand oil molecules have no such hydrogen bonding capacity and the water molecules prefer to demix into a separate phase since breaking hydrogen bonds between water molecules to accommodate the oil molecules is energetically expensive. However it is important to realize that such a phase separation is entirely due to the self attraction of water for itself since the magnitude of the interactions between water molecules is significantly greater than those between oil molecules or between oil and water molecules [3]. Actually, such demixing processes are macroscopic manifestations of a phenomenon which has microscopic origins.

Consider a simple hydrocarbon like methane. At room temperature and pressure methane is a gas and is only sparingly soluble in water. Can one immediately conclude that the water dislikes methane? Not really. When methane is dissolved in water, even though the water welcomes only a minute quantity of methane, the water is observed to warm up. This would indicate that there are energetically favourable interactions occurring between the methane molecules and water for heat to be released. Then why does the water not incorporate more methane in aqueous solution? The reason is that energetics is only part of the

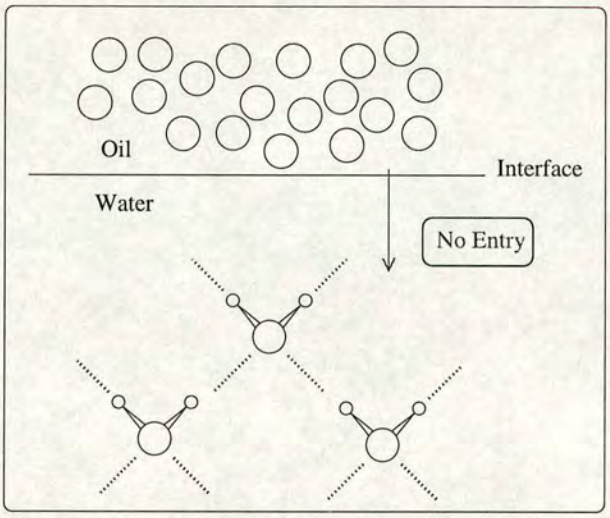

Figure 2.1: Oil and water do not mix, a schematic.

story. Favourable energetic interactions which in technical terms are defined as enthalpic contributions are not the only quantity which determines whether the mixing is a spontaneous process. Another quantity, the entropy plays an equally important role. The entropic term determines whether a process results in more order or disorder compared to the reference state (here, methane and water existing as separate systems). The dissolution of methane in water is strongly opposed by the entropic term. Apparently, dissolving methane in water increases ordering in the system which nature does not like. Thus the difference between the enthalpic (ΔH) and entropic terms (TΔS) defines the free energy of mixing (ΔG) whose sign determines whether a process occurs spontaneously. A positive ΔG implies the process cannot occur spontaneously, which in the present case translates to, *it is very difficult to dissolve methane in water.* Other nonpolar gases like argon also show similar thermodynamic signatures when they are forced into an aqueous solution. These thermodynamic properties, characteristic of dissolution of nonpolar molecules (molecular groups) in water are often referred to as *remarkable hydration properties* for these are unique to water as a solvent.

In 1945, Frank and Evans in a seminal paper provided a molecular interpretation of these thermodynamic properties [5]. They stated that " when a rare gas atom

or a nonpolar molecule dissolves in water at room temperature it modifies the water structure in the direction of greater crystallinity - the water so to speak, builds a microscopic iceberg around it" [5]. This restructuring of water was argued to be necessary in order to accommodate the solute since such structures would contain more free space. The more ordered structure of water in the hydration shell of the nonpolar solute gave rise to the large entropy loss. Other simple mixed solutes which have polar and nonpolar groups like alcohols (methanol, ethanol etc) and ketones (acetone) also exhibit similar thermodynamic properties when mixed in water. While the polar group aids the dissolution process, the entropy of mixing is still negative. Frank and Evans suggested that such solutes also affect the hydration water molecules like their corresponding hydrocarbons would. A recent experimental investigation by Bowron *et al* [12] confirmed the presence of such a hydration shell around krypton in aqueous solution. This hydration shell was significantly disordered and loosely defined compared to the clathrate hydrate they observed in the solid. This experiment indicates that Frank and Evans could not have been right. In fact an earlier experiment by Soper and Finney [13] which aimed at determining whether the water molecules were more ordered than bulk water in the methyl group environment had reached similar conclusions.

In 1959 Kauzmann introduced the concept of hydrophobic interactions which was defined as the attraction between nonpolar molecules (or groups) in an aqueous environment which drove them to aggregate in order to release water from their immediate neighbourhood which would otherwise be more structured and would be entropically highly unfavourable [4]. Kauzmann argued that the hydrophobic interaction was the prime intermolecular interaction responsible for the folding of proteins in unique three dimensional structures. The folding process involves the collapse of the protein into a compact globule in which amino acids having significant nonpolar groups are clustered in the core of the globule sheltered from the aqueous medium in which they exist. Hydrophobic interactions were also shown to drive the assembly of amphiphilic macromolecules into micelles and

vesicles. Amphiphilic molecules consist of a long hydrocarbon tail and a polar head group which is capable of forming hydrogen bonds with water. In aqueous media these hydrocarbon tails cluster to avoid contact with water [3]. In both self assembly processes the polar domains of the macromolecules form the interface with the aqueous solvent phase.

A significant effort by numerous researchers to understand the origins of these unusual solvent properties of water has resulted in several thousands of publication over the past several decades. A recent review by Blokzijl and Engberts [6] crystallises the varied viewpoints which emerged by the early 1990's from these investigations.

What follows is a summary of the advances made over the past decade in unravelling the microscopic origins of the peculiar properties exhibited by water as a solvent. A primer on the terminology used in the scientific literature precedes the review of recent results.

2.2 Basic Concepts: Hydrophobic Effects

There have been varied definitions in literature of the hydrophobic effect [6] and this has led to some confusion. Hence it is important to define some concepts for clarity.

Hydrophobic hydration refers to the way in which a nonpolar solute (molecular group) affects the structure of water in its immediate vicinity. This process results in thermodynamic properties of the solution which are unique to water as a solvent. These properties are a negative solution enthalpy and entropy and a positive solution free energy*. Hence the negative solution entropy governs the dissolution process of a nonpolar solute in water. This negative solution entropy

*All thermodynamic measurements are made relative to a reference state which could be a hypothetical solution at unit mole fraction or the ideal vapour state of the solute. Defining the reference state is important when thermodynamic quantities are reported.

results in a positive heat capacity of these infinitely dilute aqueous solutions. Within the framework of the "iceberg" model this could be explained by the requirement that heat needs to be supplied to melt these iceberg structures around the nonpolar solutes. Dilute aqueous solutions of alcohols and other mixed solutes (containing polar and nonpolar groups) also showed similar thermodynamic solution properties.

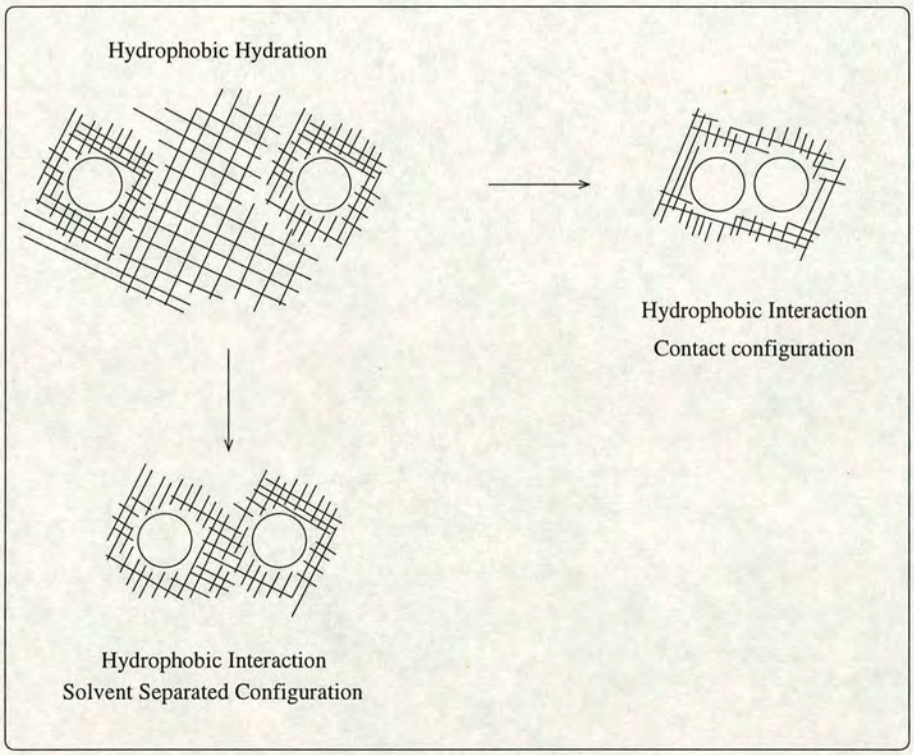

Figure 2.2: A schematic representation of hydrophobic hydration and the hydrophobic interaction (*see text for details*). The nonpolar solutes are represented as circles.

The hydration of nonpolar species in water thus, has a free energy cost which results in a net attraction between these molecular species in water. This attraction is responsible for their tendency to aggregate in aqueous solution to minimise their surface area of contact with water. This attraction is referred to as the hydrophobic interaction (see fig. 2.2).

To be more precise, the process of hydration of a single nonpolar solute which

involves the transfer of the solute from its gaseous phase to an infinitely dilute aqueous solution results in positive free energy and heat capacity changes over the entire temperature range accessible to calorimetric experiments. The enthalpy and entropy changes are negative at low temperatures and positive as temperatures are increased. The thermodynamic quantities associated with this transfer process are defined as the hydration thermodynamic properties as opposed to solution thermodynamic properties where the transfer process is from the pure liquid to the aqueous solution.

The best way to determine whether a solute affects the structure of water in its neighbourhood is to determine the distribution of water molecules around the nonpolar solute [6]. The technical term used to denote the distribution of atoms (or molecular centres) in a liquid is the "radial distribution function" or the "pair distribution function". The general shape of a radial distribution function g(r), for a liquid is shown in fig. 2.3. For low r values g(r) is zero. This corresponds to a volume around a reference atom which is empty and is a result of strong repulsions between atoms. This is the familiar hard-core repulsion which restricts the approaching atoms from coming too close to each other and prevents atomic overlap. The first peak position denotes the distance at which the first shell of nearest neighbours exists. As the distance from the reference atom increases the oscillations in g(r) diminish rapidly and the function approaches unity (*since the radial distribution function is normalised to the average atomic density of the liquid*).

Consider a solute in aqueous solution with its molecular centre defines as "A". Then $g_{AOw}(r)$ is the pair distribution function which is determined from the average number of water oxygen atoms in a thin spherical shell of width Δr and at radius r from the solute molecular centre A [†]. Similarly one can also determine $g_{AHw}(r)$ as well as $g_{OwOw}(r)$, $g_{OwHw}(r)$ and $g_{HwHw}(r)$ for pure water. One approach adopted to investigate the degree to which the water structure is affected due to the presence of the nonpolar solute is to determine the distribution function of

[†]The subscript w is used to define the water oxygen and hydrogen atoms.

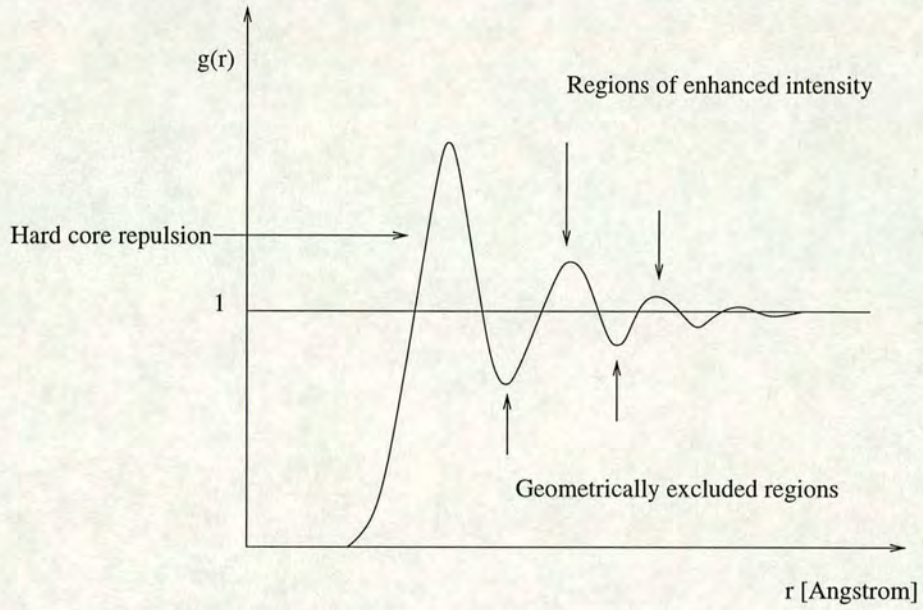

Figure 2.3: Typical radial distribution function for a liquid (*see text for details*).

the water molecules in the first hydration shell of the solute and comparing this with the same distribution function from pure water. Another way of addressing the issue is to determine the distribution functions for water in the aqueous solution and compare it with pure water. The latter approach is particularly useful when the aqueous solutions have solute concentrations which result in almost all the water molecules participating in the hydration of the solute.

To investigate the origin of the hydrophobic interaction, one needs to investigate the forces between nonpolar solutes in water as a function of their relative distance. The chance of finding a second solute particle at a distance r from the centre of the first solute particle is a direct measure of the magnitude of the interactions between the solute particles. The potential of mean force ΔW is defined as the work done to bring two nonpolar solutes from infinite separation to a separation r in solution which is of the order of the diameter of the solute [6]. It takes into account the direct pair interaction potential between two solutes in the absence of the solvent as well as the effects of the solvent. The potential of mean force is related to the solute-solute pair distribution function by the following equation [14]:

$$g_{AA}(r) = e^{-\frac{\Delta W}{kT}} \tag{2.1}$$

Clearly, the potential of mean force can be defined for any value of r. Specifically, it will have a minimum corresponding to the peak in first coordination shell of the solute-solute pair distribution function and it will have a maximum at r values lying between the first and second coordination shells.

Theoretical approaches aim to provide a description of the experimentally determined pair distribution functions or of predicted potentials of mean force / pair distribution functions from computer simulations.

The stage is now set to present a synopsis of important advances made over the past decade in increasing our understanding of hydrophobic effects, i.e. hydrophobic hydration and the hydrophobic interaction.

2.3 Progress Over the Past Decade

2.3.1 Hydrophobic Hydration: Recent Theoretical Models

Numerous models have been developed to account for the positive free energy of hydration of nonpolar solutes in water. A theoretical model developed by Lee [15] offered a completely different explanation than the then prevalent iceberg model. Lee took a cue from the Scaled Particle theory (reviewed by Blokzijl and Engberts [6] and references therein) which postulates that the dissolution of a solute in water is decomposed into two steps; the first is that of cavity creation to accommodate the solute and the second is that of the onset of solute-water interactions. Physically cavity formation represents a fluctuation in the equilibrium structure of water. The scaled particle theory uses statistical arguments to determine the work done in creating a cavity of appropriate size in the water net-

work to accommodate the solute. Both solute and solvent are treated as spherical particles. The crux of this theory is that creation of such a cavity requires the exclusion of solvent particles from the volume occupied by the solute and this process involves a certain amount of work. This work done (which is the same as the excess chemical potential) is related to the probability p_0 of finding a cavity of a given radius in water via a Boltzmann equation: Work done = $\Delta\mu^{ex} = -kTlnp_0$. It has been postulated for quite some time that the essence of hydrophobicity lies in the difference in the work of cavity creation in water and other organic solvents [16]. Lee's model indicated that the reason behind the low solubility of nonpolar solutes in water is due to the small size of the water molecule. Lee argued that the small size of the water molecule defines the length scale of the system and if all else were equal then it would be harder to insert a solute in a solvent made of smaller molecules than in a solvent made of larger molecules. Using his theory, Lee was able to explain the hydration thermodynamics of noble gases [15].

Compensation models were also developed in light of some interesting experimental data. It was noted that the Gibbs energy of solvation (ΔG) on the transfer of argon from a hydrocarbon solvent like cyclohexane to water, hydrazine and ethylene glycol was remarkably similar in magnitude and sign, indicating that the dissolution of argon in cyclohexane was more favourable than in these hydrogen bonded solvents (see table 2.1). The low solubility of argon in hydrazine and ethylene glycol was due to an unfavourable enthalpy change. What was surprising however was that the transfer of argon from either hydrazine or ethylene glycol to water produced compensating enthalpy and entropy changes resulting in a net zero change in the Gibbs energy. These observations led to the suggestion that the thermodynamics of solvation of nonpolar molecules in water was governed by (a) the extensive hydrogen bond network of water, a feature which it shared with other hydrogen bonded solvents and (b) due to the fluctuating nature of the hydrogen bond network of water which distinguishes itself from other hydrogen bonded solvents. The latter factor was thought to be responsible for the compensating enthalpy and entropy contributions.

Solvent I	Solvent II	ΔG [kJ mol^{-1}]	ΔH [kJmol^{-1}]	$-T\Delta S$ [kJ mol^{-1}]
Cyclohexane	Water	10.4	-11.2	21.6
Cyclohexane	Hydrazine	11.9	9.5	2.4
Cyclohexane	Ethylene Glycol	10.3	0	10.3
Ethylene Glycol	Water	0	-11.3	11.4
Hydrazine	Water	-1.5	-20.7	19.2

Table 2.1: Thermodynamic parameters for the transfer of one mole of argon from solvent I to solvent II at 298 K. Data taken from ref. [6] and references therein.

Lee [17] analysed these ideas of compensation of enthalpic and entropic terms by investigating which processes in the solvation of nonpolar solutes in water are compensating and which are not. Lee's theory of nonpolar solute hydration states that there exist two opposing factors which determine the hydration Gibbs energy. One is the excluded volume entropy change associated with the creation of a cavity in the water network to accommodate the solute which is unfavourable while the other is the direct van der Waals interaction between the solute and water which favours the hydration process [‡]. The excluded volume effect overwhelms the hydration process and is the primary reason behind the low solubility of nonpolar solutes in water. The structural reorganisation of the hydrogen bonds of water around the solute which accompanies the dissolution is a compensating process which does not affect the Gibbs energy change [18]. It however contributes to the enthalpy and entropy change associated with the hydration process and is responsible for the large heat capacity change [19]. This is where the importance of the hydrogen bonds between water comes in. As mentioned before, these theoretical results are in significant disagreement with the classic 'iceberg model'

[‡]Note that Lee used these ideas from the Scaled Particle Theory earlier to understand hydration of noble gases as well

of Frank and Evans [5].

Using Lee's theory Graziano was able to explain the physical origins behind the increase in solubility of noble gases with increasing size and the decrease in solubility of hydrocarbons with increasing size as observed in transfer experiments [20]. For noble gases it was shown that the van der Waals attractive interaction increases with solute size due to the increasing number of weakly bound electrons which interact favourably with the water dipole moment. This interaction energy increases more steeply with size than the competing cavity creation energy. The trend is opposite for the hydrocarbons where the cavity creation term rises faster than the interaction term as a function of increasing solute radius. Clearly Graziano's work casts doubt on the claimed reinforcement of water structure in the hydration shell of a nonpolar solute as the physical origin of the low solubility of such solutes in water.

The success of a molecular theory of hydration of nonpolar groups in water would lie in the ability of the theory to explain the hydration thermodynamics of solutes like alcohols which due to the presence of the polar hydroxyl group have stronger energetic interactions with water. While the hydroxyl group of the alcohols is responsible for their solubility, the hydration entropy change is large and negative where as the hydration heat capacity change is large and positive just like their corresponding aliphatic hydrocarbons. It was argued [1] that all available evidence suggested that the nonpolar group of the alcohol played an important role in the hydration of alcohol molecules and the thermodynamic hydration data were interpreted using the traditional 'iceberg model'. Graziano has gone a step further to use Lee's theory to explain the hydration thermodynamics of these simple amphiphilic molecules. He showed [21] that the contribution from water-alcohol hydrogen bonds is fundamental in describing alcohol solubility in water over a the temperature range (5-100)°C. The physical origin of the negative entropy of hydration was indeed the excluded volume effect with the hydrogen bond reorganisation in the alcohol hydration shell being an entirely compensating process which however did give rise to the large and positive change in the

hydration heat capacity.

Computer simulation studies of hydrophobic effects have also helped provide deeper insight into the phenomenon. Key results obtained in the past decade will be reviewed next.

2.3.2 Computer Simulations of Aqueous Solutions

Following the review by Blokzijl and Engeberts [6] in 1993, there has been considerable progress in understanding hydrophobic hydration and the hydrophobic interaction using computer simulations. It is essential to present a synopsis of what was learnt via simulations by the early 1990's in order to appreciate how much progress has been made since then. This synopsis is presented below.

Simulations performed in aqueous solutions are either the monte carlo (MC) type or the molecular dynamics (MD) type. Either method is useful for determining static properties such as radial distribution functions. However only the MD method can be used to determine dynamic properties such as diffusion coefficients. These simulations are carried out on small system sizes, about 500 molecules or so and the system size is often dictated by the nature of the problem at hand, available computer memory and the speed of the computer. A configuration of the molecules of the system under study is set up using intermolecular potentials. In MC simulations several configurations of the system are obtained by randomly moving the atoms in the system. An acceptance term (Boltzmann weighting) is defined to either accept or reject a configuration once it is generated. Structural quantities are then obtained as averages over several hundred configurations which are generated in the course of the simulation. In MD simulations particle trajectories are monitored using equations of motion. After several thousand time steps the time average of a particular property is obtained by integrating over the entire trajectory [22].

Dilute aqueous solutions were studied to investigate hydrophobic hydration and

the hydrophobic interaction using prototypical solutes such as methane or the noble gases. Normal butane was used to study conformational changes induced by the presence of water in a hydrocarbon chain. Results obtained from all these simulations were all in qualitative agreement in spite of the different time scales, intermolecular potentials and type of simulations that were run. Several conclusions were reached. These are summarised here. Water molecules avoided pointing their OH bonds directly towards the nonpolar solute. Further, depending on the size of the solute, the number of water molecules in the first hydration shell ranged from around 20 for methane to about 34 for n-pentane. Introduction of a polar group was found to strongly facilitate the hydration of nonpolar groups of an amphiphilic molecule. Structural changes between the hydration shells of the polar and apolar moieties indicated that these hydration shells are mutually obstructive in regions of spatial overlap. Structural analysis of the hydration shells around nonpolar solutes has revealed the existence of clathrate like[§] structures. However these structures have been noted to be extremely labile clearly discounting the presence of any frozen water patches.

To determine the contribution of hydration shell water molecules to the hydration entropy, Paulaitis *et al* have used a statistical mechanical formulation for the entropy of hydration of simple hydrophobic solutes [23]. Their investigations revealed that the small size of the water molecule resulted in a high packing efficiency of water molecules in the hydration shell of simple nonpolar solutes. This packing gave rise to strong solute-water translational correlations which contributed significantly to the entropy of hydration. The hydrogen bonding nature of the water molecules resulted in their tangential orientation around the solute and this gave rise to strong orientational correlations between the water molecules and the solute. Further simulations were reported for hydrophobic chains using multiparticle correlation functions to determine the hydration entropy and the proximity approximation where the structure of the hydration shell was assumed

[§]In such structures the water molecules orient their dipole moments tangential to the surface of the nonpolar solute. This orientation reduces the loss of hydrogen bonds incurred by the water molecules due to the incorporation of the nonpolar solute in the water network.

to be a sum of contributions from individual sites on the molecule [24]. Calculated and simulated solute-water radial distribution functions were found to be in good agreement. It remains to be seen whether these methods can be applied to simple amphiphilic solutes where there would a preferential hydrogen bonding interaction between the solute and water [25, 26].

In a different approach to model the observed hydration free energies of nonpolar solutes, Hummer *et al* [27, 28] have developed a model based on original developments in Scaled Particle theory and Information theory. Current predictions by this theory have been quite accurate.

Although progress is being made in the modelling of solute-water interactions, there has been no work done on simple amphiphilic solutes. However, experimental structural determination of aqueous solutions of simple amphiphilic molecules is now possible and considerable progress is expected in this area. Experimental solute-water radial distribution functions could help the modelling community enormously. Advances in the experimental area of structure determinations will be discussed later.

Several simulations also addressed the issue of hydrophobic interactions. In all these studies either the solute-water potential of mean force or the solute-water radial distribution function was evaluated. The first minimum in the potential of mean force corresponds to a solute-solute contact configuration where as the second minimum indicates a solvent separated contact. Similarly, the radial distribution function had a first peak corresponding to a direct solute-solute interaction and a second peak which represented a solvent mediated solute-solute interaction. There have been conflicting results on the height of the barrier between the contact pair and solvent separated configurations. No spontaneous association of nonpolar solutes was noted in simulations on picosecond time scales. It seemed that the simulations would need to run for longer times. The simulations hence failed to obtain a clear signature of the hydrophobic interaction. It was apparent that in order to investigate hydrophobic interactions higher solute

concentrations would be necessary. This would prevent the water molecules from forming hydration shells.

Over the past eight years or so almost all simulations reported similar conclusions. Presented below are some of the most important studies as viewed by the author. Methane has remained the most favoured solute. Skipper investigated the tendency of methane molecule to aggregate in a mixture of 4 methane and 256 water molecules. Solute-solute, solute-solvent and solvent-solvent radial distribution functions were evaluated. The methane molecules showed an increasing tendency to aggregate as the temperature was increased [29]. These results were supplemented by another report by Skipper *et al* a few few years later where the authors investigated concentrated mixtures of methane in water across a temperature range of 270°K - 380°K. At low temperatures the authors found that the methane molecules actually repelled each other weakly implying that the water molecules preferred to remain in the hydration shells of the methane molecules. Solute-solute hydrophobic interactions became attractive only around room temperature of 300°K and reached a maximum around 340°K. The water molecules preferred to be in the bulk as the temperature was increased. There was some evidence pointing to enhanced solvent hydrogen bonding at low temperatures [30]. Almost simultaneously Ludemann *et al* reported a similar temperature effect on methane hydrophobic association, i.e. increasing temperature favours association and that the most pronounced temperature effect was seen in the temperature region of 300°K - 305°K [31].

Recently, Mancera *et al* [32] have reported another set of results from long (1 nanosecond) MD simulations run on the methane-water system to supplement earlier information [30]. Here the authors confirm yet again that that the contact configuration peak in the methane-methane radial distribution function increases with increasing temperatures. Mancera investigated hydrogen bond changes in the hydration shell of methane and ethane compared to bulk water and found that there was a large fraction of broken bonds in the hydration shell as compared to bulk water. The hydrogen bonds were also found to be stronger in the hydra-

tion shell [33]. Very recently Silverstein *et al* computed the change in enthalpy resulting from the breaking of a hydrogen bond in pure water and that in the water molecules forming the hydration shell around Argon. This was found to be 1.9 kcal mol^{-1} for the case of bulk water and 2.4 kcal mol^{-1} for hydration shell waters [34]. These results add weight to the conclusions reached by Mancera. Results reported in a recent simulation of methane in water by Hernández-Cobos *et al* [35] indicate that the water structure in methane - water mixtures is not very different from that of water at all temperatures [298 K - 600 K] in their study. Further the energetically favourable solvation enthalpy was found to be determined by the methane - water interactions with a small positive reorganisation energy of water which was not favourable. The negative change in entropy was attributed purely to excluded volume effects. This last result was echoed in several other reports. Specifically, Mountain and Thirumalai indicated that the only penalty to solute dissolution was the excluded volume of the solute which results in a negative entropy. The authors found no evidence in favour of changes in water structure even in the case of the largest solute (octane). Hydrophobic hydration resulted purely from the strong tendency of the water molecules to preserve their hydrogen bonds [36]. In an independent study, Durell and Wallqvist found that the favourable enthalpy change accompanying the transfer of Krypton from the gas phase to water at room temperature was due to the strong van der Waals interaction between the solute and solvent [37].

The study of conformational changes in higher alkanes in the presence of water has continued to receive attention with possible implications to the study of protein folding. Paulaitis and Ashbaug confirmed earlier predictions of the gauche conformer of the normal butane being more stable than the trans conformation [24]. However Mountain and Thirumalai found little evidence for water mediated interactions between the non - bonded carbon atoms even for octane and they concluded that transition to globular conformations can only occur for very long hydrocarbon chains [36].

There is one aspect about hydrophobic hydration which has still not been dis-

cussed and that is of the heat capacity changes associated with this effect. Sharp and Madan in a key study address the issue of heat capacity changes associated with the hydration of apolar and polar solutes in water [38]. Their study was motivated by the fact that there is a large positive change in the hydration heat capacity of apolar solutes while it is negative in the case of polar solutes. The authors found that there were significant changes in the mean hydrogen bond length and the root mean square hydrogen bond angle of the first hydration shell water molecules. Hydration water molecules around apolar groups showed decreased bond length and bond angles while those around polar solutes showed the opposite. The authors concluded that at infinite dilutions the apolar solutes affected water like a decrease in temperature would. Calculated changes in hydration heat capacities reproduced the experimental trends qualitatively though the quantitative values were underestimated systematically by as much as 50%. The authors suggest that perturbation to water structure beyond the first hydration shell may be important. It was also pointed out in another study [39] that the large magnitude of the heat capacity of hydration for nonpolar solutes comes about from the flattening of the water orientational distribution with respect to the solute.

Hydrophobic hydration and the hydrophobic interaction are intimately connected. The presence of a solvent separated minimum noted in the simulations of hydrophobic interactions implied that the water preferred to hydrate nonpolar solutes (small solutes like methane). So how and when does the hydrophobic interaction dominate over hydrophobic hydration? Over the past five years there have been reports which have addressed the issue of hydrophobic interactions in reasonable depth. The most striking study has been by Rascke *et al* who performed nanosecond molecular dynamics simulations on increasing numbers of hydrophobic solutes in water [40]. Three types of solutes were considered, alkanes (methane and butane), isobutylene and benzene. The canonical ensemble method used in the MD simulation was NVE, i.e. constant number of molecules, volume and energy. This differs from experimental conditions which are NPT,

i.e. constant number of molecules, pressure and temperature. The former was adopted because the simulation software developed by one of the authors of that report has been highly optimised to run at constant energy. Several conclusions were reached in this study. Over the time scale of the simulation transitions from small to large cluster sizes were noted with the larger clusters being more stable and persisting over longer periods of time. The formation of clusters was also found to depend on solute concentration. Hence the likelihood of aggregation increased with increased number of solutes in the simulation box or with a reduced box size (see fig. 2.4 for a snapshot view of the simulation) The most striking result from these simulations was the observation that the free energy of adding a solute to a cluster of a given size becomes more favourable as the cluster size increases showing clear cooperativity in cluster formation.

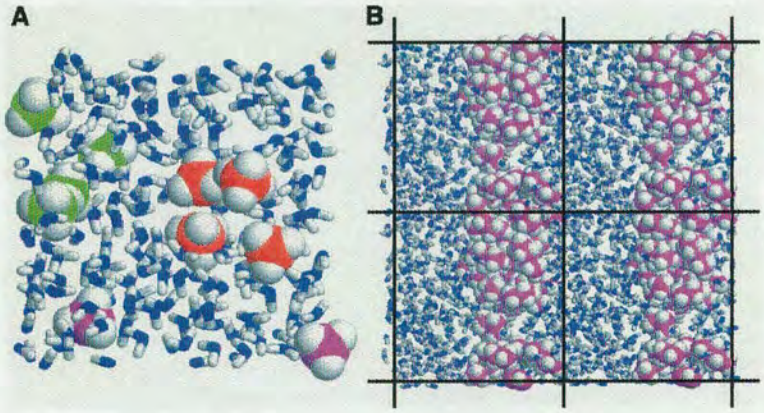

Figure 2.4: Snapshots from the simulations of Raschke *et al* [40]. (A) Ten methane and 204 water molecules in a 6700 $\AA^3$ box. Methane molecules are space-filled, and water molecules are represented as sticks. (B) A projection of four adjacent 13,500 $\AA^3$ periodic boxes each containing 20 butane and 338 water molecules.

Thus it was concluded that studies involving methane dimers were too limited to reveal this important aspect of the hydrophobic interaction. The formation of small clusters (number of methane molecules less than five) was found to be thermodynamically unfavourable corroborating previous potential of mean force calculations on methane which showed the solvent separated configuration being more favourable than the contact pair. Interestingly Rank and Baker [41] found

a solvent separated barrier to the contact interaction for a methane dimer and trimer in their MC simulations. Dimer formation of a larger solute (radius = 2.6 $\AA$) compared to methane (radius = 1.85 $\AA$) was also investigated. The free energy minimum was found to be more shallow for the larger solute compared to that of methane. These results are consistent with the fact that the solubility of noble gases in water increases with solute size [20]. Rank and Baker also reported results from Monte Carlo simulations which aimed at investigating contributions of the hydrogen bonding property of water and the van der Waals interaction to the attraction between methane molecules in water [42]. They found that the magnitude of the attraction between methanes was not significantly changed when the hydrogen bonding interaction between the water molecules was switched off and the resulting fluid was maintained in the liquid state by either increasing the pressure or the magnitude of the solvent van der Waals interaction. However, when all solvent-solvent interactions were turned off, the authors found that the attraction between the two methane molecules was no greater than in the gas phase. These results on the potential of mean force between two methane molecules in water add further weight to similar results reported in earlier literature [43, 44] which concluded that the small molecular size and the density of water were responsible for the positive free energies of hydration of nonpolar solutes.

While prior to the 1990's some simulations seem to have been performed on amphiphilic molecules detailed simulations of such solutes in water are only now beginning to be reported. Since dilute aqueous solutions of such solutes (acetone, alcohols, amines etc) have thermodynamic properties similar to those of hydrocarbons in water, detailed calorimetric investigations of such systems have been the subject of several studies [45, 46]. While thermodynamic properties do yield useful information on bulk properties of these systems little can be deduced about the microscopic structure of these systems. Almost all recent reports on amphiphilic molecules in water aim at investigating hydrophobic hydration. Alcohols have been a favourite, with changes in water structure being reported [47] in dilute aqueous solutions of methanol. It was found that water far from the solute

retained its bulk structure where as water in the immediate vicinity of the solute seemed to show a lower local density. No evidence of clathrate like (tangential orientation of water molecules around the solute) structure of the hydration water was reported in a study of infinitely dilute aqueous alcohol solutions [48]. Kusalik *et al* reported the structure of dilute methylamine-water solutions and showed that methyl-methyl association exists in the mixture and that these associations are not strongly directionally specific [49]. The presence of the polar group in these molecules implies solubility in water across a significant concentration region at least for simple amphiphiles. This fact immediately opens up a whole new concentration regime, where there is a significant amount of the amphiphilic molecule but comparatively little water. Clearly in such a situation the classical hydrophobic effect cannot operate. How does water respond to the presence of the apolar groups in such concentrated mixtures? With hydrocarbons this is an impossible scenario to explore. It is remarkable that this avenue has been so under explored. Such concentration regions may be important to understand how aggregation occurs on a microscopic scale.

Amphiphiles are realistic solutes to study because all self assembly processes such as micelle formation or membrane formation in macromolecular assemblies and intra molecular processes such as protein folding involve a large number of molecules with different functional groups. While protein folding is a much more complex process compared to say micelle formation due to the chemical diversity of the amino acids which form the protein polymer and the constraints introduced due to the chain connectivity, the fact that hydrophobic interactions are important in both types of self assembly is not disputed [50]. Just how important it is relative to other intra molecular interactions such as hydrogen bonding, dipole interactions etc. for the folding problem is a question whose answer has been largely elusive over the past forty years. In an attempt to address this issue Durell *et al* [51] performed molecular dynamics simulations to determine the potential of mean force between two hydrophilic solutes in dilute aqueous solution. Another set of simulations was also performed with partial charges on

the hydrophilic solutes switched off to examine 'hydrophobic analogs'. It was found that the maximum solvent induced contribution to the potential of mean force between the solutes was calculated to be four times more negative for the hydrophilic solutes than for the hydrophobic ones. From their work, the authors conclude that solvent induced forces between polar amino acid residues could be more important in the folding of proteins than the hydrophobic interaction. Similar conjectures were also raised in another study by Shimizu and Chan [52] in which the authors address the issue of anti-cooperativity in the association of a methane molecule with an existing methane dimer in aqueous solution. By comparing the potential of mean force between the methane molecule and the methane dimer with that obtained by assuming pair additivity as a function of angle of approach of the methane molecule with respect to the axis of the dimer, the authors conclude that their simulations predict anti-cooperative interactions between a methane dimer and a single methane molecule at most positions where they are in relatively close proximity. If such anti-cooperative effects do exist in the hydrophobic core formation in the folding of proteins, the authors postulate that interactions besides the hydrophobic effect may play an important role in maintaining the stability of these macromolecules. The results of Shimizu and Chan consider cooperative effects which have a different definition from those studied by Rascke *et al* [40], the later refer to cooperativity as the more favourable total interactions among a larger cluster of hydrophobic solutes than among a smaller cluster of such solutes.

With all this progress on the modelling and simulation front, experimentalists have also made some useful discoveries. Emerging techniques such as neutron diffraction coupled with sophisticated data modelling techniques are beginning to provide answers to the subtleties of the chemical nature of the solute and the resulting intermolecular interactions in aqueous media which dictate the structure of these mixtures. A systematic structural investigation of aqueous solutions is now possible in unprecedented detail. These techniques are expected to bridge the gap between real structural information and simulated data and provide re-

searchers with valuable information to validate predictions from theory.

Advances in this area are summarised next.

2.3.3 Probing Aqueous Solution Structure

Aqueous solutions of simple amphiphilic solutes lend themselves easily to neutron diffraction experiments. Neutrons are well suited for diffraction studies of aqueous mixtures because neutrons are scattered differently by hydrogen and deuterium isotopes of hydrogen. Put in another way, hydrogen and deuterium have different neutron *scattering lengths* [53] thereby making the diffraction patterns from H_2O and D_2O distinct. The scattered intensity from the samples when Fourier transformed after appropriate corrections yields a pair distribution function which is a measure of the structure of a liquid. Aqueous solutions of simple amphiphilic solutes are however quite complex and typically, both the solute and solvent contain hydrogen atoms. The use of multiple isotope substitution [54] helps to pick out specific hydrogen-hydrogen pair distribution functions. These methods are called second order substitution methods and have been in use over the past decade to probe the structure of such mixtures [55]. Even so, there is still information not within direct experimental access such as the pair distribution functions of atoms which do not have isotopes which can be used for neutron diffraction. Sophisticated data modelling procedures similar to the reverse Monte Carlo method have been developed by Soper [56] in the mid 1990's to tackle the problem. Without going into further details here, it is sufficient to state here that these procedures yield details on the orientation of the constituent molecules in the mixture, yielding molecular centres' correlation functions and hence map the structure of the mixtures in great detail. A considerable literature has been continuously building up of studies of aqueous solutions of molecules of chemical and biological importance. Specifically, studies on the tetraalkylammonium ion - water, methanol - water and tertiary butanol - water system have revealed relevant structural information which has helped verification of theories (see the reference

to the work of Paulaitis *et al* [25] where the experimental data on tetramethyl ammonium ion -water mixtures is used) as well as provide new insights into the standard model hypothesis of Franks and Evans [5].

Results from these diffraction experiments are summarised below. Soper and Finney reported in a first detailed experiment on a 0.1 mole fraction methanol in water mixture the structure of the hydration shell around the methyl group of the alcohol [13]. Their results were able to show that the orientation of the water molecules around the methyl group was tangential much like that predicted by the standard model. However, this orientational arrangement was significantly disordered; the cage-like water shell was *not* long-lived. Further, this structural rearrangement of the water molecules did not result in an over all change in the water HwHw pair distribution function when compared to that of pure water. Hence there was no evidence to be found to support the presence of a more ordered water structure.

Turner *et al* [57, 58] investigated the effect of tetraalkylammonium ions on the structure of water. They found that the water molecules adopt distinct tangential arrangements around the ion and that even if there are any significant electrostatic interactions between the ion charge and water, these do not influence the average water-ion distance which implied that the water structure is influenced significantly by the apolar alkyl groups of the ion. Again, the water structure was not found to be more ordered than that of pure water.

In a series of experiments on the tertiary butanol - water system Bowron *et al* [59, 60, 61] have found significant interactions between the non polar groups of the alcohol in a dilute mixture of tertiary butanol in water (0.06 mole fraction). These findings lend strong support to the notion that these molecules form small clusters in dilute aqueous mixture and the interaction of the alcohol molecules in the clusters is via the nonpolar groups. Such behaviour is a direct manifestation of the hydrophobic interaction. As the concentration of the alcohol was increased to 0.16 mole fraction it was found that there was no change in the hydrogen bond

environment of the alcohol hydroxyl group, i.e. the water molecule hydration number of the hydroxyl group did not change. What did change was the number of butyl groups on an average in the vicinity of a reference tertiary butanol molecule. In fact, the dominant nonpolar group interaction noted in the 0.06 mole fraction mixture gave way to some mixed polar group to nonpolar group contacts as the alcohol concentration was increased.

While alcohols and tetraalkylammonium ions have now been shown to display hydrophobic behaviour recent experiments on dimethyl sulfoxide - water mixtures have reported [62] that there was no evidence for any hydrophobic association of these molecules in water at a concentration of 2 water molecules to 1 dimethyl sulfoxide molecule. If anything there is some indication in this report that the water structure is more pronounced in this mixture than in pure water. However, the significance of these results on water structure enhancement need to be addressed with some caution since such deductions are made by comparing the heights of the first peak if the water-water radial distribution functions of pure water with that found in the mixture under consideration and excluded volume effects need to be accounted for in the case of mixtures [63].

While most of the structural work using neutrons has been done on simple amphiphilic solutes there have been attempts to determine direct information on water structure in methane - water mixtures. In a recent report Koh *et al* [64] determine the nature of the hydration shell around methane as the hydrate is formed. The methane - water mixture held at a pressure of 14.5 MPa was cooled in successive steps to determine the diffraction patterns as the hydrate was formed. The authors found the methane molecules adopting contact configurations (contact distance of around 4 $\AA$) as well as solvent separated configurations (solvent separated methanes occurring at a distance of around 7 $\AA$ on an average). As the hydrate formed on cooling, the contact configuration peak in the carbon-carbon pair distribution function diminished in intensity while the solvent separated peak becomes marked only when the hydrate is actually formed. These results agree with the simulation results of Ludemann *et al* [31] who showed that the contact

configuration peak corresponding to methane aggregation decreases as the temperature is decreased while the solvent separated configurations become prominent. Plots of the orientations of the water molecules in the hydration shells of methane which were obtained from modelling of the experimental data reveal that the orientation of the water molecules in the hydration shell in the solution is similar to that found around the hydrate (see fig. 2.5). This conclusion is in contrast to the structure of hydration shells around nonpolar groups of simple amphiphilic solutes in aqueous solutions [13, 57]. Koh *et al* point this difference to the "presence of a hydrogen-bonding hydroxyl radical or ionic charge on the molecule which would in every likelihood affect any conclusions about structural changes considerably". These results are in conflict with the results reported by Bowron *et al* [12]. Koh *et al* indicate that this may be due to the different radius of the krypton atom compared to methane.

It remains to be seen whether future investigations of other small amphiphile - water systems reveal anything new, especially about how the fine balance between the various chemical groups of a molecule determine the dominant intermolecular interactions of solutes in an aqueous medium.

2.4 Full circle: Macroscopic effects

So far the discussion has focused entirely on hydrophobic interactions involving small nonpolar or amphiphilic solutes. Some general conclusions can be reached. When water is required to accommodate small solutes (with radii less than ≈ 4 Å) with nonpolar groups which are incapable of hydrogen bonding with the solvent molecules, the water molecules reorganise themselves and simply go around the solute. They orient tangentially around the nonpolar groups of the solute in order to maximise their hydrogen bonds: losing hydrogen bonds is very expensive, more expensive than the entropic cost of reorganisation. This reorganisation leads to loss of orientational freedom of the water molecules around the solute. The current view is that for such solutes, water is a poor solvent not because

the energetic interactions between the solute and water are unfavourable, they are in fact pro-dissolution, what comes in the way is the entropic cost due to excluded volume effects. Water exerts a strong squeezing out force on such solutes compared to other organic solvents. Hence nonpolar solutes are sparingly soluble in water, it is amazing they are soluble at all.

However, all is not well when water molecules are faced with nonpolar solutes which are significantly bigger than a few angstroms or with a collection of nonpolar solutes which extend spatially for lengths greater than several angstroms. The water molecules cannot go around the solutes easily and hydrogen bonds are lost. This is energetically costly and the water molecules pull away form such extended nonpolar regions rather willingly.

In a recent article, Lum *et al* present a theory to account for the radically different responses of water to the presence of nonpolar solutes (or surfaces) depending on their spatial extent [65]. Their theory shows how for solutes with radii less than 4 $\mathring{A}$ the free energy of hydration is in agreement with the information theory model of Hummer *et al* [27] which was mentioned in an earlier section. However as the solute size approaches that of 10 $\mathring{A}$ and beyond, the predictions of this theory deviate strongly from the approach used in the information theory model. This difference is essentially due to the drying of extended hydrophobic surfaces in water. Hence Lum *et al* conclude that a ball of oily groups with a radius larger than 10 $\mathring{A}$ (approximately 20 methyl groups) is sufficient to induce drying. Similar results were also reported by Southall and Dill [66] in another report following that of Lum *et al.* In fact Southall and Dill also concluded from their simulations that the energetics of nonpolar solute hydration also depends on the solute shape and curvature. Surface topography has been shown to play a decisive role in the hydration of biomolecular surfaces [67].

2.5 New Frontiers

The present views on hydrophobic effects clearly indicate that while hydrophobic intermolecular interactions do affect the self assembly of macromolecules it is still a matter of debate to what extent. There have been indications of hydrophilic interactions between water and polar groups of amphiphilic molecules as also being important [6, 52] in maintaining the stability of self assembled structures. The relative importance of these two competing intermolecular interactions is still an open question at both length scales, microscopic and macroscopic. We still do not know how water interacts with simple amphiphilic solutes like alcohols as a function of concentration in the mixture. Exactly when does the hydrophobic interaction give way to hydrophobic hydration? How does the balance between polar and nonpolar groups govern interactions between water and such mixed solutes? As or more important is the physics which governs assembly at the nanometer length scale, in light of the recent theoretical advances made by Lum *et al* [65] to understand drying at macroscopic surfaces. Advances in our understanding of these complicated responses of water to the presence of different molecular assemblies are eagerly awaited.

The work reported in this thesis addresses a small part of the intricate nature of various intermolecular interactions in aqueous media. Methanol is chosen as a model amphiphile-like solute and its hydration as a function of increasing dilution in water is mapped out in detail. This work aims to investigate the relative importance of the methyl and hydroxyl groups in determining the structure of these aqueous solutions.

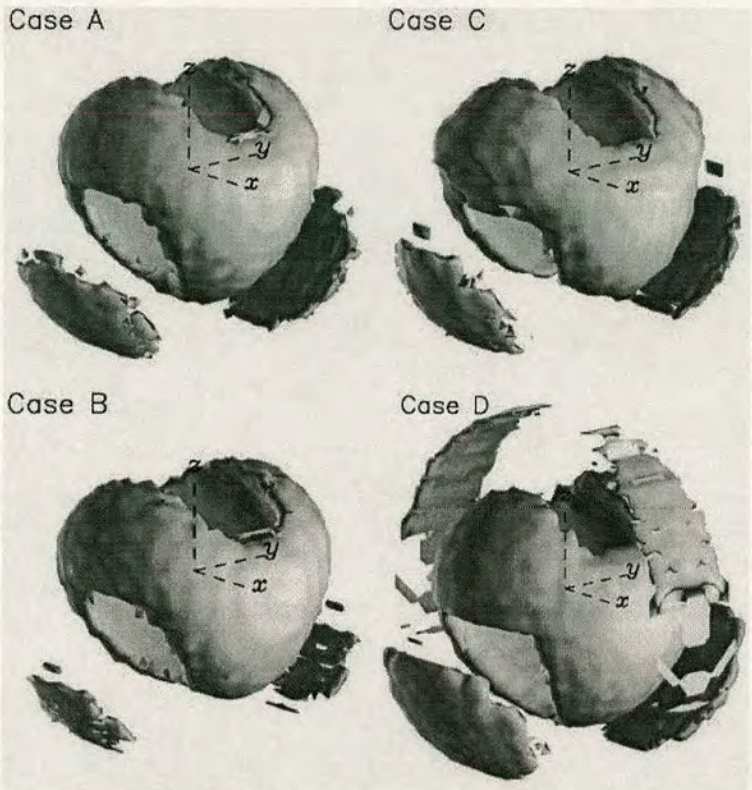

Figure 2.5: Density distribution of the orientations of a water molecule's dipole moment vector in the hydration shell around methane in aqueous solution. Lobes of density in the z-y plane correspond to rotations of the dipole moment vector about an axis perpendicular to the plane of the water molecule, while those in the z-x plane correspond to rotations about an axis parallel to the H-H vector within the molecule. A methane molecule is at the centre of the coordinate system and the orientational distribution functions of the water molecule have been averaged over the orientations of the central methane. It can be seen that these orientational correlations are similar in shape in the stable solution, when hydrate is forming, and in the hydrate crystal. The greatest densities are observed for water molecule orientations, where both hydrogens and lone pairs are kept as far away as possible from the methane, thus reinforcing the hydrogen bonding between water molecules. The four situations shown are: +18°C (case A), +10°C (case B), and +4°C (case C) and +4°C on heating from -10°C to (case D, hydrate). For all cases the pressure was held at 14.5 MPa. It is also seen that these orientational correlations extend to the second shell. For case D there is a notable expansion in the cage, and the ordering in the second shell becomes more marked [64].

Chapter 3

Methanol-Water System: A Preliminary Study

In this chapter the motivation behind choosing the methanol-water system to study hydration effects in aqueous media will be presented. A preliminary spectroscopic investigation of the hydration of methanol in aqueous solutions with increasing quantities of water is also reported.

3.1 Methanol- A Simple Amphiphilic Solute

Methanol is the simplest alcohol and is soluble in water in all proportions. Methanol has a methyl group which cannot form hydrogen bonds with water while it has a hydroxyl group which can form as many as three hydrogen bonds with water as shown in fig. 3.1. It is well known that the miscibility of methanol in water in all proportions is due to the presence of the polar hydroxyl group as well as the small size of the methyl group. In higher alcohols the increasing size of the alkyl residues renders them insoluble in water at most concentrations [68]. Hence the lower alcohols (methanol,ethanol) form ideal systems to study hydration effects as a function of solute concentration.

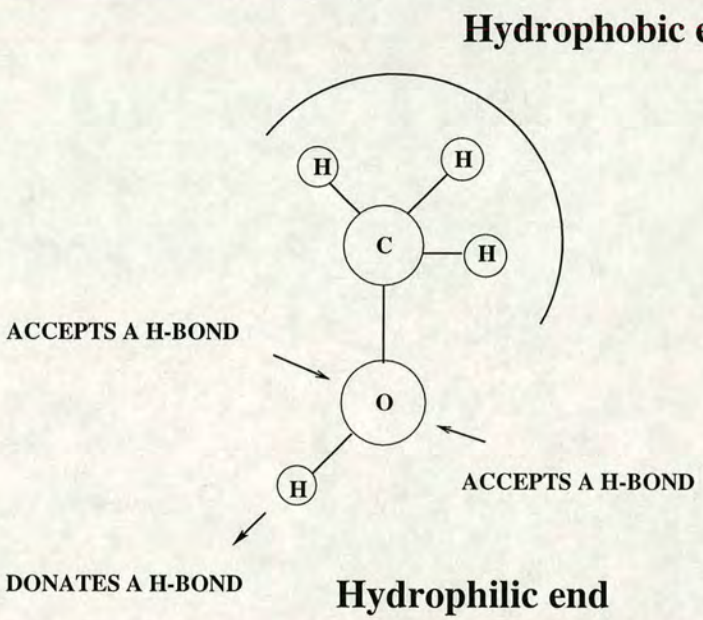

Figure 3.1: Maximal hydrogen bonding capacity of the methanol hydroxyl group.

Optical spectroscopy measurements on the methanol-water system prior to the mid 1990's [69, 70, 71] have reported a progressive breakdown of methanol hydrogen bonds with increasing dilution with water, with the methanol hydroxyl group forming hydrogen bonds with the water molecules. Some investigations were also aimed at determining whether the methanol molecules interacted with each other preferentially [72, 73] in these mixtures. Specifically the work of D'Angelo *et al* on a series of alcohol-water mixtures (methanol, ethanol, propanol, tertiary butanol) indicated that at high concentrations, the interactions between alcohol-water molecules are random. As the concentration of water increases, microaggregates of the alcohols are formed and finally when the solutions are significantly dilute the water molecules form an extended network like that found in pure water and hydrate the nonpolar alkyl residues.

Recent advances in the theoretical and experimental understanding of molecular interaction in aqueous media have brought such simple amphiphilic molecules to the forefront of active research again. Since some old concepts about the hydration of nonpolar species in water have been questioned, as explained in the preceding chapter, the emphasis is once again on probing the structure of aqueous

solutions. Such efforts have a three fold purpose:

- To further our understanding of the interaction of water with different chemical species in an effort to understand hydration effects on water structure.
- To determine how the fine balance between various chemical residues on a molecule can determine dominant intermolecular interactions in aqueous media.
- To ascertain what happens when the quantity of water in the medium is not sufficient to give rise to the classical hydrophobic effects reported so far.

Surprisingly, even for a simple solute such as methanol there has been very little work done to understand how increasing concentrations of methanol affects the hydration of the the polar and nonpolar groups. In the present work Raman spectroscopy is used to sketch a global picture of the progressive hydration of methanol, beginning with concentrated solutions where there is very little water to extremely dilute solutions where the water can hydrate the entire methanol molecule.

3.2 Raman Scattering

3.2.1 Theory

When a material is illuminated with a powerful source of light, some of the light scattered from the sample may have a frequency different from the incident light. This is the *Raman effect* and was discovered by Raman and Krishnan early in the 20th century [74].

In quantum mechanical terms, this effect can be described as an inelastic collision between a photon and the molecules in the scattering medium. In such a collision, the photon exchanges energy with a molecule. This results in an altered

frequency of the scattered photon. Since the total energy of the system (which comprises of the scattering molecule and the interacting photon) must be conserved, the energy change of the scattered photon must be exactly equal to the energy gained by the molecule. For such an energy exchange to be *allowed*, the energy lost by the photon must equal the energy difference between the quantised molecular energy levels. This leads to the scattering molecule exchanging energy with the photon in discrete units. At a molecular level, a Raman scattering event involves transitions between vibrational levels of a specific vibrational mode in the scattering molecule. If the molecule gains energy from the photon, it gets excited to a higher vibrational energy level and the scattered photon has a frequency which is red-shifted relative to the incident beam. This is a *Stokes* process. If the molecule already exists in an excited state it can also give some energy to the interacting photon thereby de-exciting to a lower energy level itself. In such a situation, the photon frequency is blue-shifted relative to the incident beam. This is an *Anti-Stokes* process. At room temperatures almost all molecules are in their ground state and hence most experiments look at the red-shifted part of the Raman spectrum.

The interaction of the incident light with the molecules in the scattering medium is dominated by elastic scattering in which the scattered beam is of the same frequency as the incident light since there is no exchange of energy between the molecules in the scattering medium and the incident photons. This mechanism results in an intense band in the scattered spectrum. On either side of this band are less intense bands at frequencies which are red and blue-shifted due to Raman scattering. Peak frequencies of these Raman bands contain information about bond force constants, bond lengths and charges about specific bonds in the molecule [75]. Any change in the environment of the scattering molecule which affects any of the above mentioned bond parameters will result in the peak frequencies being altered relative to the pure material under ambient conditions. Several intermolecular interactions can also affect the environment of a scattering molecule. Specific examples include hydrogen bonding with another molecular

species and dipolar interaction between induced dipoles. Application of external hydrostatic pressure would be an example of an external perturbation.

Typically in an experiment, an intense monochromatic source of light is used (a laser) in the visible region of the electro-magnetic spectrum. The wavelength of such a source is around 500 nm which is much greater than the size of a molecule. Hence the molecule *sees* a time varying electric field which for all practical purposes has no spatial variations. This electric field exerts the same electric force on all electrons in the molecule thereby displacing them from their average positions giving rise to an induced dipole. The magnitude and direction of the induced dipole depends critically on the polarizability of the molecule.

Polarizability can be best described as the softness of the electron cloud [76] in a molecule. It is a measure of the molecule's response to an electric field and its ability to acquire an electric dipole moment. Quantum mechanics tells us that for a particular molecular vibration to be Raman active, the polarizability of of the molecule must change with respect to that specific vibration. For polyatomic molecules it is difficult to determine which vibrational modes are Raman active given the vast number of vibrations such molecules can have [77]. Without going into details, it is sufficient to note that group theory explains how the polarizability of the molecule couples to a specific vibrational mode of the molecule in determining whether a vibrational mode is Raman active.

The polarizability of the molecule is a tensorial quantity (3×3 matrix). When a plane polarised beam of light interacts with a molecule, the induced dipole moment can have a direction different to that of the incident field. The off-diagonal components of the polarizability tensor determine those components of the induced dipole which are not parallel to the incident field. Hence, the scattered light, whose direction depends on the direction of the induced dipole moment need not be parallel to the incident field.

The scattered light can thus be separated into a polarised component whose plane of polarisation is parallel to the incident beam (VV spectrum) and a depolarised

component whose plane of polarisation is perpendicular to the polarisation of the incident beam (VH spectrum). This leads to Raman scattering being observed in two scattering geometries with respect to the polarisation of the incident radiation. A typical experimental set up is shown in fig. 3.2.

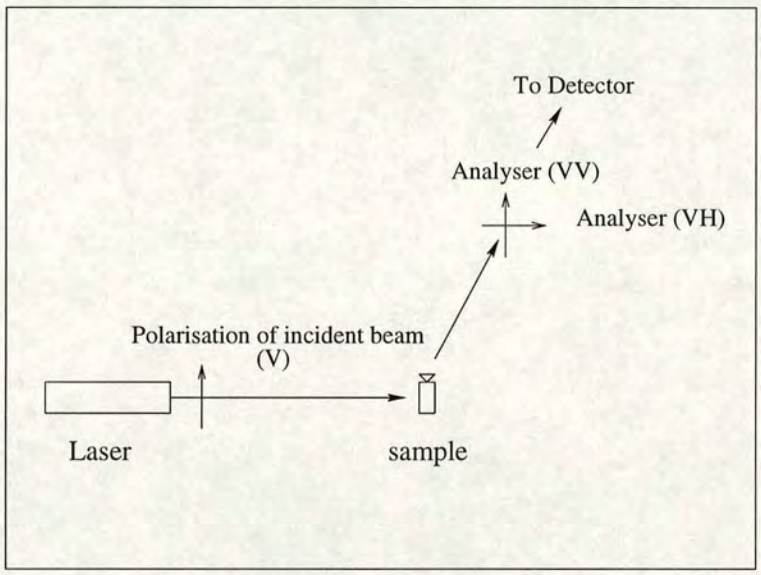

Figure 3.2: Experimental set-up to collect Raman spectra.

Normally, peak frequencies obtained either from the VV or the VH spectrum of molecular liquids coincide. However there have been instances where this is not the case. Typical examples are: the C=O stretch mode of acetone [78], C-O stretch mode of methanol [71] and O-H stretch mode of alcohols [69]. Theoretical formulations developed by Wang and McHale indicate that an angular dependent intermolecular potential gives rise to the non-coincidence of peak frequencies of some molecular vibrational modes [79, 80] as indicated in the examples above. Such intermolecular potentials could arise for example due to hydrogen bonding or transition dipole interactions (dipole derivative with respect to the specific molecular vibration which shows the non-coincidence effect). Particularly in the case of associated liquids (hydrogen bonded liquids), this non-coincidence effect can be used to monitor how external environmental changes affect inter-species association (which is due to the formation of hydrogen bonds). The specific case of methanol will be discussed next.

3.2.2 Raman spectra of methanol and water

The Raman spectra of water and methanol in the VV and VH geometries are shown in figs. 3.3 and 3.4 respectively. It is at once obvious that the Raman spectrum of water is very weak. This makes Raman spectroscopy a particularly attractive technique to investigate structural changes occurring in water-organic liquid mixtures as a function of concentration of either molecular species since there is minimum overlap between the water spectrum and that of the organic liquid.

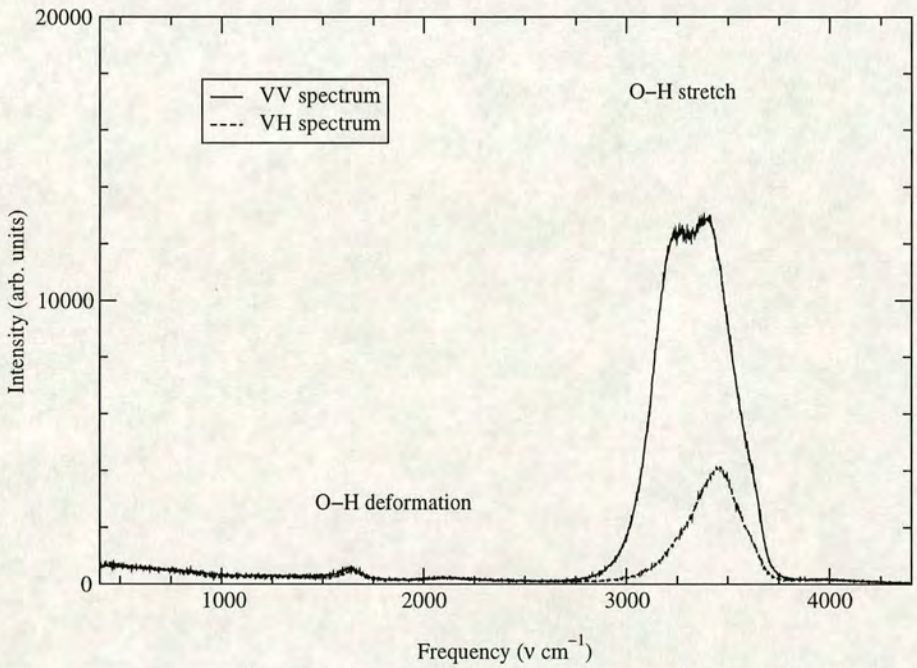

Figure 3.3: Raman spectrum of water.

In the case of methanol, (see figs. 3.3 and 3.4) the two spectra overlap only in the region of the O-H stretch around 3200 cm^{-1}. Both molecular species have strong signatures due to their -OH groups. Hence this spectral region is not useful to study how increasing dilution with water would affect the hydration of the methanol hydrophilic (hydroxyl) moiety.

The adjacent molecular bond, which is the C-O bond helps in this particular case. The frequencies of the C-O stretch mode (ν_{CO}) do not coincide in the VV and VH

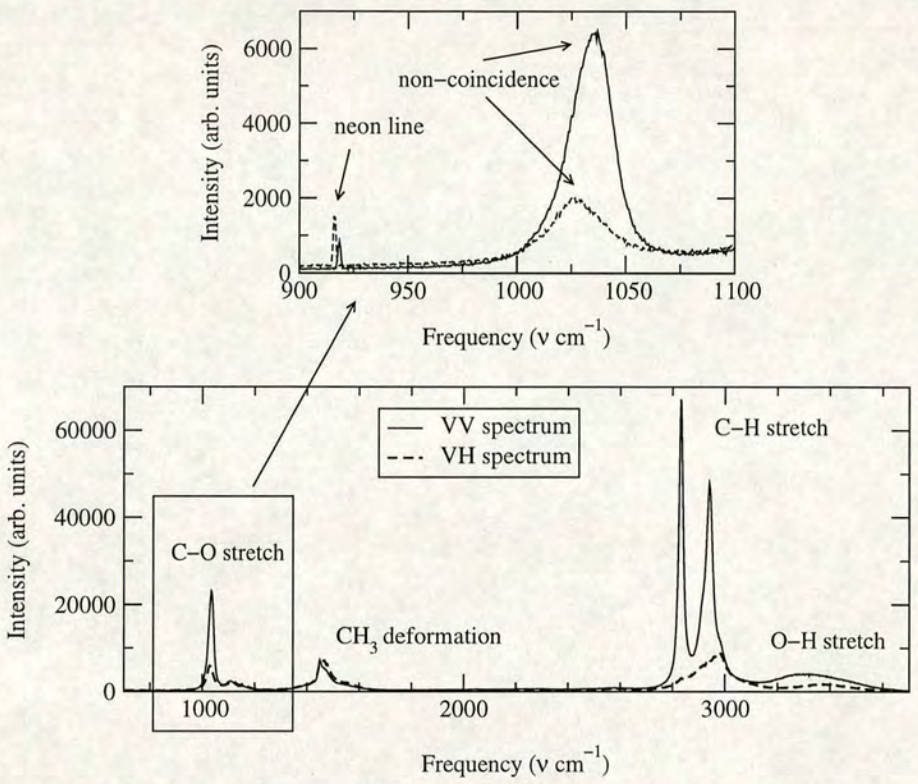

Figure 3.4: Raman spectrum of methanol.

spectra. In pure liquid methanol, $\nu_{CO}^{(VV)} \simeq 1036$ cm^{-1} while $\nu_{CO}^{(VH)} \simeq 1029$ cm^{-1}. A detailed analysis of the non-coincidence effect in pure methanol for the C-O stretch mode has been carried out recently by Torii and Tasumi [81] using the model developed by Wang and McHale [79, 80]. This provides a molecular level explanation of the observed non-coincidence. Methanol molecules hydrogen bond to form chains in the liquid state [82]. While coupling of the transition dipoles (for the C-O stretch mode) is responsible for the non-coincidence of the peak frequencies in the VV and VH mode, the relative position and orientation of the molecules is governed by hydrogen bonds. Hence the C-O mode frequencies have different values in the two scattering geometries. This non-coincidence effect provides a useful means of monitoring the degree of inter methanol hydrogen bonds in mixtures of methanol with other liquids.

Detailed investigations by Kabisch and Pollmer [70] have shown that the C-O stretch mode of methanol is sensitive to the type of hydrogen bonds formed via

the hydroxyl group of the alcohol in mixtures with other liquids. When methanol donates a hydrogen bond via its hydroxyl hydrogen, the frequency of the C-O mode is seen to blue-shift with respect to the monomer value whereas the same mode red-shifts from the monomer value when the hydroxyl group accepts a hydrogen bond.

In the specific case of adding water to methanol, hydrogen bonds form between the two molecular species [71] since the hydroxyl group of methanol can act as a hydrogen bond acceptor and a hydrogen bonds donor (see fig.3.1). The C-O stretch mode which is isolated in the methanol spectrum would thus respond to a changing hydrogen bond environment at the hydroxyl group end of the alcohol.

Previous reports on the variation of ν_{CO} with methanol concentration (mole fraction, x) in methanol-water mixtures have been conflicting. Zerda *et al* [71] reported, in a study otherwise devoted to high-pressure effects, that ν_{CO} is a *linear* function of x, contradicting Kabisch and Pollmer [70] who reported a nonlinear trend. More recently, Kamogawa and Kitagawa reported *both* ν_{CH} and ν_{CO} [72, 83], but did not comment on their correlation. They however interpreted their results in terms of inter-molecular contributions of each species (water and methanol) to the observed frequency shifts of the C-H stretch mode. None of these authors use the spectroscopic data to give a *global* picture of the progressive hydration of methanol, concentrating instead on the particulars of hydrogen bonding in special regimes (mostly at small x).

The results reported by Gruenloh *et al* [84] which are described next enable precisely such an interrogation of the observed spectroscopic trends. A combination of spectroscopy and computational methods were used by the authors to investigate the response of the C-H stretch modes of methanol to specific hydrogen bond environments at the hydroxyl end of the alcohol. The spectroscopic measurements were performed in the gas phase. The C-H stretch frequency was found to increase (decrease) from the gas phase monomer value depending on whether the hydroxyl group of methanol accepted [A] (donated [D]) a hydrogen

bond. This result was also found to be valid in condensed phases. The authors report a study of mixtures of methanol with acetone/water/chloroform where the methanol is involved in different types of hydrogen bonds with the complexing species. They found ν_{CH} increasing by as much as 10 cm^{-1} when methanol was sufficiently diluted in water, confirming their prediction from gas phase results, i.e. when the hydrogen bond environment at the hydroxyl end of methanol transferred from an AD (pure methanol is a hydrogen bonded liquid, see fig. 3.5) to an AAD hydrogen bond configuration *, the C-H stretch frequency blue shifts. Similarly, in the case of diluting methanol in acetone, ν_{CH} was found to decrease in frequency by about 4 cm^{-1}, again consistent with their prediction for methanol going from an AD to a D hydrogen bond configuration. Acetone, does not have a hydrogen to donate but does have an oxygen which can accept a hydrogen bond via the methanol hydroxyl hydrogen.

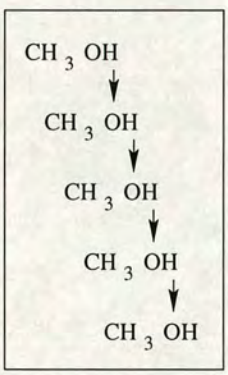

Figure 3.5: Schematic representation of the chain structure in liquid methanol.

It is thus possible to probe the hydration of the -OH group of methanol in methanol-water mixtures by monitoring changes in the C-O and the C-H stretch frequency.

In the next section results obtained from the Raman spectra of methanol at various concentrations of methanol in water are presented. These are discussed in detail to obtain a global picture of hydration of methanol in aqueous solutions.

*Water molecules can donate and accept hydrogen bonds. In a very dilute mixture, the water molecules will try to maximise their hydrogen bonds with methanol molecules.

3.3 Experimental Procedure

Methanol was purchased from Sigma and used without further purification. Deionized water was boiled and filtered through a 0.2 Millipore filter. Mixtures of methanol-water ranging from pure methanol to 0.01 mole fraction of methanol in water (x) were prepared and sealed in glass bottles. They were used within 72 hours of preparation. This was because a small change in the mixture concentration was noted after about three days. Raman spectra were excited at room temperature (290±2) K using 400 mW of the 514.5 nm line of an Argon ion laser. A Coderg T800 triple axis spectrometer was used to collect Raman spectra in a 90° geometry. Spectral resolution was 1.2 cm^{-1}. The incident laser was always polarised in a plane perpendicular to the scattering plane. For the C-O stretch of methanol both VV and VH spectra were recorded while for the C-H stretch only the VV spectra were recorded. A neon emission line was used as an internal frequency standard. Peak frequencies were determined by inspection.

3.4 Results and Discussion

Measured values of the C-O stretch frequency, ν_{CO} (VV and VH) and the C-H stretch frequency, ν_{CH} (VV) are shown in fig. 3.6 and fig. 3.7 respectively. The observed frequency shifts of both stretch modes are nonlinear with respect to the methanol mole fraction, x. The C-O mode is seen to red-shift while the C-H mode is seen to blue-shift.

The results shown here are in agreement with those of Kabisch and Pollmer [70] and Kamogawa and Kitagawa [72].

Three distinct regions can be identified from fig.3.6 and fig.3.7. The first concentration region is above $x \approx 0.7$. Here $\nu_{CO}^{(VV)}$ is seen to red-shift by about 5 cm^{-1} whereas $\nu_{CO}^{(VH)}$ remains constant. Further, ν_{CH} does not blue-shift significantly. In the next concentration regime, between $x \approx 0.7$ and $x \approx 0.25$, $\nu_{CO}^{(VV)}$ red-shifts

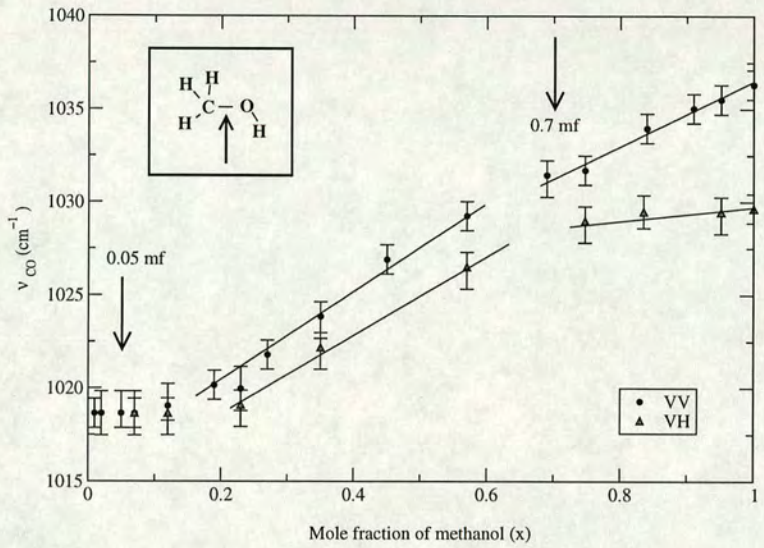

Figure 3.6: Change in CO stretch frequency with increasing mole fraction of water.

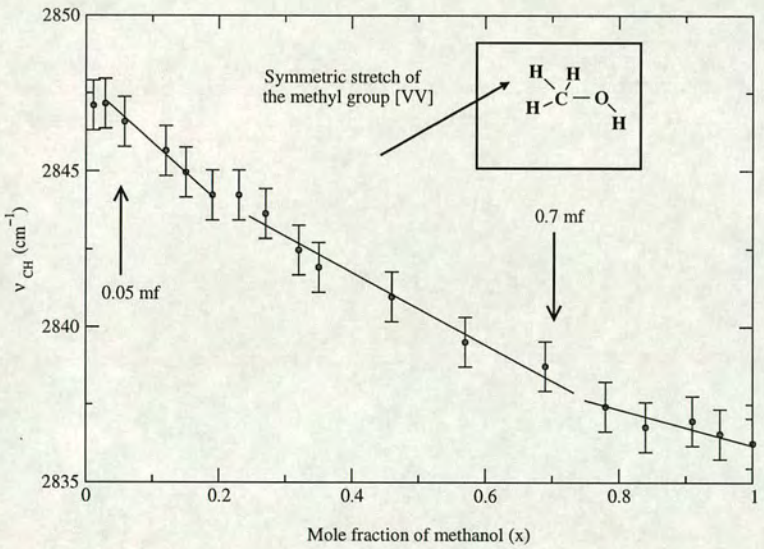

Figure 3.7: Change in CH stretch frequency with increasing mole fraction of water.

further and is accompanied by a dramatic red-shift in $\nu_{CO}^{(VH)}$. Also observed is a rapid blue-shift in ν_{CH}. In the last concentration region which is below $x \approx 0.25$, both $\nu_{CO}^{(VV)}$ and $\nu_{CO}^{(VH)}$ saturate and coincide within error at about 1018 cm^{-1}. However, ν_{CH} seems to blue-shift further on.

As mentioned earlier, molecules in pure liquid methanol hydrogen bond to form chains. On an average at 25°C these chains are about five molecules long [82]. A schematic picture is shown in fig.3.5. Up to $x \gtrsim 0.7$ it appears that water molecules do not affect the chain structure of methanol drastically. There are at least three arguments to support this statement. To begin with, the non-coincidence effect, which is a measure of the difference between $\nu_{CO}^{(VV)}$ and $\nu_{CO}^{(VH)}$ is still nonzero indicating that inter methanol hydrogen bonds still exist. Next, while $\nu_{CO}^{(VV)}$ red-shifts, curiously $\nu_{CO}^{(VH)}$ remains constant within error. Further ν_{CH} also does not blue-shift dramatically. Gruenloh *et al.* [84] measured ν_{CH} in methanol molecules in which the polar moiety participates in hydrogen-bond complexing to other species. They found that ν_{CH} is sensitive to the *configuration* of hydrogen bonds at the polar moiety, but not to the kind of complexing species giving rise to a particular hydrogen bond configuration. A single methanol molecule can, at most, accept two and donate one hydrogen bond, (see fig. 3.1). For such an 'AAD' configuration, Gruenloh *et al.* always found ν_{CH} blue-shifting.

In light of the results reported by Gruenloh *et al* [84], the almost constant ν_{CH} is indicative of very few methanol molecules having an AAD hydrogen bond configuration. Hence the water molecules form hydrogen bonds with the methanol chain ends. The red-shift in $\nu_{CO}^{(VV)}$ implies weakening of the C-O bond. This would occur if strong hydrogen bonds form between water and the oxygen lone pair of methanol. This would result in electrons being sucked into the C-O bond due to the hydrogen bond at the oxygen atom. Chain-end hydration in this concentration regime has also been suggested very recently by Sato *et al* [85] based on reorientation relaxation time measurements using dielectric spectroscopy.

A dramatic red-shift is seen in $\nu_{CO}^{(VH)}$ between $x \approx 0.7$ and $x \approx 0.25$. This is accompanied by an equally steep blue-shift in ν_{CH}. The red-shift in $\nu_{CO}^{(VV)}$ continues. In this region the chain structure of methanol is broken down. This is quantified by the saturation and coincidence of $\nu_{CO}^{(VV)}$ and $\nu_{CO}^{(VH)}$ at 1018 cm^{-1} by $x \approx 0.25$. Water molecules completely hydrate the -OH group of methanol. All inter methanol hydrogen bonds are broken. Moreover, at $x \approx 0.25$, the blue-shift

in ν_{CH} appears to saturate at around 2844 cm^{-1} in agreement with predictions made by Gruenloh *et al* for methanol molecules in AAD configurations, suggesting that the hydrogen bond configuration round the hydroxyl groups in methanol has stabilised.

Blue-shift in ν_{CH} starts again at $x \sim 0.15$. By this stage,the primary 'AAD' hydration shell of the hydroxyl group is associated with a further 3 or so water molecules. When this process of hydroxyl solvation is complete, further hydration takes the form of water molecules forming structure round the methyl groups. This is proposed as the hydration process below $x \sim 0.15$. Indeed, very recent neutron scattering and simulation work by Finney and Soper [13] reports a more or less complete shell of water molecules surrounding each methanol at $x = 0.1$. Interestingly, even though the average hydrogen bonding configuration of the hydroxyl group is not expected to change in this regime, ν_{CH} continues to blue-shift. The conclusion of Gruenloh *et al.* [84] from gas-phase work, that ν_{CH} in methanol molecules is sensitive to the hydrogen bond configuration at the polar moiety, therefore needs supplementing in the condensed phase, where ν_{CH} clearly also responds to the immediate environment of the non-polar moiety. The C-H stretch frequency appears to roll off again at $x \sim 0.05$. This might point to primary solvation of methanol molecules being complete.

There is just one comment which seems necessary before concluding this section. The trend seen in the behaviour of $\nu_{CO}^{(VV)}$ and $\nu_{CO}^{(VH)}$ up to $x \sim 0.7$ is almost identical to the behaviour of this mode in pure liquid methanol under pressure [71]. In pure methanol under pressure, $\nu_{CO}^{(VV)}$ red-shifts by about 2 cm^{-1} at 4 kbar of hydrostatic pressure while $\nu_{CO}^{(VH)}$ remains constant. Detailed modelling of the non-coincidence effect in pure methanol based on the model of McHale [80] has been carried out by Torii and Tasumi [81]. They suggest that the initial increase in density on application of pressure is largely absorbed by closer packing of methyl groups, leaving the hydrogen bonding structure at the methyl moieties (and therefore the chain structure) little affected. That there is little change in the chain structure is consistent with the author's interpretation of what happens

in the regime $1 > x \gtrsim 0.7$. Furthermore, thermodynamic measurements on methanol-water mixtures have yielded a *decrease* in the methanol partial molar volume for all concentrations down to $x \sim 0.1$ [86]. The partial molar volume at $x \sim 0.7$ is equivalent to an effective methanol density of $\rho \sim 0.8$ g/cm^3. This is equivalent to pure bulk methanol at ~ 0.5 kbar [71]. It is therefore at least plausible that the behaviour of the non-coincidence effect in ν_{CO} in the concentration range $1 > x \gtrsim 0.7$ basically reflects an increase in methanol packing density due to the presence of water [87].

3.5 Summary and Conclusions

The behaviour of ν_{CO} and ν_{CH} in methanol-water mixtures suggests three regimes of hydration. At $1 > x \gtrsim 0.7$, the addition of water leaves the chain structure of pure methanol substantially intact; hydration takes place at the chain ends, where the methanol molecules act principally as H-bond acceptors. For intermediate concentrations, $0.7 \gtrsim x \gtrsim 0.25$, water progressively breaks up methanol chains; individually molecules become hydrated, accepting two and donating one H-bond with water. Below $x \approx 0.25$, when the hydroxyl groups are completely surrounded by water, hydration of the methyl groups take place, resulting in their complete primary solvation by $x \approx 0.05$. The naive picture of water hydrating amphiphile-like molecules, namely, that it solvates the polar moiety before the non-polar moiety, is therefore seen to be essentially correct.

Detailed thermodynamic measurements reported by Koga *et al* [45] also point to three mixing schemes in water-alcohol mixtures which support the interpretations from the Raman data reported here. Corroboration for this proposed picture has come from a number of sources, including dielectric spectroscopy and neutron scattering [13, 85]. The comparison of the effect of dilution with water and hydrostatic pressure is intriguing.

Clearly a detailed structural investigation is necessary to validate the interpre-

tations made from the Raman data. From the results obtained using Raman spectroscopy, two concentrations clearly demand a more detailed investigation, $x \approx 0.7$ and ≈ 0.05. The former will yield information on how water begins to disrupt the methanol chain network and whether the presence of water affects the methanol interactions like external pressure would. The latter concentration is sufficiently dilute for a water network to exist. Hence a structural investigation at this methanol mole fraction will point to whether the methyl group ($-CH_3$) interferes with the water network at all. It is important to note that the methyl group is hydrophobic and hence would prefer to not be in contact with water. However its small surface area enables water molecules to form a disordered cage around it [13].

Neutron scattering has been used over the past decade to provide structural information on disordered materials. The recently developed Empirical Potential Structure Refinement technique [56] to analyse data resulting from neutron scattering experiments has opened new vistas for condensed matter research in the area of disordered materials like liquids. The next chapter will provide a review of the neutron scattering technique and its use in structural studies of liquids as well as a formal introduction to the EPSR technique which was developed in the late 1990's by Dr Alan Soper. The thesis will then focus on results obtained from neutron scattering experiments on methanol-water mixtures at the above mentioned concentrations.

Chapter 4

Neutron Scattering: Tool for Liquids Research

In order to probe the structure of matter at a molecular level one needs to resort to indirect methods. Scattering techniques allow the investigation of structure over a wide range of length scales. Structure on a molecular scale is of the order of angstroms ($\mathring{A}$) and neutrons are increasingly being used to determine the structure of liquids. This chapter introduces the theory behind neutron scattering. An introduction to recently developed modelling techniques to extract information from the data collected from neutron scattering experiments is also presented.

4.1 Neutron Scattering

4.1.1 Theory

The simplest way to introduce the idea behind scattering is to appreciate that the incident radiation used should have a wavelength comparable to the length scale of the system under investigation. If a beam of radiation is incident on a target, the scattered intensity will contain information on the positions of the

scattering centres in the target. Neutrons with wavelengths in the range 1-10 $\AA$ are ideal to investigate structural correlations in condensed matter systems. These wavelengths correspond to energies of the order of meV which are routinely obtained at most neutron facilities.

What follows next is a more quantitative explanation of how the scattered intensity maps onto the spatial structure of many particle systems. This explanation is extremely general and applies to all types of particles. To begin with fig. 4.1 shows a typical scattering geometry with the incident, final and scattering wave vectors. Let $\vec{k}$ and $\vec{k'}$ ($|\vec{k}| = 2\pi/\lambda$) define the incident and final wave vectors of the scattered particle.

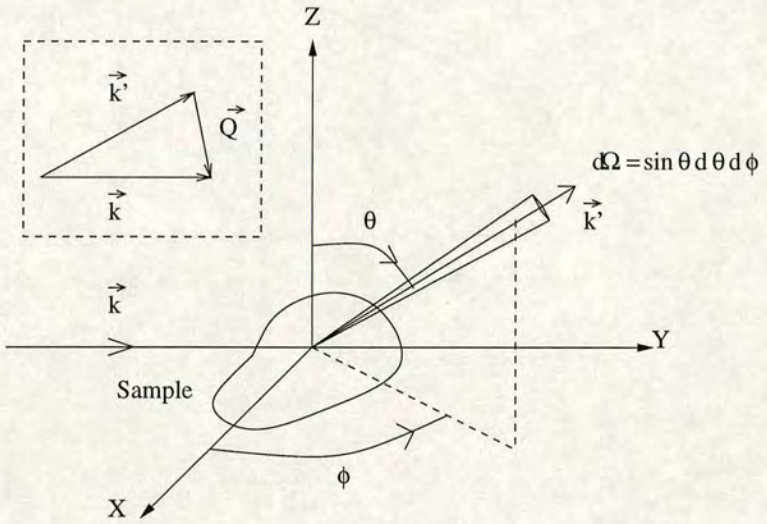

Figure 4.1: Geometry for a typical scattering experiemnt. The incident and scattered wave vectors and energies are given by ($\vec{k}$,E) and ($\vec{k'}$,E') respectively. The solid angle dΩ is defined about a specific direction θ and a detector collects particles scattered in the direction defined by the angle θ.

If the particle interacts with the scattering centres in the medium via a potential U, quantum mechanics tells us that if this interaction is sufficiently weak thereby resulting in only the lowest order term in the scattered wave [88], the scattering amplitude is proportional to the matrix element formed by the incoming wave function of the incident particle, the scattering potential and the outgoing wave

function of the scattered particle;

$$amplitude \approx \langle out \mid U \mid in \rangle \tag{4.1}$$

This amplitude is denoted by $A_{\mathrm{k,k'}}$ where the two plane wave states of the scattered particle are characterised by the above mentioned wave vectors [88].

Thus:

$$A_{\mathrm{k,k'}} = \int e^{-i\vec{k'}.\vec{r}} U(\vec{r}) e^{i\vec{k}.\vec{r}} d^3\vec{r} \tag{4.2}$$

where $e^{i\vec{k}.\vec{r}}$ is the wave function of the incident particle and $e^{i\vec{k'}.\vec{r}}$ is the wave function of the scattered particle.

A scattering medium is a multi particle system. The interaction potential $U(\vec{r})$ can be written as:

$$U(\vec{r}) = \sum_{\alpha} U_{\alpha}(\vec{r} - \vec{r_{\alpha}}) \tag{4.3}$$

Here $\vec{r}_{\alpha}$ is the position of an atom labelled arbitrarily as α. The amplitude of the scattered wave is given by:

$$A_{\mathrm{k,k'}} = \sum_{\alpha} \int e^{-i\vec{k'}.\vec{r}} U_{\alpha}(\vec{r} - \vec{r}_{\alpha}) e^{i\vec{k}.\vec{r}} d^3\vec{r} \tag{4.4}$$

Defining a new variable $\vec{R}_{\alpha} = \vec{r} - \vec{r}_{\alpha}$ the above equation reduces to:

$$A_{\mathrm{k,k'}} = \sum_{\alpha} \int e^{-i\vec{k'}.[\vec{r}_{\alpha}+\vec{R}_{\alpha}]} U_{\alpha}(\vec{R}_{\alpha}) e^{i\vec{k}.[\vec{r}_{\alpha}+\vec{R}_{\alpha}]} d\vec{R}_{\alpha} \tag{4.5}$$

Grouping the terms in $\vec{R}_{\alpha}$ together and defining the scattering wave vector as $\vec{Q} = \vec{k} - \vec{k'}$ such that $\hbar\vec{Q} = \hbar\vec{k} - \hbar\vec{k'}$* is the momentum transfered to the scattering

*See figure 4.2

centre we get:

$$A_{\mathrm{k,k'}} = \sum_{\alpha}[\int e^{i\vec{Q}.\vec{R}_\alpha} U_\alpha(\vec{R}_\alpha) d\vec{R}_\alpha] e^{i\vec{Q}.\vec{r}_\alpha} \tag{4.6}$$

The integral in the above equation can be denoted by $\mathrm{U}_\alpha(\vec{Q})$. This term contains all the information on the spatial extent of the interaction potential and is defined as the atomic form factor.

The quantity actually measured in a scattering experiment is the scattered intensity. This intensity is the square of the matrix element $\mathrm{A_{k,k'}}$ which was derived above. In a typical scattering experiment, the differential cross section is the experimentally accessible quantity. It directly maps on to the the scattered intensity and is defined as the ratio of the number of particles scattered into the direction (θ,ϕ) per unit time, per unit solid angle ($d\Omega$) divided by the incident flux [89].

It is important to mention that the differential cross-section referred to here is a static cross-section, i.e. it is obtained from a scattering experiment by integrating over all possible energy transfers to the medium. This cross-section is thus a function of the scattering vector.

The differential cross-section ($\frac{d\sigma}{d\Omega}$) can be written as:

$$\frac{d\sigma}{d\Omega} \sim \sum_{\alpha,\alpha'} U_\alpha(\vec{Q}) U^{\star}_{\alpha'}(\vec{Q}) e^{i\vec{Q}.\vec{r}_\alpha} e^{-i\vec{Q}.\vec{r}_{\alpha'}} \tag{4.7}$$

In the theory presented so far the scattering centres have been assumed to be rigid in their positions. In reality this is not the case. Experimental measurements are taken over a period of time which is much greater than thermal equilibration times. If the detector collects scattered radiation as a function of the scattering vector alone and independent of the energy change then the scattered intensity collected at a detector records a snapshot of the sample with each scattering event. These different snapshots collected over time represent a time average collected

over many sample configurations [88]. For an ergodic system time averages are equivalent to averages over all allowed configurations. If the atoms of the medium are identical the form factor neatly separates out and the scattered intensity carries information which solely depends on the positions of the atoms in the medium and hence the spatial structure of the medium. The scattering intensity can then be defined as:

$$I(\vec{Q}) = \langle \sum_{\alpha,\alpha'} e^{i\vec{Q}.[\vec{r}_\alpha - \vec{r}_{\alpha'}]} \rangle \tag{4.8}$$

4.1.2 The Structure Factor

The structure factor $S(\vec{Q})$ is traditionally defined as $N^{-1}[I(\vec{Q})]$ [88] , where N is the total number of particles in the scattering medium. A typical scattering experiment collects scattered particles over a significant $\vec{Q}$ range. It is at once clear that at $|\vec{Q}| = 0$, $S(\vec{Q}) = N$ which corresponds to the straight through beam. For all remaining values of $\vec{Q}$ the structure factor simplifies to the following;

$$S(\vec{Q}) = \frac{1}{N} \langle \sum_{\alpha,\alpha'} e^{i\vec{Q}.[\vec{r}_\alpha - \vec{r}_{\alpha'}]} \rangle \tag{4.9}$$

$$S(\vec{Q}) = \sum_{\alpha \neq \alpha'} \int e^{i\vec{Q}.\vec{r}} \langle \frac{1}{N} \delta(\vec{r} - [\vec{r}_\alpha - \vec{r}_{\alpha'}]) \rangle d\vec{r} + 1 \tag{4.10}$$

The '1' comes from the α=α' terms. The term in the angular brackets is defined as the pair correlation function multiplied by the density of the scattering medium [22].

$$\rho g(\vec{r}) = \frac{1}{N} \langle \sum_{\alpha \neq \alpha'} \delta(\vec{r} - [\vec{r}_\alpha - \vec{r}_{\alpha'}]) \rangle \tag{4.11}$$

The structure factor can now be written as:

$$S(\vec{Q}) = 1 + \rho \int [g(\vec{r}) - 1] e^{i\vec{Q}.\vec{r}} d\vec{r} \tag{4.12}$$

While the structure factor is an extremely useful quantity, it's information content is entirely in Q space. From the point of view of analysis one requires information in r-space. This is contained in the pair correlation function which will be delved into some detail. This is because ultimately, it is this quantity which the experimenter is after and understanding what it means is crucial. When the medium under investigation is a homogeneous isotropic fluid, the pair correlation function does not depend on the direction of $\vec{r}$ but only its magnitude. The resulting function, g(r) is called the radial distribution function[†] which describes statistically, the probability of finding an atom at a distance r away from any other atom.

Suppose one has a configuration of particles in a scattering medium. One of the particles is chosen as the origin. The radial distribution function is obtained by determining the number of particles whose centres line within a distance dr of a circle of radius r centred around the origin averaged over all atoms in the configuration. A simple illustration in 2 dimensions is shown in fig. 4.2.

For an isotropic medium the integral in equation 4.12 can be evaluated over the spherical polar angular coordinates. This results in a simpler version of the same equation, i.e.

$$S(Q) = 1 + 4\pi\rho \int [g(r) - 1] r^2 \frac{\sin(Qr)}{Qr} dr \tag{4.13}$$

where ρ is the number density of the atoms in the medium. While the above integral is a one dimensional integral, it is important to remember that the diffraction experiment records the structure factor in three dimensions.

The general shape of a radial distribution function for a liquid has already been shown earlier in fig. 2.3 (see chapter 2 for details). What is important to note here

[†]This quantity was introduced earlier in chapter 2.

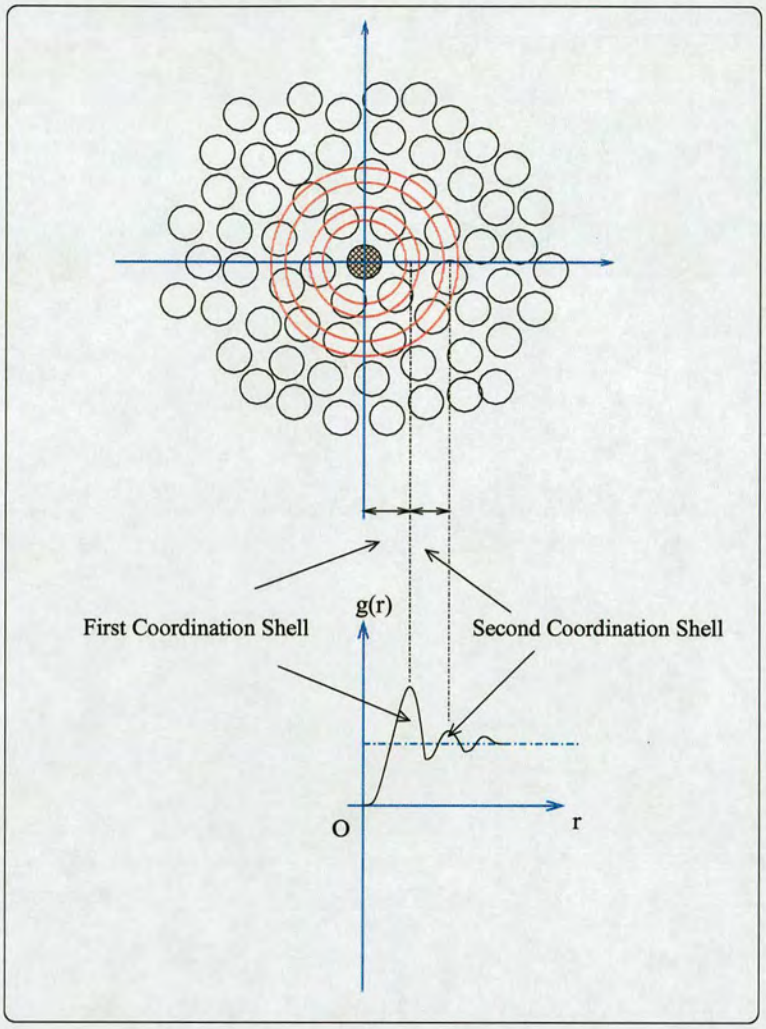

Figure 4.2: Typical radial distribution function for a hard sphere fluid shown in 2 dimensions. The particle at the origin is arbitrarily chosen. The first and second coordination shells are shown in red (*see text for details*).

is that while determining the radial distribution function or conversely the structure factor, the integration must take into account the correct number density of the atoms in the liquid. Integration under the first peak of a radial distribution function gives the first neighbour coordination number, i.e. the number of atoms in the first coordination shell.

4.1.3 Real Systems

Structural correlations in a liquid are short range, extending over a few molecular diameters. This length scale characterises the liquid state and is a direct consequence of the packing constraints in the liquid due to the rigid molecular units. It is not surprising that neutron scattering is being increasingly used as the preferred technique to study the structure of liquids at the angstrom length scale. Small angle neutron scattering is also emerging as a powerful technique to probe density fluctuations in liquids which are of the order of tens of nanometers.

Neutrons interact with matter via the nuclear force. The range of these forces is of the order of femtometers (10^{-15} m) while the wavelength of the neutrons used to probe liquid structure is of the order of an angstrom (10^{-10} m). This results in an interaction potential (*between the incoming neutron and the scattering nucleus*) which is point like and isotropic. The scattering length (*denoted by b in the literature*) of a nucleus defines the amplitude of the scattered wave. The atomic form factor introduced earlier contains precisely this information. The scattering length is unique to each element and depends on the nuclear spin and isotope. Thus the scattering length has to be averaged over the N nuclei in the sample. Consider again equation. 4.7 where the interaction potential is now substituted by the scattering length:

$$\frac{d\sigma}{d\Omega} \sim \mid \sum_{\alpha} b_{\alpha} e^{i\vec{Q}.\vec{r}_{\alpha}} \mid^2 \tag{4.14}$$

This can now be simplified [53] to yield:

$$\frac{d\sigma}{d\Omega} \sim N\langle b_{\alpha}\rangle^2 \mid e^{i\vec{Q}.\vec{r}_{\alpha}} \mid^2 + N(\langle b_{\alpha}^2\rangle - \langle b_{\alpha}\rangle)^2 \tag{4.15}$$

The scattered intensity consists of contributions from two separate differential cross sections. The first term in the above equation yields contributions from coherent scattering, the quantity of interest. It contains information on the posi-

tions of the nuclei. The phase factor ($e^{i\vec{Q}.\vec{r}_\alpha}$) considers all nuclei as the same even thought individual nuclei can have a range of scattering lengths. The second term does not contain a phase term and measures the mean square deviation of each scattering length from the mean. This term is called the incoherent scattering term since it contains no positional information. Contributions from incoherent scattering have to be removed from the measured raw data before analysis at the structure factor level can be undertaken.

In complex systems such as molecular liquids there are several atomic species and the scattering length of each has to be accounted for separately. The atomic form factor contains contributions from the scattering length of each atomic species. The total scattered intensity is a sum of several structure factors with appropriate weights proportional to the product of the scattering length and the atomic weight fraction of each atomic species in the sample. As mentioned before, the scattering lengths have to be averaged over the nuclear and isotope spin-states. Hence for a scattering system which comprises of a molecular liquid (or a mixture of molecular liquids) if α denotes the number of atomic species in the scattering system, the TOTAL structure factor measured by a diffraction experiment is a combination of two terms, a "self" term and a "distinct" term.

$$F(Q) = \sum_{\alpha} c_\alpha \bar{b^2}_\alpha [S_\alpha(Q)] + \sum_{\alpha \neq \beta} c_\alpha c_\beta \bar{b}_\alpha \bar{b}_\beta [S_{\alpha\beta}(Q) - 1] \tag{4.16}$$

where c_α is the atomic fraction of each atomic species α and b_α is its neutron scattering length. $S_{\alpha\beta}(Q)$, the partial structure factor for atom types α and β, is defined as[‡]

$$S_{\alpha\beta}(Q) - 1 = 4\pi\rho \int r^2 [g_{\alpha\beta}(r) - 1] \frac{sin(Qr)}{Qr} dr \tag{4.17}$$

where ρ is the average atomic number density of the solution under investigation and $g_{\alpha\beta}(r)$ is the partial pair correlation function for the two atom types.

[‡]This is basically equation 4.13.

The "self" term contains contributions from incoherent scattering which can be quite high for protons. The "distinct" term provides information on the correlations of distinct particles (coherent scattering) and hence is the all important quantity from the point of view of a researcher.

So far the scattering considered does not take into account any energy transfers which occur during a scattering process. Normally, in neutron scattering processes the scattering nucleus recoils under neutron impact. The neutron exchanges energy with the scattering system and inelasticity effects have to be accounted for. Thus the structure factor can no longer be considered to be a function of the scattering vector alone but is also a function of energy i.e. ω. The positions of the atoms in the system are thus a function of time. An analysis similar to that presented in the beginning of this chapter is required to explicitly account for the energy dependence of the scattering process. The resulting structure factor is then a function of Q and ω [90]. $S(Q, \omega)$ is called the dynamic structure factor. The static structure factor is obtained by integrating the dynamic structure factor with respect to ω along a path of constant Q. Hence, the scattering experiment actually integrates $S(Q,\omega)$ over all energy transfers and gets an ensemble averaged snap shot of the system at t=0.

Inelastic scattering takes place particularly due to the presence of light atoms such as hydrogen in the sample since the mass of hydrogen is comparable to that of the neutron. These scattering events affect the structure factors measured and corrections have to be made to account for their presence in systems containing light atoms. Inelasticity effects can be reduced by working with high neutron energies and low scattering angles. Pulsed neutron sources are ideally suited for such purposes and have opened up new experimental avenues for condensed matter research aimed at investigating structure in aqueous media. A pulsed neutron source not only produces intense neutron pulses but also allows scattering experiments to be performed using a spectrum of energies (or wavelengths). This implies fixed scattering geometries need to be used [53]. This is a very useful experimental setup for scattering experiments which require geometries with low

scattering angles.

The raw data collected from a scattering experiment is not useful and specific data corrections need to be done before the distinct term in the total structure factor can be obtained for further analysis.

4.1.4 Data Corrections

Data collected from a sample during a neutron scattering experiment needs to be corrected for several effects which will be outlined below. The procedures involved are standard. An in depth report of these data correction procedures are beyond the scope of this thesis. Information on all aspects of these correction procedures can be found in literature references [91, 92].

All scattering experiments reported in this thesis were performed on SANDALS, the small angle neutron diffractometer for amorphous and liquid samples at the pulsed neutron source ISIS, at the Rutherford Appleton Laboratory in the U.K. At the time when the experiments were performed, the instrument offered the following range of scattering angles (2θ) [3° - 31°] and neutron wavelengths [0.05$\mathring{A}$ - 4.5$\mathring{A}$].

The sample under investigation is housed in a can made from an alloy of Titanium (68%) and Zirconium (32%). This alloy has zero coherent scattering and hence no Bragg peaks are seen in the scattered intensity due to the can. This helps remove contributions from the can rather easily in the data correction procedures.

In a typical neutron scattering experiment four sets of data are collected.

- Background intensity
- Neutrons scattered from vanadium
- Neutrons scattered from the can housing the sample
- Neutrons scattered from the sample (+can)

Following is a step by step account of the procedures involved in determining the structure factor from the measured raw data:

- The scattered intensity (detector counts) is collected as a function of scattering angle. This intensity is then amalgamated into 14 groups. Each group is assigned to a specific scattering angle. Before this amalgamation procedure, noisy detectors are eliminated.

- Next for each detector group, the summed intensity is calculated as a function of the scattering vector $\mid \vec{Q} \mid$. The distance travelled by a neutron is calculated from the time of flight in order to calculate the value of $\mid \vec{Q} \mid$ for a given scattering angle. At this stage the incident and transmission spectra are also determined as a function of $\mid \vec{Q} \mid$.

- The transmission spectrum is then used to determine contributions from:

  1. multiple scattering events which arise due to a neutron being scattered by more than one nucleus AND
  2. attenuation which occurs due to absorption of some neutrons by the sample

  for the sample(+can), the can and Vanadium data.

- Intensity measurements from Vanadium are also corrected for noise and normalised to the number of scattering nuclei in the vanadium sample.

- Finally contributions from the can are subtracted from the intensity measurements from the sample(+can) and the background counts are subtracted from the vanadium data.

- The result is a scattering intensity which is a measure of the structure factor and is normalised to the vanadium data to get absolute intensity scales. The last normalisation involves dividing the entire intensity spectrum by the number of scattering nuclei in the sample itself.

Once these basic set of steps have been performed only one correction step remains. This is to do with the removal of self scattering terms. Measured total differential cross sections in an experiment include contributions from self scattering. These terms are difficult to subtract out especially in the case of light atoms such as hydrogen where inelastic scattering renders these self terms to be strongly dependent on the scattering angle and the neutron energy. Procedures to remove these terms can be found in the literature [92] and will not be elaborated here. These have been used in routine experiments for the past decade and provide the best estimate of the contribution of the self scattering terms in the sample. A summary of this approach will be presented once the technique of isotope substitution has been explained. It is important to emphasise at this point the importance of this correction procedure. Incomplete removal on the inelastic scattering contributions results in uncertainties in the quantitative analysis of the data at the partial radial distribution function level where coordination numbers are determined and variations in this function are used to deduce changes in local structure.

A simple flow chart (fig. 4.3) illustrates all the basic steps involved in a typical data correction procedure for experiments done on SANDALS.

The resulting experimental data after the corrections have been performed is essentially the interference term from the scattered intensity. It can either be Fourier transformed to yield the pair distribution function, g(r) or used in data modelling procedures to obtain structural models of the liquid which are consistent with the measured data.

The next two sections will explain how isotope substitution techniques have greatly enhanced the information content obtained from neutron scattering experiments and new data modelling strategies which provide unparallelled structural details of complex molecular liquids.

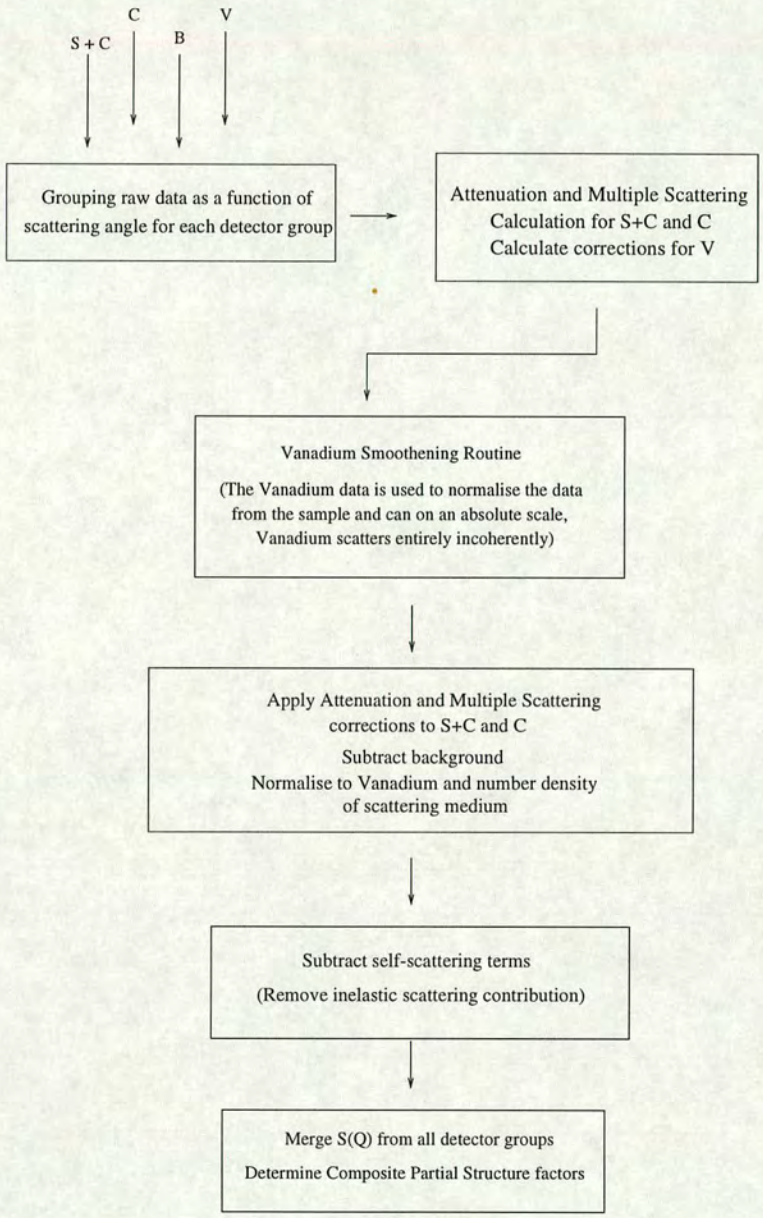

Figure 4.3: Correction factors applied to time-of-flight diffraction data collected on the SANDALS diffractometer at the pulsed neutron source ISIS, U.K. Here, S, C, V, B stand for the sample, can, vanadium and background respectively.

4.1.5 Isotope Substitution- The Technique

Perhaps, the most important aspect of neutron scattering is to do with the scattering materials themselves. The scattering length varies randomly across the periodic table but there is one element, hydrogen, whose isotope Deuterium has

a scattering length which is opposite in sign to that of hydrogen. The technique of *isotope substitution* which exploits this difference in scattering lengths between the two isotopes of hydrogen was discovered by Enderby *et al* about four decades ago [93]. Since the scattering of neutrons depends on the scattering length, experiments can be performed on chemically similar systems which have different isotopes. The scattered intensity is then different for each sample and depends on the response of the neutron probe to the isotopes. This technique allows the experimenter to essentially pin down the vantage point to the substituted atom in the liquid and survey the liquid environment around that point.

When the sample under investigation contains hydrogen this technique can be used to obtain the HH partial structure factor by performing a neutron diffraction experiment on three samples. The easiest way to illustrate this technique is to take the example of water. Three samples are used, light water (H_2O), heavy water (D_2O) and a 1:1 mixture of the two (HDO). Data are collected from each sample and routine corrections are performed as explained in the previous section. Three total structure factors are obtained;

$$F_1(Q) = c_{\mathrm{H}}^2 b_{\mathrm{H}}^2 [S_{\mathrm{HH}}(Q) - 1] + 2c_{\mathrm{O}} c_{\mathrm{H}} b_{\mathrm{O}} b_{\mathrm{H}} [S_{\mathrm{OH}}(Q) - 1] + c_{\mathrm{O}}^2 b_{\mathrm{O}}^2 [S_{\mathrm{OO}}(Q) - 1] \quad (4.18)$$

$$F_2(Q) = c_{\mathrm{D}}^2 b_{\mathrm{D}}^2 [S_{\mathrm{D}}(Q) - 1] + 2c_{\mathrm{O}} c_{\mathrm{D}} b_{\mathrm{O}} b_{\mathrm{D}} [S_{\mathrm{OD}}(Q) - 1] + c_{\mathrm{O}}^2 b_{\mathrm{O}}^2 [S_{\mathrm{OO}}(Q) - 1] \quad (4.19)$$

$$F_3(Q) = c_{\mathrm{H}}^2 b_{\mathrm{HD}}^2 [S_{\mathrm{HH}}(Q) - 1] + 2c_{\mathrm{O}} c_{\mathrm{H}} b_{\mathrm{O}} b_{\mathrm{HD}} [S_{\mathrm{OH}}(Q) - 1] + c_{\mathrm{O}}^2 b_{\mathrm{O}}^2 [S_{\mathrm{OO}}(Q) - 1] \quad (4.20)$$

Here in the case of the mixture the atomic fraction of hydrogens remains the same, since a 1:1 mixture of light and heavy water is used. However the scattering length needs to account for the in-solution isotopic exchange which occurs. Hence the scattering length in the mixture denoted by b_{HD} is a linear combination of the

scattering lengths of H and D respectively. Defining x as the fraction of light hydrogen in the mixture sample;

$$b_{\mathrm{HD}} = xb_{\mathrm{H}} + (1-x)b_{\mathrm{D}} \tag{4.21}$$

Solving equations 4.17 - 4.19 simultaneously yields each of the three partial structure factors. It is a neat idea which has tremendous use in structural studies of aqueous mixtures. Clearly, such an analysis assumes that there is no difference between the structures of H_2O, D_2O and HDO. Hence structural data obtained from the isotope substitution technique will produce less detail about any fine structure present in the water radial distribution functions since these structures do differ slightly. Further light water has a temperature of maximum density of 4°C where as heavy water has a corresponding temperature of around 11°C. Hence is is important to work at temperatures which are not close to these values since the structure of the two forms of water might be different.

Consider next a slightly more complex system, a mixture of methanol and water. Carbon and Oxygen do not have isotopes which can be used to perform isotope substitution experiments. Fortunately, the methyl hydrogens provide a unique handle on the methanol correlations as shall be demonstrated shortly. Again, one obtains a total structure factor in a scattering experiment. Three samples need to made and scattering data from each is required. Isotope substitution can be performed only on the methyl hydrogens. This results in the following samples: CH_3OD in D_2O, CD_3OD in D_2O and a 1:1 mixture of CH_3OD/CD_3OD in D_2O. Heavy water is used in this case because structural correlations between the methyl groups are sought and Deuterium has a significantly lower incoherent cross section as compared to hydrogen. Hence inelastic corrections are minimised.

The resulting total structure factor is:

$$F(Q) = c_{\mathrm{X}}^2 b_{\mathrm{X}}^2[S_{\mathrm{XX}}(Q)-1] + 2c_{\mathrm{X}}c_{\mathrm{H}}b_{\mathrm{X}}b_{\mathrm{H}}[S_{\mathrm{XH}}(Q)-1] + c_{\mathrm{H}}^2 b_{\mathrm{H}}^2[S_{\mathrm{HH}}(Q)-1] \tag{4.22}$$

Here the label X refers to unsubstituted atoms (Carbon, Oxygen and hydroxyl Deuterium) whereas the label H refers to substituted atoms (methyl hydrogens). Note that $S_{XX}(Q)$-1 and $S_{XH}(Q)$-1 are composite partial structure factors (CPSF) and are a neutron weighted average of several partial structure factors,

$$S_{\mathrm{XX}}(Q) - 1 = \frac{\sum_{\alpha \neq \mathrm{H}, \beta \neq \mathrm{H}} c_\alpha c_\beta b_\alpha b_\beta S_{\alpha\beta}(Q) - 1}{c_{\mathrm{x}} b_{\mathrm{X}}} \tag{4.23}$$

$$S_{\mathrm{XH}}(Q) - 1 = \frac{\sum_{\alpha \neq \mathrm{H}} c_\alpha b_\alpha S_{\alpha\mathrm{H}}(Q) - 1}{c_{\mathrm{X}}^2 b_{\mathrm{X}}^2} \tag{4.24}$$

A similar set of experiments can be performed with isotope substitutions on the hydroxyl hydrogens of methanol and water or on all hydrogens in the mixture. A total of nine composite partial structure factors are then obtained. Clearly the single most important quantity obtained from the above mentioned experiments is the HH partial structure factor. For the case of water all partial structure factors are obtained where as in the case of the mixture a huge amount of information remains hidden in the composite partial structure factors. Further even the HH partial structure factor cannot be assigned entirely to the HH correlations of water when the concentration of a solute containing hydrogens from the hydroxyl group is high.

Hence alternative data modelling techniques are absolutely crucial to get detailed information on all the partial radial distribution functions and intermolecular orientations which remain hidden in the composite partial structure factors mentioned above. The next section introduces such data modelling strategies which are being adopted by researchers engaged in simulations and experiments.

One point still remains to be addressed before leaving this section. It was mentioned earlier that inelastic scattering has to be subtracted from the measured intensity before any further analysis can be done. Isotope substitution is extremely useful in determine the self-scattering contribution to the total scattered intensity. A detailed report on the approach can be found elsewhere [92] and a

synopsis is presented here.

It was mentioned that the total structure factor measured in a scattering experiment contains contribution from the self scattering terms and the interference (distinct) terms. The self scattering terms have to be subtracted out since they contain no positional information. However, inelastic scattering, especially from light atoms like hydrogen make the problem quite complicated. Isotope substitution enables the determination of the self scattering contribution reasonably straightforward. The method requires the calculation of the self scattering term for a given set of three solutions (H_2O, D_2O and a mixture of the two) by taking an appropriate linear combination of the three total structure factors. Such an operation results in the XX composite partial structure factor and a residual term which is the self scattering term. This term forms a slowly varying background on which the XX function oscillates. The basic idea involves fitting a polynomial to this background but taking care that the characteristic oscillation of the XX function are not represented in the fit. This fit is a measure of the single atom self scattering term. For each solution, a correction factor is applied to this self scattering contribution to account for the atomic fraction of hydrogens which have the largest contribution the self scattering term. This is at once obvious when the incoherent scattering cross section for hydrogen and deuterium are compared (see table 4.1). Finally, the self scattering contribution for each solution is subtracted from the total structure factor. The resulting function is the distinct structure factor. Once the self scattering terms have been removed, the data are merged to yield the structure factor as a function of the scattering vector.

4.2 Data Modelling Technique

Understanding liquid structure has been a challenge for experimentalists and computational physicists and chemists alike. Part of the difficulty arises from the fact that the sheer nature of the material in question is disordered and structure implies a distribution of particles and the problem is unlike the determination

Element	Scattering length (10^{-15}m)	$d\sigma_{coh}$ ($10^{-28}m^2$)	$d\sigma_{inc}$ ($10^{-28}m^2$)
Hydrogen (H)	-3.740	1.758	79.7
Deuterium (D)	6.674	5.597	2.0
Carbon (C)	6.648	5.6	< 0.02
Oxygen (O)	5.830	4.23	< 0.02

Table 4.1: Scattering lengths and coherent and incoherent scattering cross-sections for some natural elements [53].

of crystal structures. Considerable progress has been made however in both areas of investigation. Experimentalists have obtained significant amounts of data with neutron scattering using isotope substitution techniques. However even clever isotope substitutions do not go a long way in providing structural details simply because almost all liquids are molecular and not all elements have isotopes which are useful in the above mentioned experiments. As has been shown earlier one is left with composite structure factors. There is very little one can do with this data. The true structure of a liquid is not really contained in the partial radial distribution functions which are in principle accessible via a Fourier transform of the partial structure factors (if available as in the case of water). These distribution functions are averaged over intermolecular orientations and vital information is lost. In terms of intermolecular orientations, the definition of a radial distribution function [94] is:

$$g(r) = \langle g(\vec{r}\omega_1\omega_2)\rangle_{\omega_1\omega_2} \tag{4.25}$$

Here $\vec{r}$ is a vector joining the centres of mass of two molecules and ω_i is the orientation of the ith (i=1,2) molecule in terms of the (ϕ_i,θ_i,χ_i) Euler angles defined with respect to a coordinate system local to the molecule.

Indeed, it is the intermolecular orientational pair correlation function, $g(\vec{r}\omega_1\omega_2)$ (OPCF) that is required to generate a realistic three dimensional picture of the structure of molecular liquids. The OPCF is thus a function of nine variables. In order to visualise the OPCF, the local reference frame of one molecule is made to coincide with the laboratory frame and the orientations of the second molecule are defined with respect to these axes [95]. The OPCF is then a function of six variables as shown in the fig. 4.4.

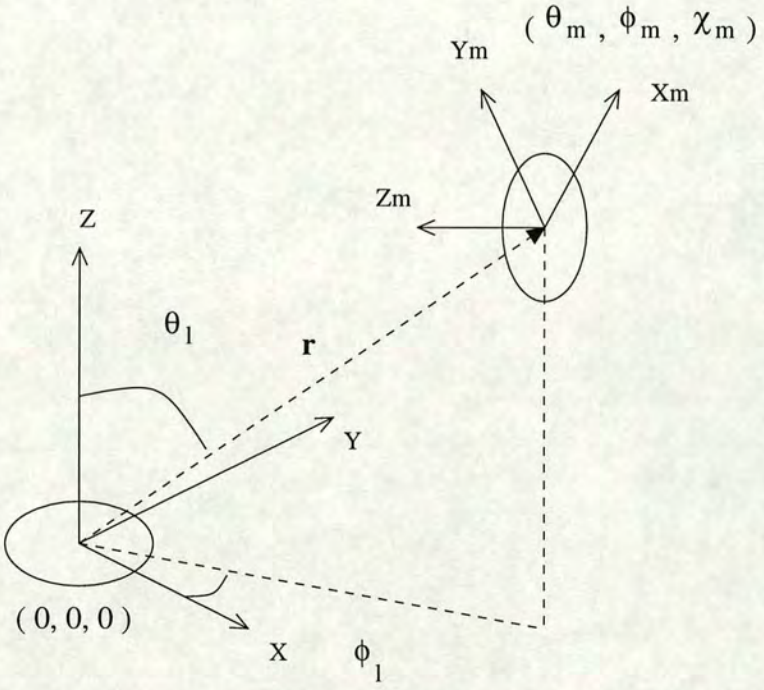

Figure 4.4: Definition of orientational coordinates of two molecules in the laboratory reference frame [95]. Molecule 1 is at the origin and molecule 2 is at a distance $(\vec{r}, \theta_1, \phi_1)$ and orientation $(\phi_m, \theta_m, \chi_m)$ from the origin.

Determining the OPCF directly from simulations is an impossible task since the number of data points required are large and well outside computer memory capabilities [95]. However, the OPCF can be evaluated using a spherical harmonic expansion [94] where the spherical harmonics play the same role in three dimensional space as sine and cosine functions do in two dimensional space. The theory behind spherical harmonic expansion of the OPCF is beyond the scope of this thesis.

The coefficients of the spherical harmonic expansion are best obtained from a simulated model of the molecular liquid with the constraint that the model should also reproduce the measured structure factors from a diffraction experiment. This would ensure that the intermolecular orientations are produced from realistic molecular configurations in the model. The empirical potential structure refinement (EPSR) technique was developed with these objectives in minds in the mid 1990's by Soper [56].

The basic idea behind the EPSR technique is to set up an ensemble of the molecules of the liquid (or liquid mixture as the case may be) whose simulated (composite)[§] structure factors agree with the experimentally measured data as closely as possible.

A standard Monte Carlo simulation is performed on a NVT (fixed number of molecules, volume and temperature) system fixed at the experimental density. The initial run in the simulation is performed using standard literature reference potentials for the liquid(s) under study. The reference potential accounts for all electrostatic interactions and takes care of any unphysical overlap between atoms that might occur during the course of the simulation. Molecular geometries are preserved by defining intramolecular harmonic potentials. This initial run brings the system into a realistic region of configuration space.

At this point all the (composite) partial structure factors accessible via the diffraction experiment are calculated from the simulated model. The difference between the measured and the simulated structure factors is calculated. This difference is Fourier transformed to r-space and is called the residual, $\Delta_{\alpha\beta}(r)$.

The residual is used to bias the reference potentials to drive the simulated (composite) partial structure factors in closer agreement with those measured from the experiment. The perturbation derived from the residual is calculated from

[§]For the rest of this chapter, the term composite is presented in brackets to remind the reader that it is not always possible to extract the partial structure factors from a diffraction experiment using isotope substitution.

the *potential of mean force* which is defined as:

$$\Psi_{\alpha\beta}(r) = -kTln[g_{\alpha\beta}(r)] \tag{4.26}$$

This equation can be interpreted by inverting it to:

$$g_{\alpha\beta}(r) = exp^{-kT\Psi_{\alpha\beta}(r)} \tag{4.27}$$

This expresses the probability that two particles, α,β, interacting via a potential of $\Psi_{\alpha\beta}(r)$ should be found in thermal equilibrium separated by a distance r. It is important to note that this potential is not a two body interaction potential since it takes into account the presence of all other particles in the system.

The perturbation which is added to the reference potential ($U^0_{\alpha\beta}$(r)) is called the empirical potential and is derived as:

$$U^{EP}_{\alpha\beta}(r) = -kTln[1 + \frac{\Delta_{\alpha\beta}(r)}{g^{sim}_{\alpha\beta}(r)}] \tag{4.28}$$

The new reference potential now becomes:

$$U^{N}_{\alpha\beta}(r) = U^{0}_{\alpha\beta}(r) + U^{EP}_{\alpha\beta}(r) \tag{4.29}$$

This perturbed potential is fed back into the simulation and the particles are moved. At the end of one interaction which involves at least one attempted translation and rotation for every molecule in the box, the new set of molecular coordinates is again used to generate the (composite) partial structure factors. A new perturbation is derived and is applied to the previous potential. This process is carried on iteratively until the simulated and measured (composite) partial structure factors agree as closely as possible and no further improvements in fits are possible. The simulation then proceeds to calculate specific quantities such

as the partial radial distribution functions and the spherical harmonic coefficients after one iteration. The information is stored and averaged over several thousand particle configurations. It is important to note that while such an interrogation of the data is done, the (composite) site-site potentials are still monitored after each iteration and modified if necessary via perturbations as described earlier. This provides a reality check on the particle configurations collected for the averaging process. Clearly, it is critical to have as many (composite) partial structure as possible to constrain the simulation. This is the key idea really. Since the refinement technique simultaneously fits several (composite) partial structure factors, it is less likely to introduce effects due to systematic errors. This is especially crucial when the removal of inelastic effects from the measured diffraction data are imperfect and subject to the order of the polynomial used to model the self scattering term as was mentioned earlier.

The EPSR technique has been used to model the diffraction data collected from the experiments conducted on SANDALS on the methanol-water mixtures. The results obtained from this analysis will be the theme in the next two chapters.

Chapter 5

A Concentrated Amphiphile-Water Mixture

The Raman frequency shifts for the C-O and the C-H stretch modes of methanol as a function of dilution in water presented earlier indicated that in the concentrated regime i.e. for methanol mole fractions greater than 0.7, the water preferentially hydrogen bonded to the hydroxyl group of methanol. The spectral shifts were interpreted as indicative of methanol molecules being pushed closer towards each other due to the presence of water.

To obtain a structural confirmation of the interpretations from the Raman data, a 0.7 mole fraction mixture of methanol in water was chosen to investigate what types of interactions exist between the methanol molecules, given that there is a dominant polar intermolecular interaction between methanol and water.

The neutron scattering experiments mentioned in the preceding chapter were performed at the ISIS spallation source. The diffraction data was modelled using the EPSR technique.

5.1 Experimental Details

Isotopically substituted, but otherwise similar mixtures of methanol in water were prepared with the correct methanol : water molecular ratio (7:3) as shown below:

1. CD_3OD in D_2O
2. CH_3OD in D_2O
3. A 50% mixture of 1 and 2.
4. CD_3OH in H_2O
5. A 50% mixture of 1 and 4
6. CH_3OH in H_2O
7. A 50% mixture of 1 and 6.

The solute-solute partial structure factor was obtained by isotope substitution on the methyl hydrogens using solutions 1,2 and 3. Isotope substitution on the hydroxyl hydrogens of water and methanol as indicated in solutions 1,4 and 5 give correlations between the hydroxyl hydrogens. Finally, solutions 1,6 and 7 provide a measure of the correlations between all the hydrogens in the solutions. Flat plate Titanium-Zirconium cells were used to house the samples. Data collected from each sample at 25°C (± 1°C) were corrected using standard data correction procedures detailed in the preceding chapter. Each of these three sets of solutions resulted in three composite partial structure factors [92], viz: $S_{HH}(Q)$-1, $S_{XH}(Q)$-1 and $S_{XX}(Q)$-1. Here, H corresponds to the labelled hydrogen and X corresponds to the remaining unlabelled atoms. The composite partial structure factors are a linear combination of several weighted partial structure factors corresponding to the various atomic species in the mixture. Tables 5.1, 5.2 and 5.3 give all the intermolecular weights for the nine composite partial structure factors obtained from the neutron scattering experiment.

XX Weights	C	O	H	H_W
C	0.05920			
O	0.14766	0.09207		
H	0.11876	0.14811	0.05956	
H_W	0.1018	0.12695	0.10211	0.04376
XH Weights	C	O	H	H_W
M	0.24332	0.30343	0.24405	0.20919
HH Weights	M			
M	1			

Table 5.1: Intermolecular weights for the 7:3 methanol-water mixture where substitutions are made on the methyl hydrogens. The atom labels M, C, O and H refer to methanol methyl hydrogen, carbon, oxygen and hydroxyl hydrogen respectively. The atom labels O_W and H_W indicate water oxygen and hydrogen. Here contributions from O and O_W are grouped together under the heading 'O'.

XX Weights	C	O	M
C	0.03619		
O	0.09028	0.05629	
M	0.21782	0.27162	0.32771
XH Weights	**C**	**O**	**M**
H	0.10244	0.12775	0.30825
H_W	0.08781	0.1095	0.26421
HH Weights	**H**	**H_W**	
H	0.28994		
H_W	0.49704	0.21302	

Table 5.2: Intermolecular weights for the 7:3 methanol-water mixture where substitutions are made on the methanol hydroxyl hydrogen as well as the water hydroxyl hydrogen. The atom labels are as mentioned in table 5.1. Here contributions from O and O_W are grouped together are grouped together under the heading 'O'.

XX Weights	C	O	
C	0.19805		
O	0.49394	0.30799	
XH Weights	C	O	
M	0.27487	0.34278	
H	0.09162	0.11426	
H_W	0.07853	0.09793	
HH Weights	M	H	H_W
M	0.38149		
H	0.25433	0.04239	
H_W	0.21799	0.07266	0.03114

Table 5.3: Intermolecular weights for the 7:3 methanol-water mixture where substitutions are made on all hydrogens, i.e. methyl and hydroxyl. The atom labels are as mentioned in table 5.1. Here contributions from O and O_W are grouped together are grouped together under the heading 'O'.

5.2 Data Modelling

The nine composite partial structure factors were used in an EPSR refinement of the measured data to obtain all the partial radial distribution functions and orientational correlations. A computer model of the mixture was set up using 245 methanol molecules and 105 water molecules. The ratio was chosen to maintain the correct mole-fraction of methanol as used in the actual experiment and a cubic box of of length 26.77 $\AA$ was used to obtain the correct density of the liquid mixture. The maximum radius values for which reliable diffraction data could be derived from the experiments are of the order of 10 $\AA$ and this set a natural length scale for the box size.

The initial run in the standard monte carlo simulation [96] was performed to bring the model system into an equilibrium configuration using literature reference potentials to determine the interactions between the molecular species in the mixture. In the present case, the SPC/E potential of Berendsen *et al* [97] was used for the water molecules and the H1 potential of Haughney *et al* [98] was used for the methanol molecules. Methanol-water interactions were modelled using standard Lorentz-Berthelot mixing rules [96]. These provide Lennard-Jones parameters which control how closely the two molecules can approach each other. The reference potentials were used to introduce as much prior knowledge into the simulation as possible. The potential was applied to all pairs of atoms on distinct molecules.

The EPSR algorithm was then executed on this model system. This refinement technique aims at generating realistic three dimensional molecular assemblies of the system under investigation which are consistent with the measured data. It is not implemented with the idea of generating realistic intermolecular potentials as well. All contributions to intermolecular interactions due to electrostatic interactions and hard core overlap due to all sites on each molecule (ten for methanol and three for water) are already accounted for by the input potentials. After initial equilibrium is reached the simulation proceeds to calculate the composite

partial structure factors which were also measured by the diffraction experiment. The nine composite partial structure factors from the simulation and experiment are compared. An iterative feedback loop was then set up to refine the potentials using perturbations derived from the difference between the measured and simulated composite partial structure factors [56] as explained in the preceding chapter. This iterative procedure continues until the residual, $\Delta_{\alpha\beta}(r)$ (see details in chapter 4), which is the difference between the simulated and measured composite structure factors, does not contain any obvious oscillatory structure. On the other hand, if the residual is nonzero and contains a slowly varying component then it is unlikely that the fits can be improved further since the residual term would then correspond to structure at unphysically short distances. This forms the guiding criterion to determine when to stop the fitting procedure [99].

The best possible fits obtained for the 7:3 mixture of methanol in water using the EPSR method are shown in fig. 5.1. The fits deviate slightly at low Q values, this is due to difficulties encountered in removing the inelastic scattering. However, these deviations correspond to low Q values and do not affect correlations at intermolecular distances which are of interest in the present work.

The simulation now proceeds to calculate quantities of interest such as the partial radial distribution functions and orientational correlations between molecular centres of both methanol and water (carbon atom for methanol, oxygen atom for water). Details of this procedure have been provided in the preceding chapter. Also shown (see fig. 5.2) are representative EPSR potentials for the case where H/D substitution is performed on the hydroxyl hydrogens at the present concentration. It is important to note that EPSR does not aim to generate realistic potentials but uses the diffraction data to generate empirical potentials to generate the measured composite structure factors which are consistent with the diffraction data.

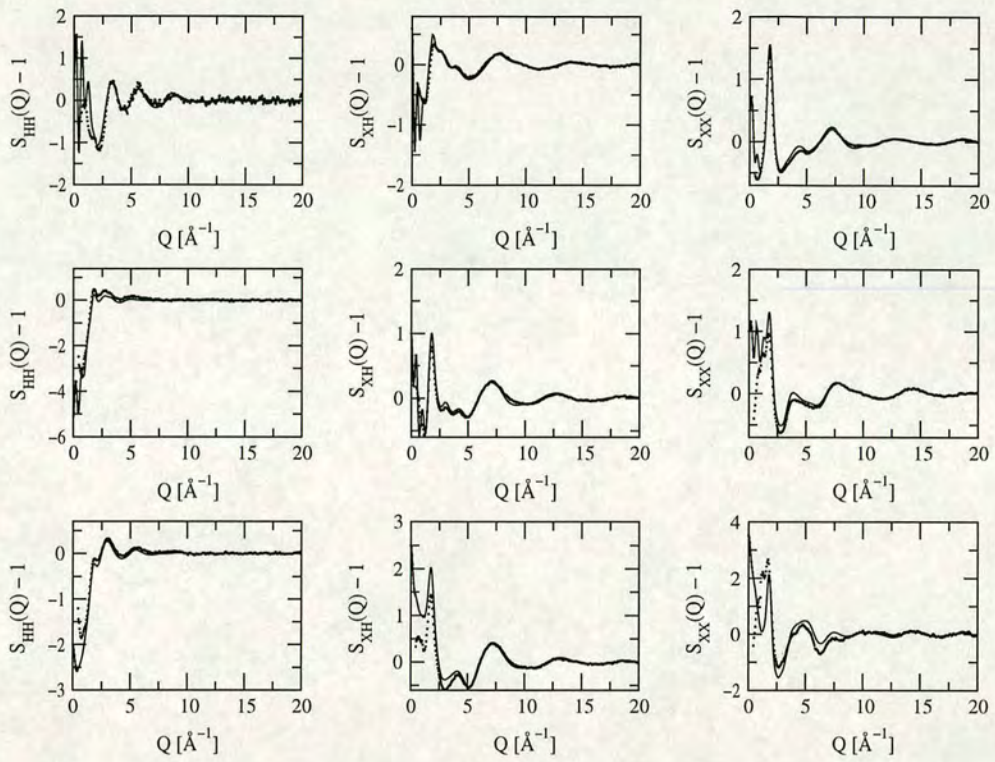

Figure 5.1: HH, XH and XX composite partial structure factors for methanol-water mixtures (70% mole methanol), for the case where H/D substitution is performed on: (a) methyl hydrogen atoms (samples 1, 6 and 7 in text) shown in the 1st row, (b) hydroxyl hydrogen atoms(samples 1, 2 and 3 in text) shown in the 2nd row and all (c) hydrogen atoms (samples 1, 4 and 5 in text) shown in the 3rd row. EPSR fits to the measured structure factors are shown as the solid circles. Note that the EPSR simulation is fit simultaneously to all 9 composite structure factors. The lack of fit in some regions, particularly for the XX function, is believed to arise from the difficulty in ensuring all the inelastic neutron scattering has been removed from the data prior to structure refinement.

5.3 Results

Carbon-oxygen stretch frequency shifts presented earlier indicate that at 0.7 mole fraction of methanol in water, the water molecules hydrogen bond to the methanol hydroxyl groups. Such a deduction was made on comparing Raman frequencies

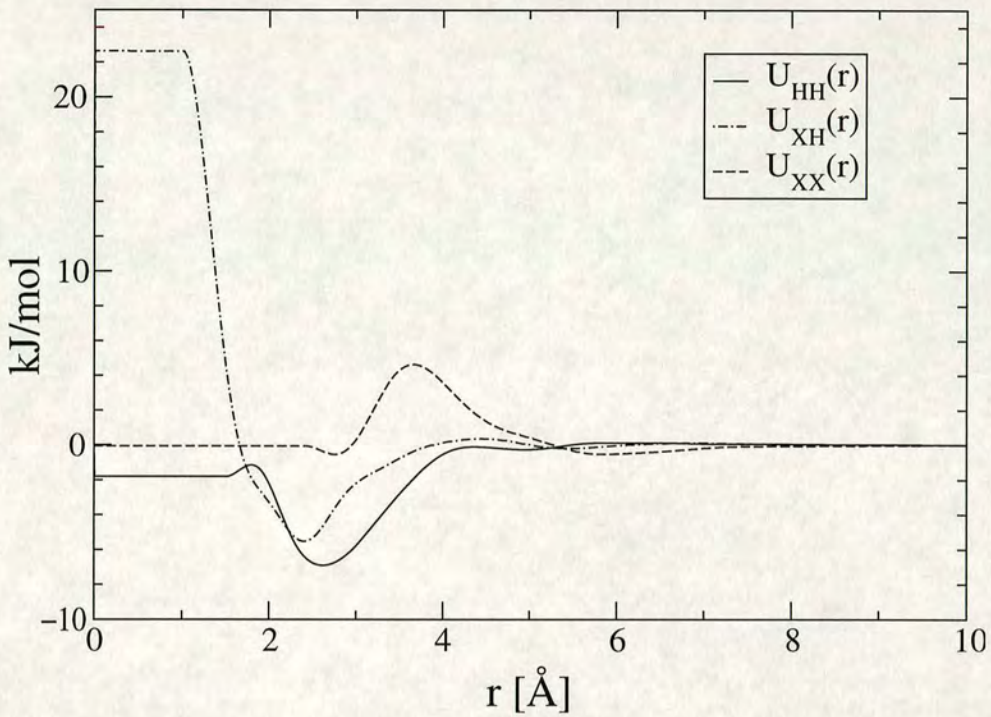

Figure 5.2: Accumulated HH, XH and XX composite *empirical potentials* for methanol-water mixtures (70% mole methanol), for the case where H/D substitution is performed on hydroxyl hydrogen atoms (samples 1, 2 and 3 in text). Note that these are not realistic potentials but take into account the presence of several atomic species, hence the term composite.

from the 0.7 mole fraction mixture with those of pure methanol. To make similar comparisons for the neutron data, information on pure methanol is required. A neutron diffraction experiment on methanol was performed by Yamaguchi *et al* [82, 100]. Their results will be used in the present discussion for all comparisons. However, the EPSR analysis performed by the authors is based in a molecular coordinate reference frame where the methanol oxygen is defined as the origin. This simulation was hence rerun using the methanol carbon as the origin, using the earlier experimental data in order to compare the data between the mixture and pure methanol.

5.3.1 Hydrogen Bond Interactions

To determine to what extent the water molecules hydrogen bond with the methanol molecules several partial radial distribution functions (g(r)'s) are required. These are shown in fig. 5.3.

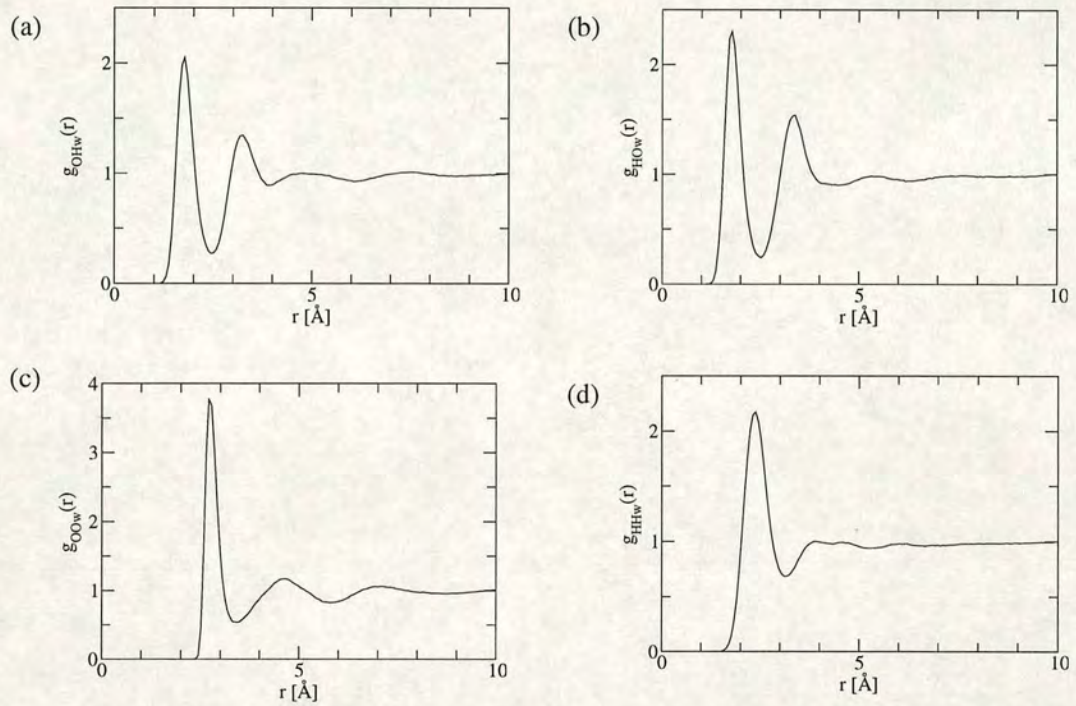

Figure 5.3: (a)OHw, (b)HOw, (c)OOw and (d)HHw partial radial distribution functions determined by the EPSR procedure for the 7:3 methanol-water mixture. These functions provide information on methanol-water hydrogen bond interactions.

To begin with $g_{OHw}(r)$ and $g_{HOw}(r)$ are interrogated. The peak around 1.75 $\AA$ is due to hydrogen bonds between methanol and water molecules. Integration under each of these peaks results in a first shell coordination number* (see table 5.4) which shows that on average there is a greater probability that a water molecule will hydrogen bond to the oxygen lone pairs than to the hydrogen of a methanol hydroxyl. This ties up with the inference made from the Raman frequency shifts where the red shift noted in the C-O stretch frequency at a similar concentration

*The errors in the coordination numbers are shown in the respective tables.

(0.7 mole fraction of methanol in water) was attributed to preferential hydrogen bonds between the methanol oxygen lone pair and water molecules. Examination of $g_{OO_w}(r)$ revealed that the hydroxyl group of methanol forms the focal point of water cluster formation. Integration under the first and second peak of this radial distribution function yielded coordination numbers of around 1 and 3 respectively. Also, the second peak is around 4.6 $\AA$ indicating that the water molecules are strongly cordinated around the hydroxyl group.

At this concentration, there are still some methanol-methanol hydrogen bonds. This is apparent from the $g_{OH}(r)$ (fig. 5.5), from which a coordination number of about 0.6 is obtained. This value is less than the corresponding value of 0.9 for pure methanol for the same radial distribution function, i.e. $g_{OH}(r)$ (see table 5.5).

The water molecules also hydrogen bond with each other. This is seen from the coordination number obtained from $g_{O_wH_w}(r)$ (see fig. 5.6). Again this is less than one. For pure water this number (table 5.6) is closer to 2 [99]. Water molecules form on average dimers, evidence for which is provided by the coordination number of around 1.2 obtained from $g_{O_wO_w}(r)$ also shown in fig. 5.6. In pure water the corresponding coordination numbers (table 5.6) is around 4.5 [99][†]. The position of the second coordination shell is taken as evidence for the extended tetrahedral network of pure water. In the 7:3 mixture this positions is at 4.5 $\AA$ just like in pure water. Clearly, the water structure at the second neighbour level still persists, even though there is very little water in the mixture. The drop in coordination number in the second shell to 3 in this mixture from around 18 [99]as observed in pure water basically reflects this decrease in concentration.

A comparison of the coordination numbers obtained from $g_{OO}(r)$ and $g_{HH}(r)$ in fig. 5.5 (1.3 and 1.5 respectively) with those of pure methanol (1.9 and 2.1 respectively, table 5.5) imply that the water molecules compete with other methanol molecules to solvate the alcohol hydroxyl group. Hence the picture that

[†]While the original paper does not mention coordination numbers, the original data were examined to determine the same to enable comparisons with values obtained in this work.

emerges is that of a network of hydrogens bonds which are mixed, with interactions between methanol molecules, water molecules as well as between water and methanol molecules. In pure methanol, the molecules hydrogen bond to form chains [100, 82]. The water molecules disturb this structure of methanol. But there is still not enough water to completely hydrate the hydroxyl group of the alcohol. This is still a significantly concentrated mixture with lots of methanol. Qualitative deductions made from the Raman data indicate that there is not much change in the chain structure of methanol up to 0.7 mole fraction of methanol in water with water molecules hydrating only the chain ends. At the present concentration, while there still exist chains of pure methanol, the average chain length is drastically reduced to about 2 molecules per chain compared to the value of around 5 for pure methanol (see fig. 5.4). The chain lengths were determined using the same algorithm as was done for pure methanol by Yamaguchi *et al* [100] where, the number of molecules in a chain were determined by starting from a single molecule and counting along a chain until either another single bonded molecule is encountered or the next molecule in the chain has three or more bonds. It may well be that at higher concentrations of methanol ($x \rightarrow 1$) the water molecules indeed hydrogen bond to chain ends. Curiously, the Raman data also suggested that the methanol molecules may be closely packed in the mixture up to concentrations of about 0.7 mole fraction of methanol in water. Do the methanol molecules respond to the presence of the water molecules if at all besides the usual hydrogen bond interactions? This issue is addressed next.

5.3.2 Methanol - Methanol interactions

Since the carbon atom has been used to define the methanol molecular centre, $g_{CC}(r)$ can provide information on inter-methanol interactions. Interestingly, this function shown in fig 5.7a moves inwards to lower r values. Integration under the first peak yields a coordination number of nearly 11 (10.8) for pure methanol (see table 5.5) and about 9 (8.85) for the 7:3 mixture. To determine whether the presence of water results in a preferential inter methanol interaction via the

Correlation	Atomic density ρ atoms per $\AA^3$	R_{min} $\AA$	R_{max} $\AA$	Coordination number 25°C (atoms)
CC	0.013	3.0	5.51	8.85 ± 0.27
CO	0.013	2.5	4.33	3.7 ± 0.12
	0.013	4.33	6.29	9.16 ± 0.19
OO	0.013	2.0	3.41	1.29 ± 0.1
OH	0.013	1.0	2.59	0.63 ± 0.05
HH	0.013	1.5	3.31	1.54 ± 0.1
CO_w	0.005	2.5	4.8	2.2 ± 0.1
CH_w	0.011	2.0	2.97	0.43 ± 0.04
	0.011	2.97	5.28	5.9 ± 0.15
OO_w	0.005	2.0	3.45	0.85 ± 0.05
	0.005	3.45	5.81	3.1 ± 0.1
OH_w	0.011	1.0	2.49	0.54 ± 0.05
	0.011	2.49	3.96	2.1 ± 0.1
HO_w	0.005	1.0	2.54	0.27 ± 0.03
	0.005	2.54	4.48	1.6 ± 0.08
HH_w	0.011	1.5	3.16	1.5 ± 0.14
O_wO_w	0.005	2.0	3.56	1.15 ± 0.14
	0.005	3.56	5.75	3.0 ± 0.23
O_wH_w	0.011	1.0	2.43	0.5 ± 0.07
H_wH_w	0.06	1.0	3.09	1.4 ± 0.1

Table 5.4: Coordination numbers obtained from the integration of the peaks observed in the partial pair distribution functions of the mixture at 25° obtained from the EPSR analysis.

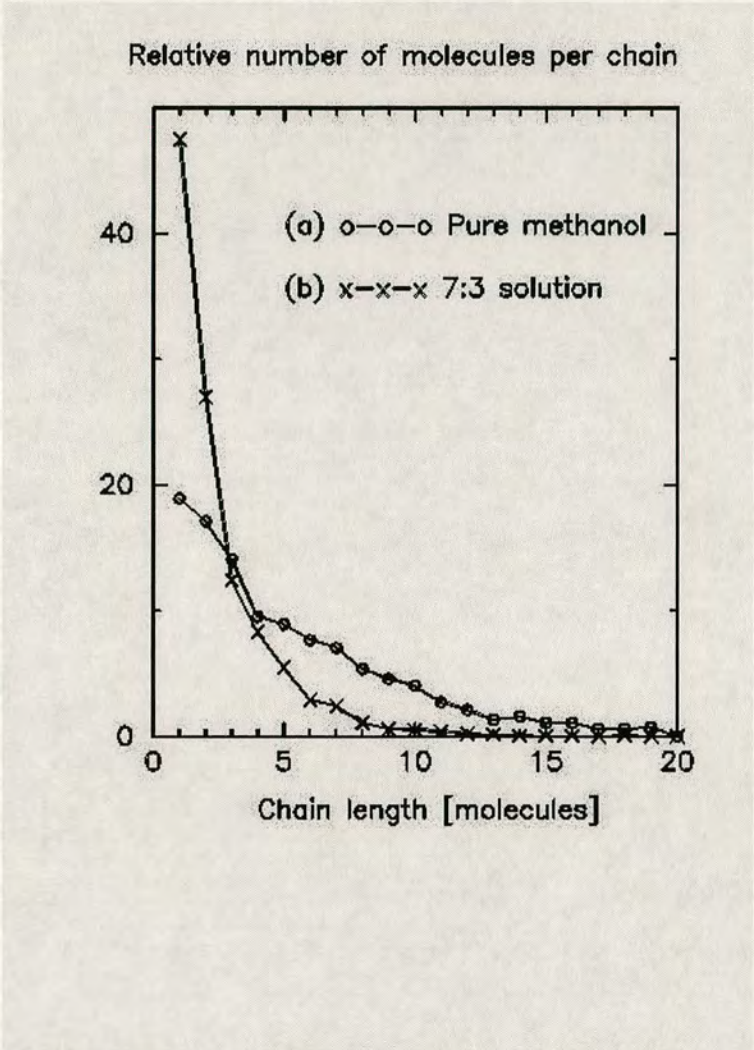

Figure 5.4: Distribution of methanol chain lengths in pure methanol [100, 82] and in the 7:3 mixture.

methyl groups, it is important to determine how many water molecules hydrate a methanol molecule on average.

This is achieved by examining the correlations between the methanol carbon and the water oxygen, $g_{COw}(r)$ shown in fig 5.8. A coordination number of around 2 is obtained. Since the water molecules interfere with inter methanol hydrogen bond interactions, it can be concluded that these water molecules in the first coordination shell around a reference carbon would be preferentially involved in hydrogen bond interactions with the methanol hydroxyl group. This observation

Correlation	Atomic density ρ atoms per $\AA^3$	R_{min} $\AA$	R_{max} $\AA$	Coordination number 25°C (atoms)
CC	0.0147	3.0	5.66	10.8 ± 0.28
CO	0.0147	2.5	4.45	4.84 ± 0.13
	0.0147	4.45	6.02	7.61 ± 0.17
OO	0.0147	2.0	3.48	1.92 ± 0.12
OH	0.0147	1.0	2.62	0.92 ± 0.06
HH	0.0147	1.5	3.28	2.1 ± 0.1

Table 5.5: Coordination numbers obtained from the integration of the peaks observed in the partial pair distribution functions of methanol [82] at 25° obtained from the EPSR analysis.

Correlation	Atomic density ρ atoms per $\AA^3$	R_{min} $\AA$	R_{max} $\AA$	Coordination number 25°C (atoms)
O_wO_w	0.033	2.0	3.4	4.6 ± 0.1
	0.033	3.4	5.58	18.6 ± 0.3
O_wH_w	0.066	1.0	2.4	1.8 ± 0.06

Table 5.6: Coordination numbers obtained from the integration of the peaks observed in the partial pair distribution functions of pure water [99].

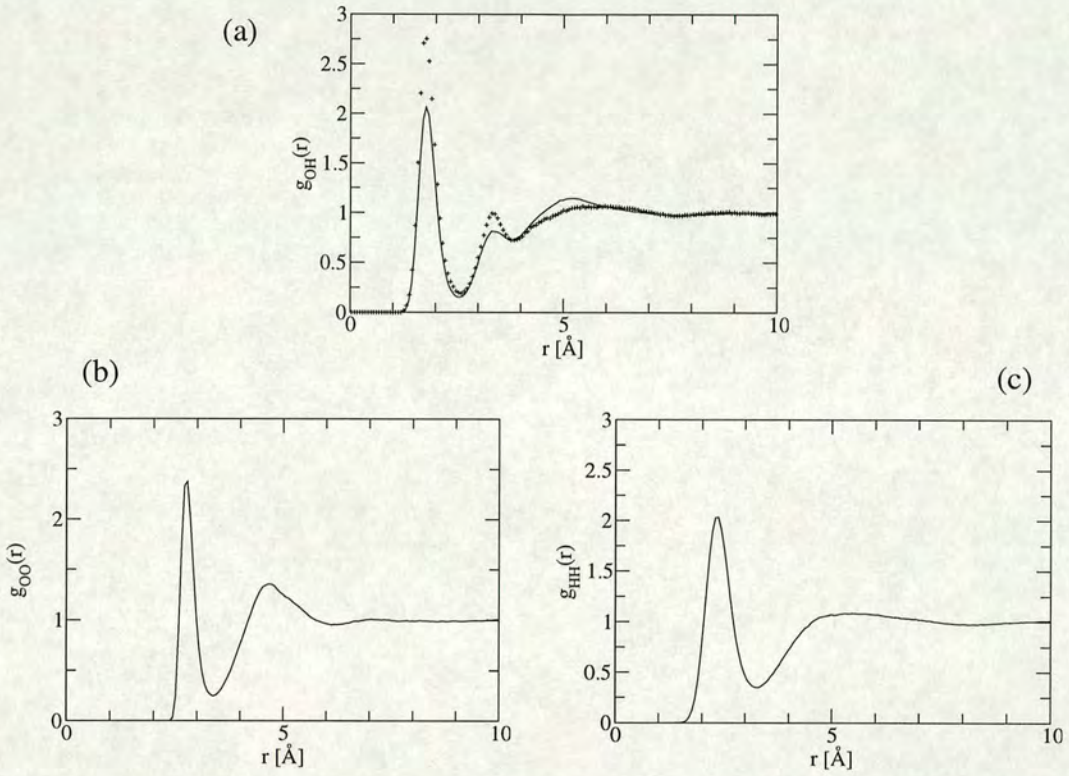

Figure 5.5: (a)OH, (b)OO and (c)HH and partial radial distribution functions determined by the EPSR procedure for the 7:3 methanol-water mixture. These functions provide information on methanol-methanol hydrogen bond interactions. Also shown in (a) is the OH function (+) for pure methanol.

suggests that if there is any increased association between the methanol molecules it should be via the methyl groups. To ascertain whether this is true, a ratio of the two coordination numbers N_{COw}/N_{CC} is considered. This ratio is then compared with the ratio of the atomic fraction of Ow and C in the mixture. Thus:

$$\frac{N_{COw}}{N_{CC}} = 0.24 < \frac{Ow}{C} = 0.43$$

This comparison shows that the methanol molecules prefer to have other methanol molecules near by rather than water molecules.

This preferential interaction also shows up in $g_{CO}(r)$, shown in fig 5.7b. The first peak of this function can be attributed to inter molecular contacts of two

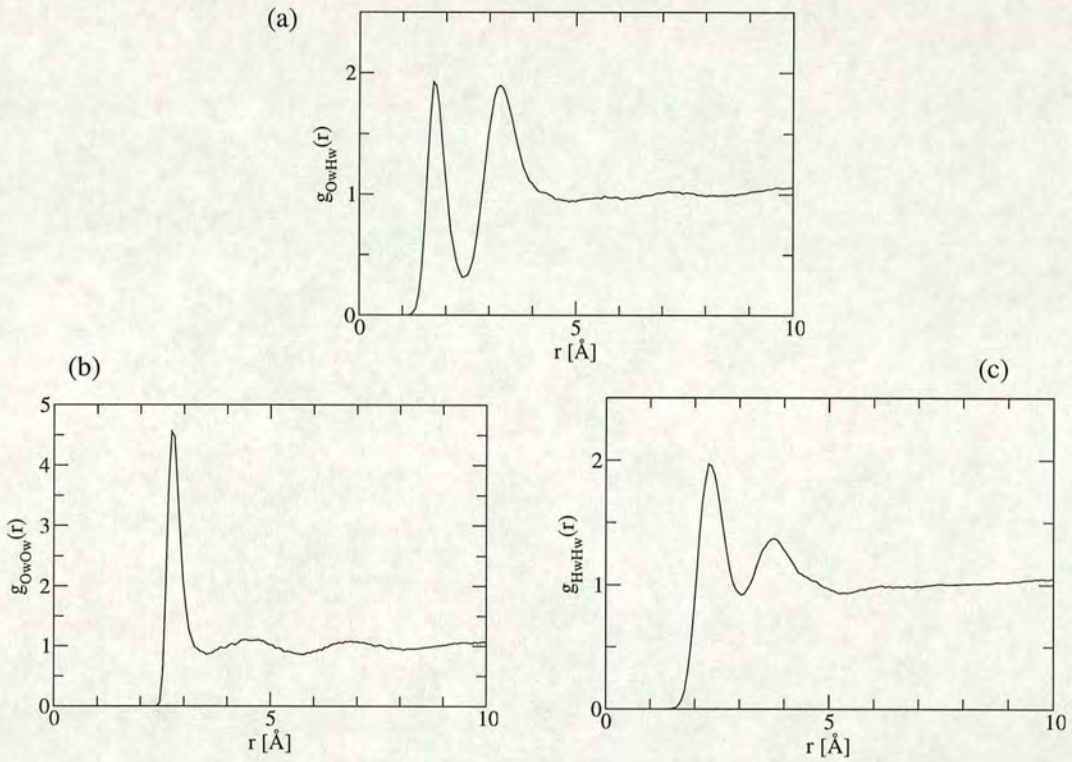

Figure 5.6: (a)OwHw, (b)OwOw and (c)HwHw partial radial distribution functions determined by the EPSR procedure for the 7:3 methanol-water mixture which provide information on water-water hydrogen bond interactions.

interacting methanol molecules via the hydroxyl group while the second peak comes from interactions via the methyl end of a methanol molecule. Simple models of these intermolecular geometries are shown in fig. 5.7c. While other contacting geometries cannot be ruled out at this stage [‡] assuming at least these intermolecular geometries, a comparison of the coordination numbers of pure methanol and the 7:3 mixture for the first and second neighbours indicate that molecular interactions via the methyl end of a reference methanol molecule are indeed enhanced. This molecular association must show up in the $g_{CM}(r)$ and $g_{MM}(r)$ functions. These are shown in fig. 5.9. Again, compared to pure methanol, the first shoulder of each function moves to lower r values by about 8% and 12% respectively and is also better defined in the mixture. Thus we can conclude that

[‡]The partial radial distribution functions are averaged over molecular orientations.

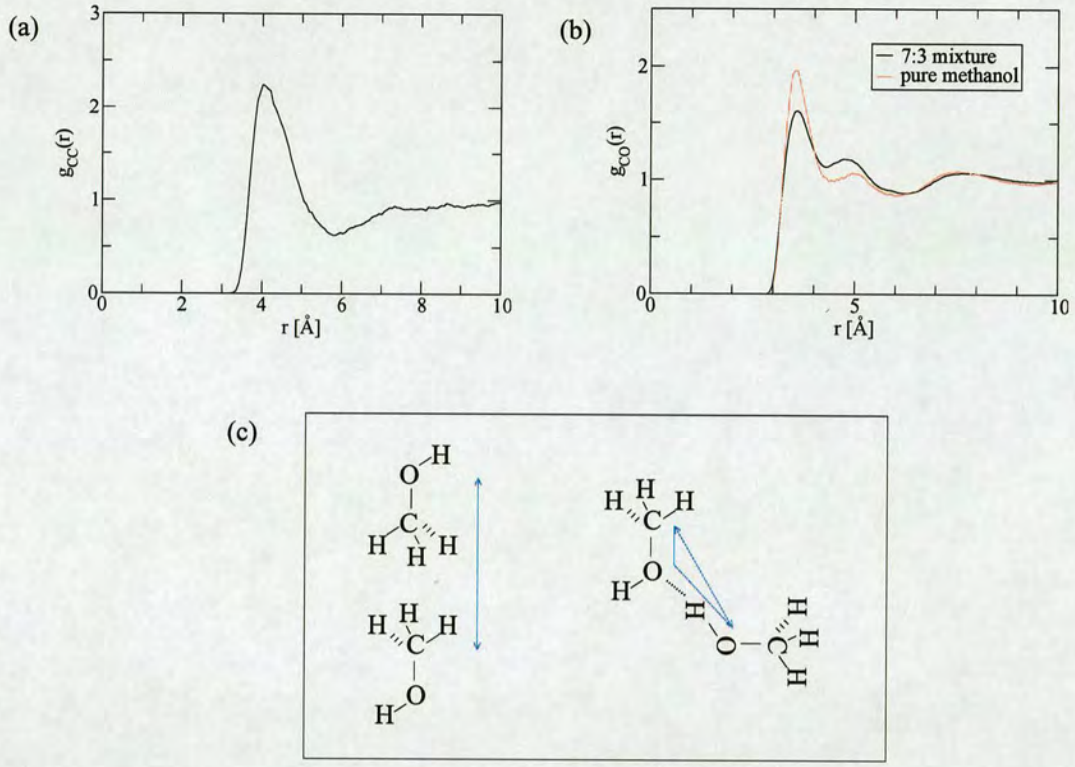

Figure 5.7: (a)CC and (b)CO partial radial distribution functions determined by the EPSR procedure for the 7:3 methanol-water mixture which provide information on methanol-methanol interactions. (c) Simple models of intermolecular geometries corresponding to the peaks in $g_{CO}(r)$.

adding as little as 30 mole % water to methanol results in an enhancement of the contact between the non-polar groups of this amphiphile, an enhancement which is quantified by not only an enhanced methyl-methyl coordination number but also through a significantly reduced intermolecular contact distance. There appears to be an increase in the packing of the methyl groups induced by adding water and confirms qualitative deductions made from the Raman spectral shifts.

5.3.3 Orientational Distributions

The partial radial distribution functions discussed above do not provide any detailed information on intermolecular geometries even though some preliminary

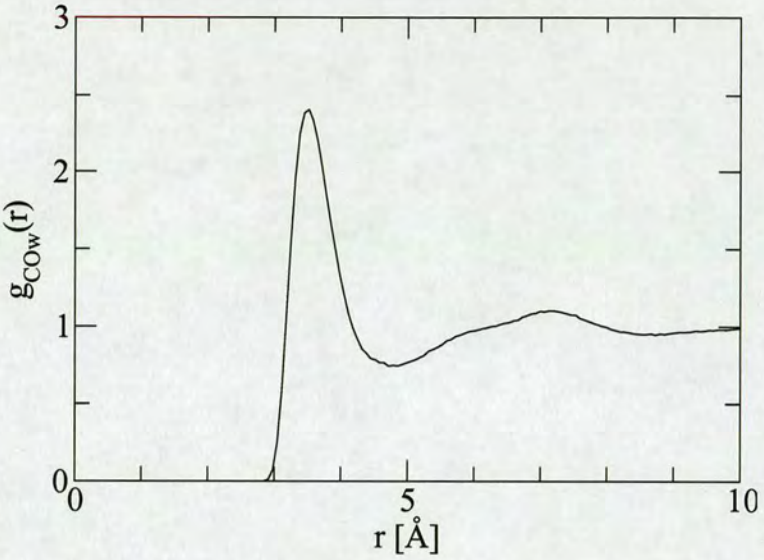

Figure 5.8: (a)COw partial radial distribution functions determined by the EPSR procedure for the 7:3 methanol-water mixture.

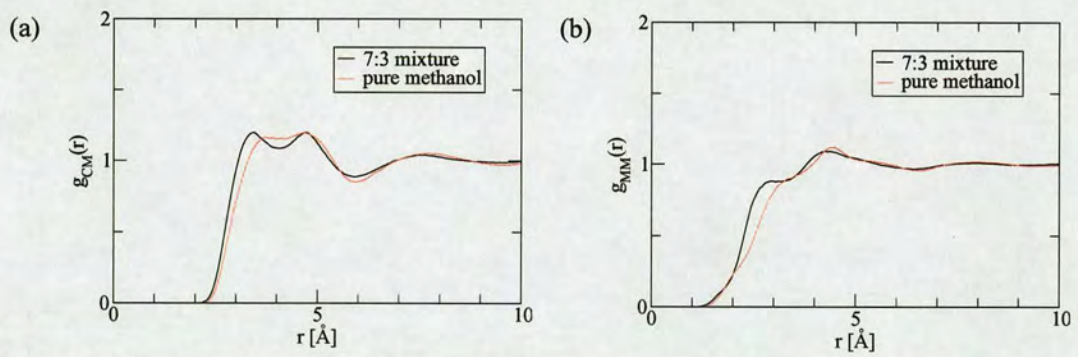

Figure 5.9: (a)CM and (b) MM partial radial distribution functions determined by the EPSR procedure for the 7:3 methanol-water mixture.

conclusions have been drawn using simple molecular models. Information on intermolecular geometries can be obtained from the spatial density functions and orientational distribution functions. The coordinate system used to define these correlations is shown in fig.5.10. The spatial density function is defined as the density of neighbouring molecular centres as a function of distance and direction away from a central molecule. The orientational distribution function is usually plotted along one direction in the spatial density function, and represents the

density of neighbouring molecules as a function of their orientation and distance relative to a central molecule. In the figures shown here these densities and correlations have been averaged over the rotation of the molecules about their axes (the O-C bond for methanol and the bisector of the H-O-H angle for water). The orientational plots hence show only the orientation of the axis of a neighbouring molecule relative to that of a central molecule.

The spatial densities of methanol molecules around a reference methanol for the pure liquid and the 7:3 mixture are shown in figs 5.11 (a) and (b) respectively. Pronounced lobes around $\theta_l = 0°, \pm 90°$ and $180°$ are seen for pure methanol. However for the mixture not only do the lobes around $\theta_l = 0°$ and $\pm 90°$ increase in intensity; they also merge giving increased brightness at $\theta_l = \pm 45°$. Further, the intensity around $\theta_l = 180°$ is significantly reduced in the mixture. In interpreting these plots, we note that θ_l values between $0°$ and $\pm 90°$ correspond to approach towards the methyl group of the central methanol molecule, while θ_l values around $180°$ relate to approaching the central molecule at the hydroxyl group end. Thus a comparison of figs 5.11 (a) and (b) lead us to conclude that, in the mixture, the dominant intermolecular methanol interaction is through the methyl 'head group', while in the pure liquid there are also significant methanol contacts through hydrogen bonding between adjacent hydroxyl groups of neighbouring molecules.

More detailed geometrical information on the angular orientations of an approaching methanol molecule with respect to the reference methanol can be obtained by examining the distributions of orientations θ_m of a neighbouring molecule at $\theta_l = 0°, 45°$ and $135°$ (see fig. 5.12, fig. 5.13 and fig. 5.14 respectively). In pure methanol, for an approach directly above the reference methanol's methyl group the dominant contribution is from edgewise ($\theta_m = \pm 90°$) and 'head on' ($\theta_m = 180°$) methyl-methyl contact (fig.5.12(a)). There is some probability for an apolar to polar contact at this approach angle, this feature is seen in the $\theta_m = 0°$ direction in fig. 5.12(a) at slightly longer distances of approach. This situation changes in the mixture. The lobe between $\theta_m = +90°$ and $\theta_m = -90°$ directions is much more continuous (fig. 5.12(b)), showing that there is a more uniform angu-

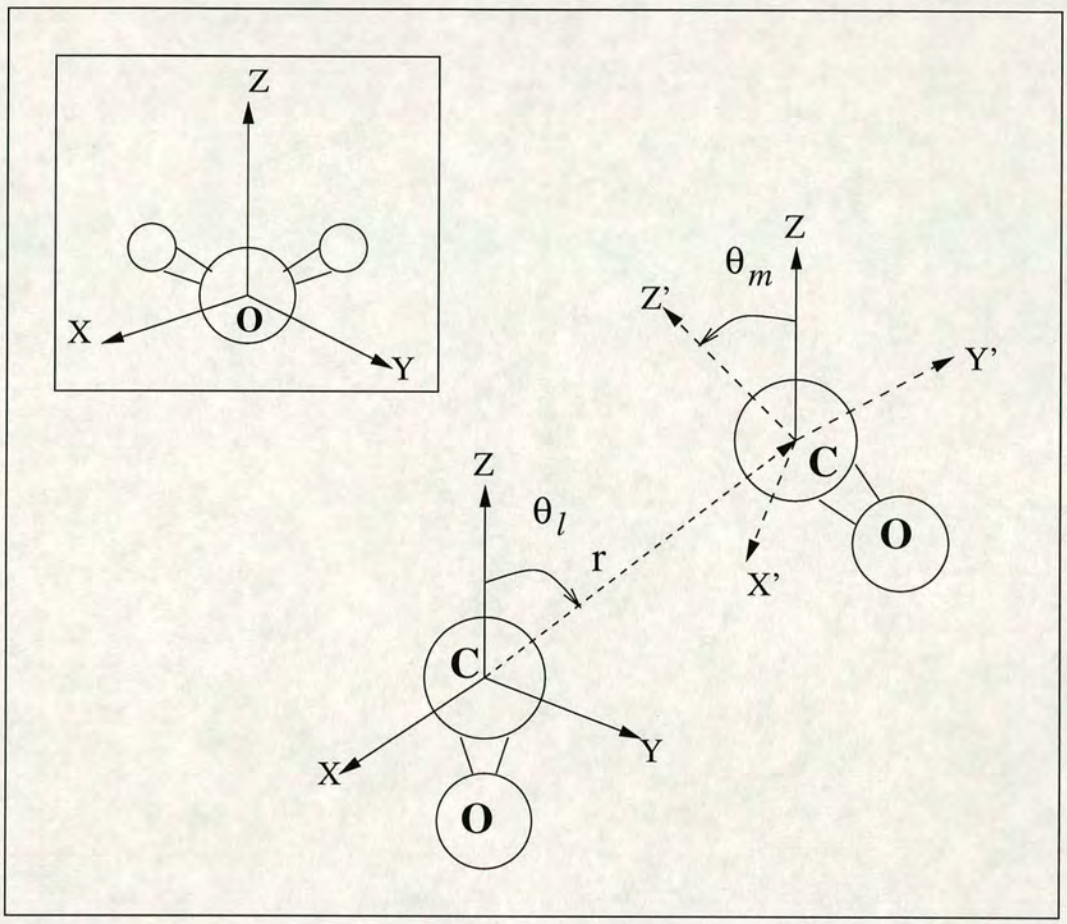

Figure 5.10: Coordinate system used to determine the intermolecular orienational correlations. The carbon atom of methanol is chosen as the molecular centre with the z axis along the OC bond. For the water molecule, the oxygen atom is chosen as the origin (see insert) with the z axis along the water dipole moment i.e. bisecting the H-O-H angle. The position of a neighbouring molecule is defined by the vector (r, θ_l). The orientation of the OC bond of a neighbouring methanol molecule or of the dipole moment of a neighbouring water molecule relative to the z axis of the molecule at the origin is defined by the Euler angle θ_m.

lar distribution of approaching methanol molecules, including a larger population of molecules in contact with their OC vectors pointing at the central molecule at angles between the edge- ($\theta_m = \pm 90°$) and head-on ($\theta_m = 180°$) directions. The probability of finding methanol molecules with an apolar to polar group contact is significantly reduced in the mixture at this angle of approach.

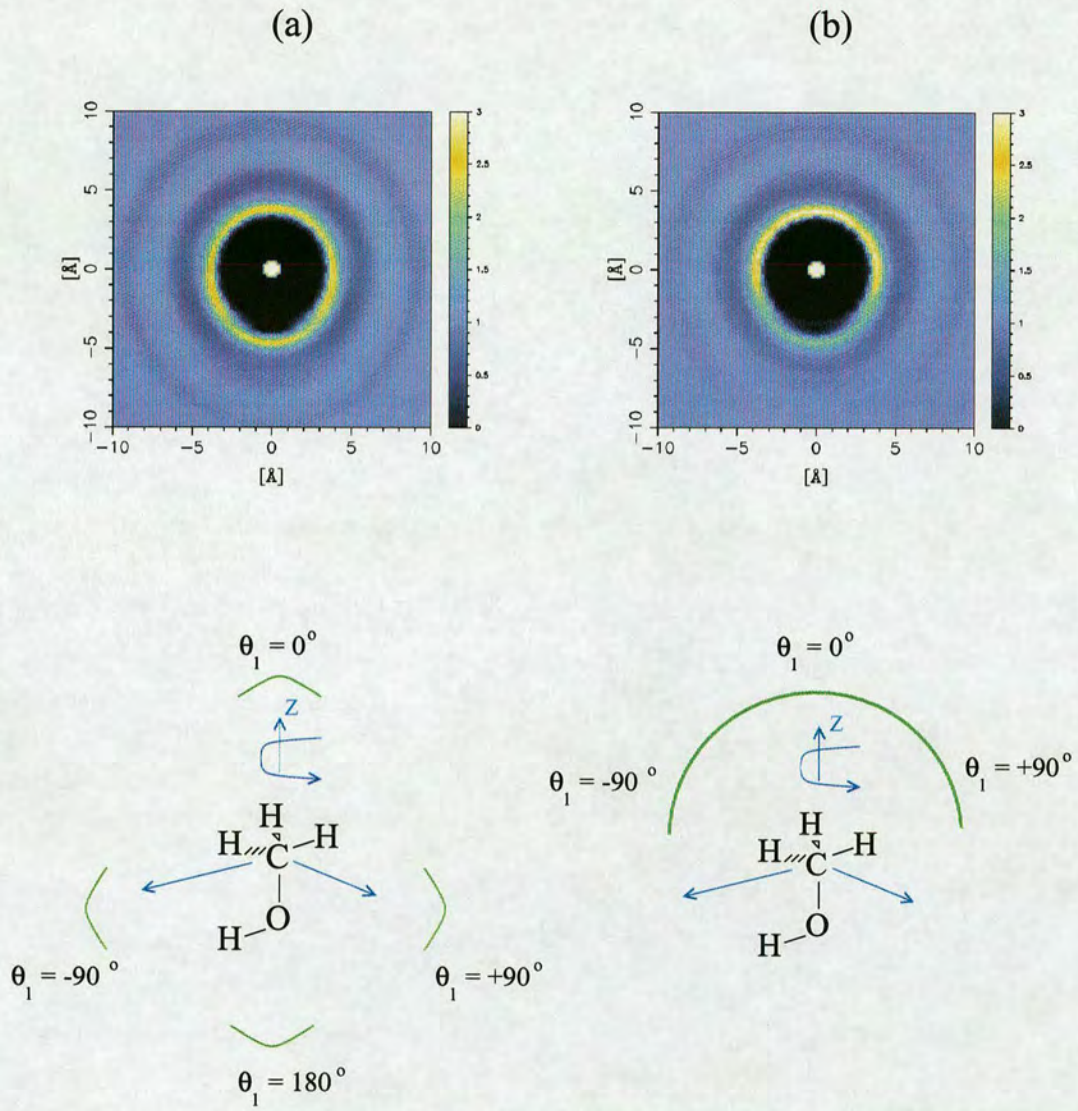

Figure 5.11: (a)Average intermolecular spatial density map of neighbouring methanol molecular centres around a central methanol molecule in pure methanol as a function of (r, θ_1) after averaging over rotations about the O-C axis on both molecules. (b) Same as in (a) but for the 7:3 mixture.

The same conclusion can be drawn from similar plots for an approach angle of $\theta_l = 45°$. The corresponding orientational correlation plots for pure methanol and the 7:3 mixture are shown in fig. 5.13(a) and (b) respectively. In the mixture, there is a more uniform distribution of the OC vectors between the $\theta_m = 135°$ and $\theta_m = -45°$ directions again indicating that the methanol molecules in the mixture prefer to interact directly via the methyl groups, a scenario which is

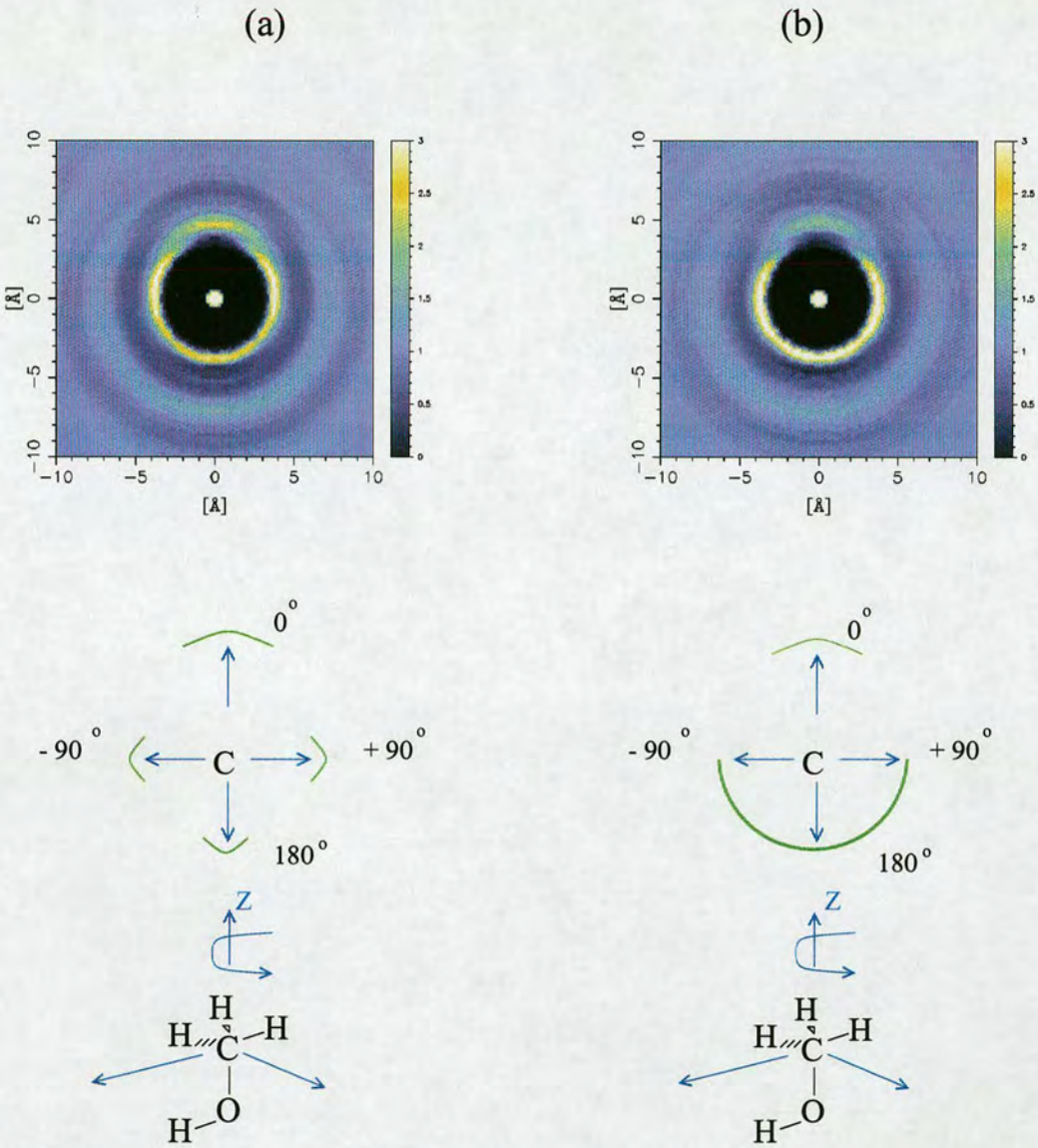

Figure 5.12: (a) Orientational distribution map of the methanol OC vector around a central methanol molecule in pure methanol as a function of (r,θ_m) with θ_l = 0° after averaging over rotations about the O-C axis on both molecules. In the schematic, the arrows around an approaching methanol molecule indicate the possible directions of the local Z axis (OC bond) of that molecule. (b) Same as in (a) but for the 7:3 mixture.

distinctly different from that found in pure methanol. Taken together, these orientational functions show that the increase in the coordination number noted from the second peak of $g_{CO}(r)$ is due to more methanol molecules interacting via

the methyl headgroup in the first coordination shell of a reference methanol. The slight inward shift of this peak can be attributed to the significant decrease in the polar-methyl group contact between a neighbouring methanol and the reference methanol.

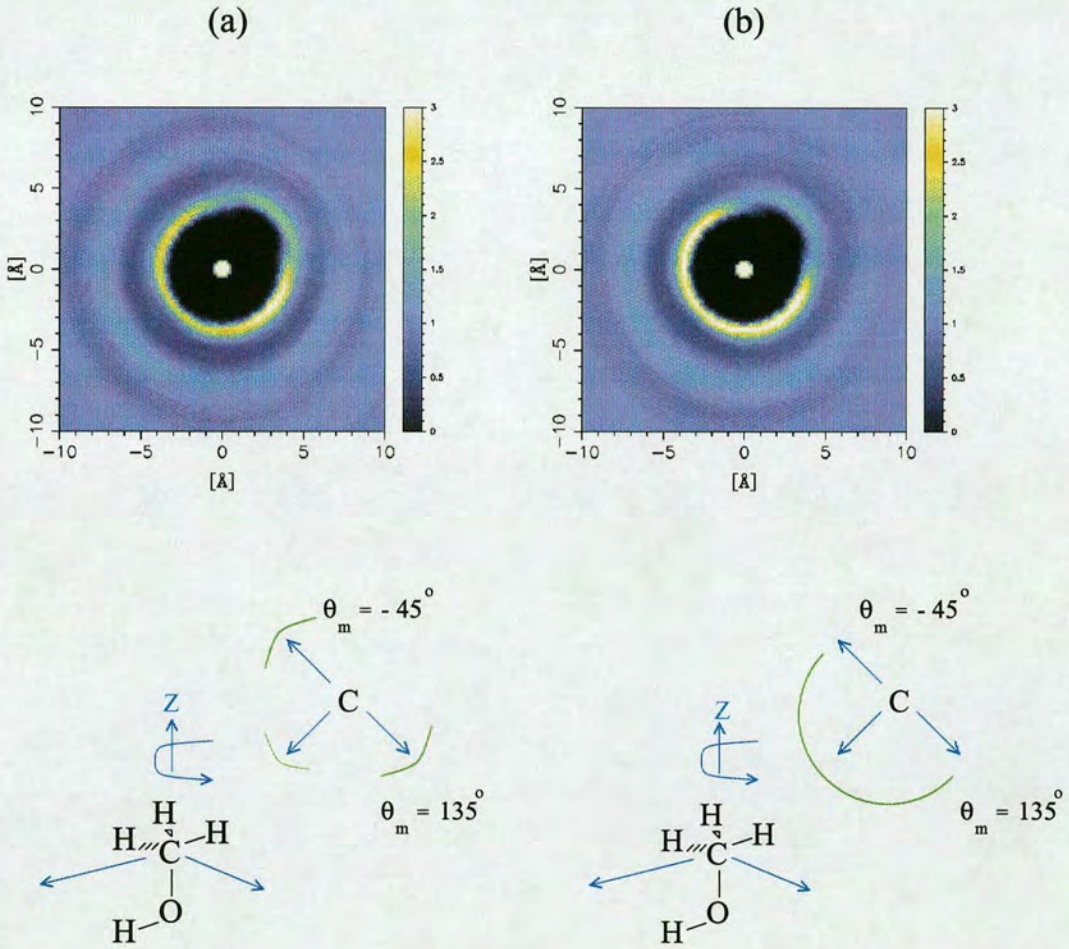

Figure 5.13: (a) Orientational distribution map of the methanol OC vector around a central methanol molecule in pure methanol as a function of (r,θ_m) with θ_l = 45° after averaging over rotations about the O-C axis on both molecules. In the schematic, the arrows around an approaching methanol molecule indicate the possible direction of the local Z axis (OC bond) of that molecule. (b) Same as in (a) but for the 7:3 mixture.

The orientational distribution plot of methanol-methanol interactions at approach angles corresponding to the hydroxyl group of a reference methanol (θ_l = 135°)

is shown next. While in pure methanol (see fig. 5.14 (a)) the dominant interaction is through hydrogen bonds at this approach angle, note the intensity around the θ_m = 135° direction, there is some indication of a polar to apolar group contact indicated by the intensity in the θ_m = -60° direction. In the case of the mixture (see fig. 5.14 (a)) there is a drop in intensity around the θ_m = 135° direction which signals a reduced probability of hydrogen bond formation between methanol molecules. Further there is also a significant decrease in intensity around the θ_m = -60° which implies a much lower chance of finding a polar to apolar contact as compared to the pure alcohol. Again, these plots confirm the interpretations made from the trends seen in the coordination numbers obtained from $g_{CO}(r)$. The decrease in the coordination numbers obtained from the first peak is due to significantly reduced polar to polar contacts via the hydroxyl end of methanol.

Such a structural response is entirely due to the presence of water. The water molecules are primarily engaged in hydrogen bond interactions with the methanol molecules. Hence their interaction with the methanol hydroxyl groups dominates over the inter methanol hydrogen bond interactions via the polar group of the alcohol. This situation is pictorially clearer from the spatial density plot of water molecules around a reference methanol molecule shown in fig. 5.15. The water molecules preferentially hydrate the methanol hydroxyl group, with little chance of them hydrating the methyl group.

5.4 Discussion and Conclusions

This is a first *structural experimental study* in a alcohol-water mixture where the water content is low. The results presented here demonstrate the preferential hydrogen bond interaction between water and methanol in the 7:3 mixture. This is in agreement with previous simulation studies of this system at similar concentrations where there is very little water [101] which conclude that the water molecules get easily incorporated in the chain like structure of methanol. The

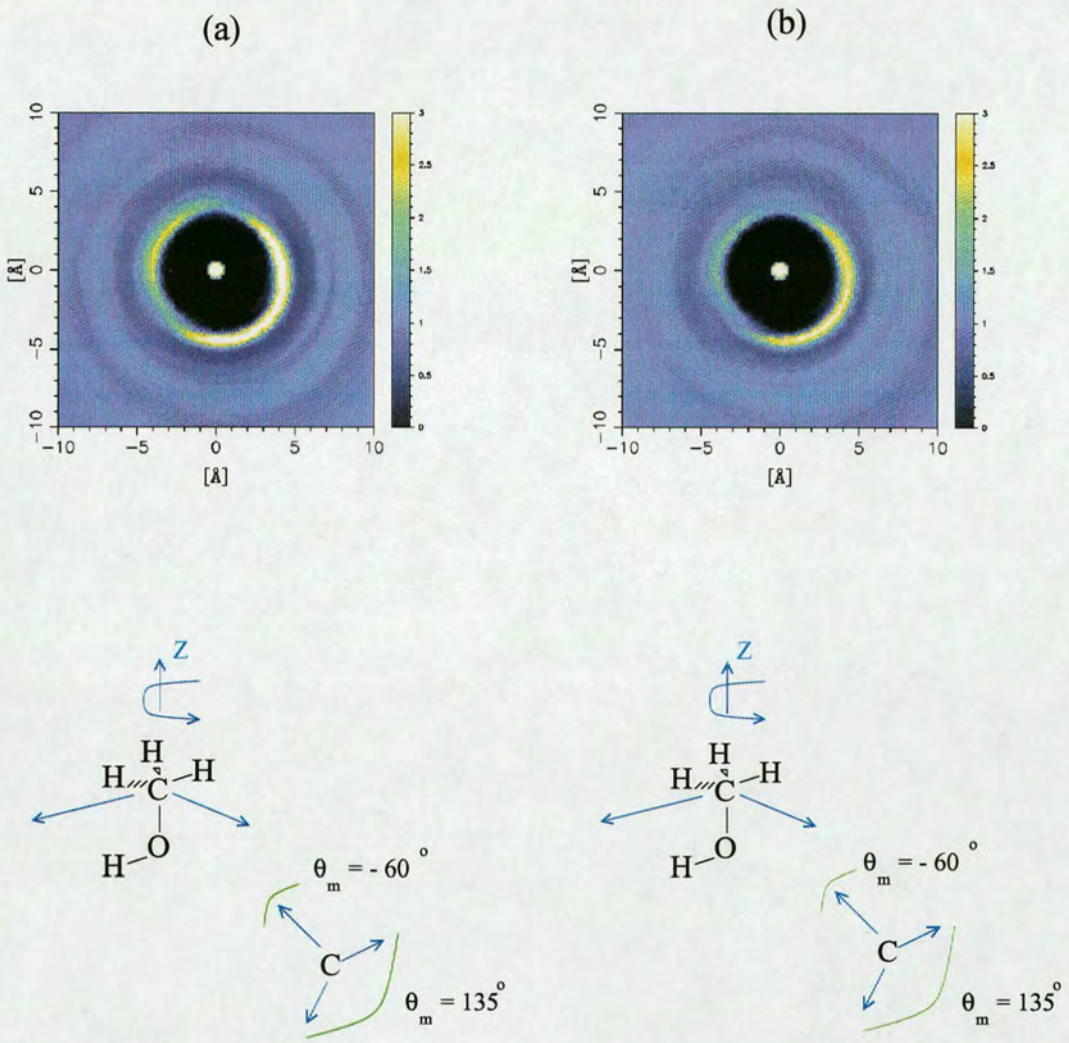

Figure 5.14: (a) Orientational distribution map of the methanol OC vector around a central methanol molecule in pure methanol as a function of (r,θ_m) with θ_l = 135° after averaging over rotations about the O-C axis on both molecules. In the schematic, the arrows around an approaching methanol molecule indicate the possible direction of the local Z axis (OC bond) of that molecule. (b) Same as in (a) but for the 7:3 mixture.

$g_{OwOw}(r)$ reported here has a second shell which is quite distinct. Such a signature is absent in the $g_{OwOw}(r)$ reported by Laaksonen *et al* [102] in their simulation study of a 0.75 mole fraction mixture of methanol in water. However, their simulation was performed on a smaller system (number of methanol molecules = 192, number of water molecules = 64). The authors also compared the heights of

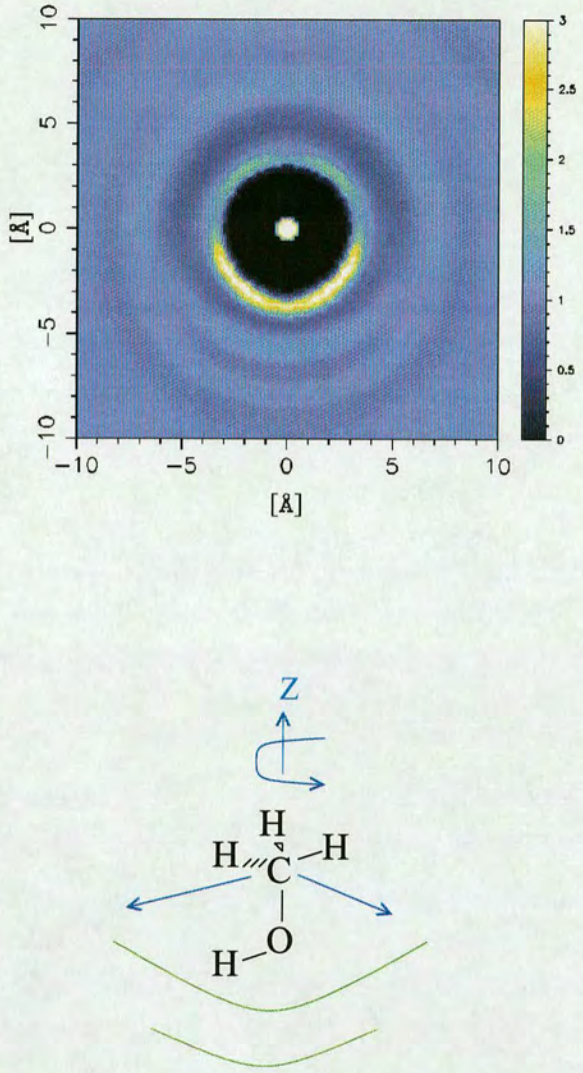

Figure 5.15: Average intermolecular spatial density map of neighbouring water molecular centres around a central methanol molecule in the 7:3 mixture as a function of (r, θ_1) after averaging over rotations about Z axes on both molecules (OC bond for methanol and the dipole moment for water).

$g_{OwOw}(r)$ from the mixture with that of pure water and concluded that the height increases significantly in the mixture. A similar conclusion is reached by Tanaka *et al* [103] and Ferrario *et al* [104] from their simulation data of a 7:3 methanol in water mixture. Tanaka *et al* attributed this increase in peak height to association between the water molecules. The present results not only indicate that

the water molecules indeed form dimers on an average but *cluster* around the hydroxyl group of methanol. Earlier reports have emphasised that in concentrated methanol-water mixtures, the water water molecules are dispersed randomly in the mixture [10, 73] and the water network is broken down completely. The other two reports, i.e. those by Laaksonen *et al* and Ferrario *et al* attributed this increase in height to the enhancement of water structure in the presence of methanol as proposed by Frank and Evans [5]. However, it has been argued in recent literature that an increase in peak height cannot be taken as evidence for enhanced structure since excluded volume effects need to be accounted for before any comparison is made between the radial distribution functions in a mixture and the pure liquid [63]. Further, the reasoning of Frank and Evans [5] concerned water structure enhancement around the methyl group. The present data show clearly that there is a negligible probability of finding water molecules hydrating the methyl group. The only definite conclusion that can be made from the present data is that the water molecules do associate to form clusters and that this clustering is driven by the polar interaction between the water and methanol hydroxyl groups [105].

More surprising however, is the stunning revelation that the methanol molecules also interact preferentially, not via hydrogen bonds but via their methyl groups. The presence of this interaction is demonstrated by a *reduced* contact distance between methanol molecules at direct *head on* approach directions. Further the spatial density plot and the coordination number obtained from $g_{CC}(r)$ also demonstrate that this preferential association is accompanied with an increase in the number of methanol molecules in the first coordination shell of a reference methanol compared to values expected from random mixing of the two species. This increase in the coordination number is entirely in the methyl environment of a reference methanol molecule as is evident from the spatial density plots. Orientational correlations between methanol molecules indicate unambiguously that this preferential interaction occurs via the methyl groups. Taken together, these results imply an increased packing of the alcohol molecules. Mass spectroscopy

and fluorescence measurements by Wakisaka *et al* [106] indicate that methanol molecules self associate to form microscopic clusters in concentrated mixtures with water. Measurements using a a hydrophobic fluorescence probe indicated that in the concentrated mixtures the methanol molecules self associate to form microscopic hydrophobic environments. It is unclear from their measurements whether water molecules form clusters in the concentrated mixtures and whether there are any hydrogen bond interactions between the methanol molecules. The present results show unambiguously that methanol molecules indeed interact preferentially via their methyl groups, an interaction which is driven by the hydrogen bonding between water and methanol.

Also, the results reported by Tanaka *et al* [103] show the first peak of $g_{CC}(r)$ actually move to *higher* r values in a 7:3 methanol-water mixture which does not agree with the results reported here. None of the simulation studies mentioned in the cited publications report any coordination numbers there by making any comparisons beyond those of the peak positions of the carbon-carbon radial distribution function difficult.

We note here that the enhancement of methyl-methyl group contacts, with an association of these molecules through their non-polar head groups, is classically the kind of behaviour expected as a result of hydrophobic driving forces. In this concentrated methanol-water mixture however, there is insufficient water to result in intermolecular solvent-solvent interactions giving rise to classical hydrophobic effects [6]. While observations of self assembly of amphiphiles in macromolecular systems have been investigated in detail [3] it has not been possible to probe the structure of aqueous solutions of simple amphiphiles like alcohols until recently. It was postulated by F. Franks in the now famous treatise on water [1] that scattering methods would be able to investigate in microscopic detail the conditions which govern the hydrophobic clustering of molecules in aqueous mixtures. The shrinking of the carbon-carbon distance reported here is the first observation of its kind in this simplest possible amphiphile-water system. In fact, it is the simplicity of the amphiphile (methanol) which renders such detailed investigations at

the atomic level possible. The significant changes noted in the methanol molecular orientations in this work show unambiguously at a microscopic level how amphiphilic molecules change their orientations in a direct response to the presence of water to form microscopic regions in the mixture which exclude water. Indeed, higher order self assembly processes which are accessible visually have their origins in such simple systems. While this has been always accepted, the present results give direct verification of ideas on which the study of self assembly of macroscopic systems is based, i.e. preferential interaction of water with polar sites of the amphiphile and changes in molecular orientations of the amphiphile to form a hydrophobic regions. It is useful to emphasise the need to get structural information on other simple amphiphilic-water systems (acetone), where the polar site is aprotic. There is no way to tell with certainty, without structural information whether water would cluster in this system and the nonpolar headroups of acetone would exclude water. It remains to be seen how sensitive is the water interaction with polar groups as a function of their chemical nature.

The next chapter deals with structural investigations in a dilute methanol-water mixture. The association of methanol molecules in this mixture could be classified as classical hydrophobic interactions if evidence for a preferential methyl-methyl association is found since this system does have a significant amount of water. It will be interesting to see how the structure of the two mixtures differs in moving from a system where largely bulk hydrophobic interactions between the amphiphile are noted (7:3 mixture) to a system where classical hydrophobic interactions are expected to be operative (1:19 mixture).

Chapter 6

New Insights into the Hydrophobic Interaction

Dilute aqueous solutions of hydrophobic solutes have been a topic of intense experimental, theoretical and simulation study for the past five decades. The interest stems from the fact that the remarkable thermodynamic properties of these solutions have been interpreted in the past as due to the solute enhancing the structure of the water network surrounding it. As already discussed, this interpretation has been questioned recently in light of several results from simulation and experiment. Neutron diffraction experiments on a 0.1 mole fraction methanol in water mixture (1 methanol: 9 waters) reported by Soper and Finney [13] gave the first unambiguous proof of a disordered cage surrounding the methyl group of methanol in the mixture. This shell of water molecules was found to be achieved without a significant modification of the orientational order between the water molecules. In that report, the authors compared the water structure in the mixture with that of pure water. In the present work an even more dilute mixture was investigated.

In this chapter experimental results from a neutron diffraction experiment on a 0.05 mole fraction of methanol in water mixture (1 methanol : 19 waters) are reported. At this concentration, the Raman stretch frequencies of the C-O and C-H

vibration modes of methanol reach saturation in the red and blue shifts they experience on dilution with water compared to their values in pure methanol. It was deduced that the methanol molecules in the 1:19 mixture and in more dilute mixtures have a complete hydration shell. The present experiment was performed in order to determine how the hydration shell around a methanol molecule changes with dilution by comparing results from this experiment with the previous report of Soper and Finney [13]. Further the issue of methanol association remained unresolved since the spectroscopic data did not yield any conclusive evidence and simulation results in literature have so far provided conflicting pictures. Thus another motivation for the present study was to determine the degree of association between the methanol molecules, especially via the methyl groups. The importance of the hydrophobic interaction between such non polar groups in water has been addressed previously.

6.1 Experimental Details

Isotopically substituted, but otherwise similar mixtures of methanol in water were prepared with the correct methanol (1) : water (19) molecular ratio as shown below:

1. CD_3OD in D_2O
2. CD_3OH in H_2O
3. A 50% mixture of 1 and 2
4. CH_3OH in H_2O
5. A 50% mixture of 1 and 4

The above substitutions yielded correlations between the hydroxyl hydrogens (mixtures: 1, 2, 3) and between all hydrogens (mixtures: 1,4,5). Methyl group

substitutions were not performed in this case since the mixture is too dilute and a significant diffraction signal from the methyl hydrogens is not detectable. Each of these three sets of solutions resulted in three composite partial structure factors [92], viz: $S_{HH}(Q)$-1, $S_{XH}(Q)$-1 and $S_{XX}(Q)$-1. As mentioned earlier, H corresponds to the labelled hydrogen and X corresponds to the remaining unlabelled atoms. The composite partial structure factors are a linear combination of several weighted partial structure factors corresponding to the various atomic species in the mixture. The following tables (6.1,6.2) give all the intermolecular weights for the six composite partial structure factors obtained from the neutron scattering experiment.

6.2 Data Modelling

The data modelling performed using the EPSR technique [56] for the six composite partial structure factors is done exactly on the same lines as mentioned in the previous chapter. A computer model of the mixture was set up using 28 methanol molecules and 532 water molecules. The ratio was chosen to maintain the correct mole-fraction of methanol as used in the actual experiment and a cubic box of of length 26.08 $\AA$ was used to obtain the correct density of the liquid mixture. The EPSR fits obtained for the 1:19 mixture of methanol in water are shown in fig. 6.1. The EPSR fits deviate slightly at low Q values, this is due to difficulties encountered in removing the inelastic scattering. The slight deviations seen in at intermediate Q values are probably due to imperfections in the polynomial used to subtract the inelastic scattering. It is most difficult to remove inelastic scattering for the XX composite partial structure factor. To understand why, consider the set of samples 1,2 and 3 mentioned above. The polynomial that is used to fit the self scattering term (see chapter 4 for details) is used to remove contributions from all the data sets measured in the experiment taking into account the concentration of the hydrogen atoms for each set. The resulting total structure factor is then an amalgamation of this corrected data. The resulting

XX Weights	C	O	M
C	0.00217		
O	0.07576	0.6145	
M	0.01306	0.2280	0.01965
XH Weights	**C**	**O**	**M**
H	0.00119	0.02085	0.00359
H_W	0.04539	0.79245	0.13661
HH Weights	**H**	**H_W**	
H	0.00066		
H_W	0.04997	0.94938	

Table 6.1: Intermolecular weights for the 1:19 methanol-water mixture where substitutions are made on the methanol hydroxyl hydrogen as well as the water hydroxyl hydrogen. The atom labels M, C, O and H refer to methanol methyl hydrogen, carbon, oxygen and hydroxyl hydrogen respectively. The atom labels O_W and H_W indicate water oxygen and hydrogen. In the present case, contributions from the methanol and water oxygen atoms are grouped together under the heading 'O'.

XX Weights	C	O	
C	0.00293		
O	0.10248	0.89466	
XH Weights	C	O	
M	0.00387	0.06756	
H	0.00129	0.02252	
H_W	0.04901	0.85579	
HH Weights	M	H	H_W
M	0.0051		
H	0.00340	0.00057	
H_W	0.12924	0.04308	0.81859

Table 6.2: Intermolecular weights for the 1:19 methanol-water mixture where substitutions are made on all hydrogens, i.e. methyl and hydroxyl. The atom labels are as mentioned in table 6.1.In the present case, contributions from the methanol and water oxygen atoms are grouped together under the heading 'O'.

total structure factors from these samples are defined as:

$$F(Q)_{\mathrm{H}} = c_{\mathrm{X}}^2 b_{\mathrm{X}}^2[S_{\mathrm{XX}}(Q) - 1] + 2c_{\mathrm{X}}c_{\mathrm{H}}b_{\mathrm{X}}b_{\mathrm{H}}[S_{\mathrm{XH}}(Q) - 1] + c_{\mathrm{H}}^2 b_{\mathrm{H}}^2[S_{\mathrm{HH}}(Q) - 1] \quad (6.1)$$

$$F(Q)_{\mathrm{D}} = c_{\mathrm{X}}^2 b_{\mathrm{X}}^2[S_{\mathrm{XX}}(Q) - 1] + 2c_{\mathrm{X}}c_{\mathrm{H}}b_{\mathrm{X}}b_{\mathrm{D}}[S_{\mathrm{XH}}(Q) - 1] + c_{\mathrm{H}}^2 b_{\mathrm{D}}^2[S_{\mathrm{DD}}(Q) - 1] \quad (6.2)$$

$$F(Q)_{\mathrm{HD}} = c_{\mathrm{X}}^2 b_{\mathrm{X}}^2[S_{\mathrm{XX}}(Q) - 1] + 2c_{\mathrm{X}}c_{\mathrm{H}}b_{\mathrm{X}}b_{\mathrm{HD}}[S_{\mathrm{XH}}(Q) - 1] + c_{\mathrm{H}}^2 b_{\mathrm{HD}}^2[S_{\mathrm{HH}}(Q) - 1] \quad (6.3)$$

Note that the subscript 'HD' refers to the mixture sample. The scattering length in the mixture b_{HD}^2 has been defined in chapter 4. The HH structure factor is then calculated by summing the hydrogen and deuterium rich samples and subtracting the mixture sample.

Thus:

$$S_{\mathrm{HH}}(Q) - 1 = \frac{xF(Q)_{\mathrm{H}} + (1-x)F(Q)_{\mathrm{D}} - F(Q)_{\mathrm{HD}}}{c_{\mathrm{H}}^2(xb_{\mathrm{H}}^2 + (1-x)b_{\mathrm{D}}^2 - b_{\mathrm{HD}}^2}) \quad (6.4)$$

This leads to cancellation of any residuals which remain after subtracting the polynomial fits [107]. Next, the $S_{\mathrm{XH}}(Q)$-1 composite is calculated. This is done as follows:

$$S_{\mathrm{XH}}(Q) - 1 = \frac{F(Q)_{\mathrm{H}} - F(Q)_{\mathrm{D}} - c_{\mathrm{H}}^2 b_{\mathrm{H}}^2[S_{\mathrm{HH}}(Q) - 1] + c_{\mathrm{H}}^2 b_{\mathrm{D}}^2[S_{\mathrm{HH}}(Q) - 1]}{2c_{\mathrm{X}}c_{\mathrm{H}}b_{\mathrm{X}}b_{\mathrm{H}} - 2c_{\mathrm{X}}c_{\mathrm{H}}b_{\mathrm{X}}b_{\mathrm{D}}} \quad (6.5)$$

Again, the subtraction removes any residual inelastic scattering that may be present.

Finally, the $S_{\mathrm{XX}}(Q)$-1 composite is calculated.

$$S_{XX}(Q) - 1 = \frac{F(Q)_H - 2c_X c_H b_X b_H[S_{XH}(Q) - 1] - c_H^2 b_H^2[S_{HH}(Q) - 1]}{c_X^2 b_X^2} \quad (6.6)$$

Here, no differences between the 'H' and 'D' samples are involved. Hence, any residual inelastic scattering does not cancel out. Also, the present sample is very dilute, it is mostly water and the XX composite involves correlations primarily from the oxygen atoms whose signal is quite weak. It rides on the inelastic scattering background and it can be quite hard to remove the background reliably. The situation changes as the concentration of methanol is increased since, the contribution from the *unsubstituted* atoms is quite high, especially when they include the methyl hydrogens. Hence the XX fits for the 7:3 mixture were of a superior quality. However, the deviations noted in the XX composite in the 1:19 mixture will not affect the hydroxyl correlations (water and methanol) obtained from the models generated from the simulation since the HH and XH composites provide unique constraints to the fits. However, the methanol-methanol correlations could be affected not only by the deviations of the XX fits from the measured data at intermediate Q values but also because this is an extremely dilute solution and the statistics obtained on these correlations will be poor. Hence the results presented here on the methanol-methanol correlations should be considered bearing in mind the level of the present analysis.

Once the fits could not be improved further, the simulation was allowed to proceed to calculate various structural quantities of interest, namely the partial structure factors and the spatial and orientation distribution functions.

6.3 Results

In order to determine whether methanol molecules in this dilute mixture interact via their methyl groups without any interfering hydration water molecules several partial radial distribution functions are examined. These are reported along with

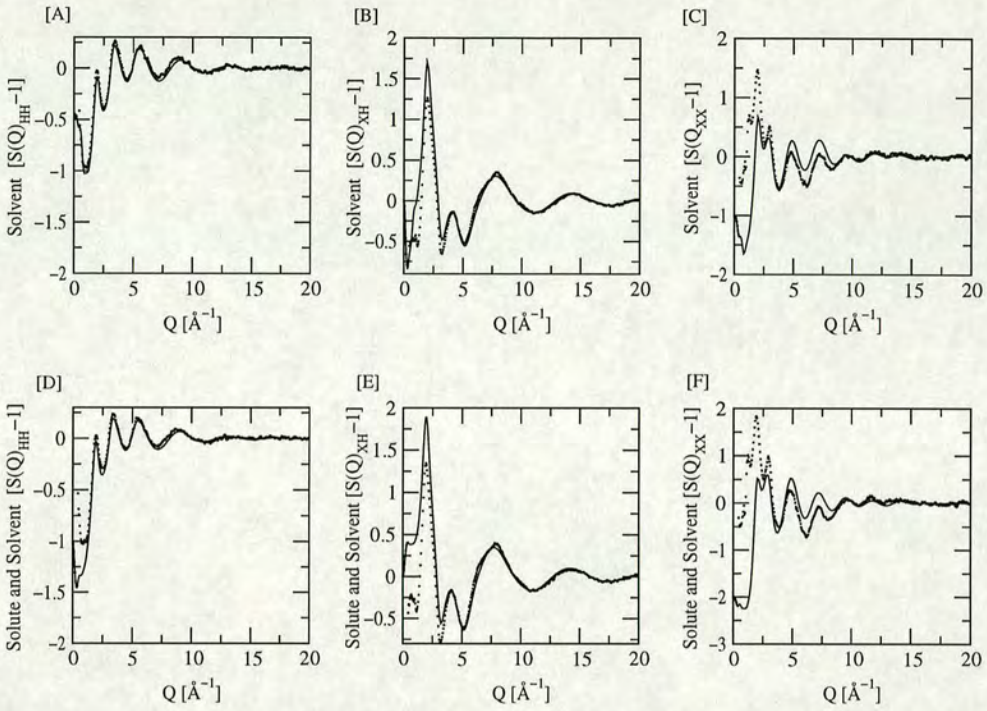

Figure 6.1: HH, XH and XX composite partial structure factors for methanol-water mixtures (5% mole methanol). Frames A,B and C correspond to the case where H/D substitution is performed on hydroxyl hydrogen atoms(samples 1, 2 and 3 in text); Frames D,E and F correspond to the case where H/D substitution is performed on all hydrogen atoms (samples 1, 4 and 5 in text). EPSR fits to the measured structure factors are shown as the solid circles. Note that the EPSR simulation is fit simultaneously to all 6 composite structure factors. The lack of fit in some regions, particularly for the XX function, is believed to arise from the difficulty in ensuring all the inelastic neutron scattering has been removed from the data prior to structure refinement (see text for details).

detailed orientational distribution plots of inter molecular correlations. In the dilute mixture an extended water network is expected, hence, comparisons are also made with the structure of pure water [99] where appropriate.

6.3.1 Methanol intermolecular correlations

To investigate the degree and the nature of methanol-methanol interaction in this dilute mixture, intermolecular correlations (partial radial distribution functions) were calculated from the model structures obtained by the EPSR method, defining the methanol molecular centre as the carbon atom. The centres correlation function, $g_{CC}(r)$ that describes the methanol-methanol correlation is shown in fig.6.2a. A distinct and broad first coordination shell is noted with a peak at $4.06\mathring{A}$ indicating solute (methanol) molecular contacts centred on this distance. Also shown in the figure is the same centres function for pure methanol [82]. Whereas adding a small amount of water (7 methanols:3 waters) shifts this centre's radial distribution function to lower r values (see fig. 5.7a) compared to pure methanol, adding more water to achieve the present 1:19 dilute solution shifts the first peak outwards. The peak is also broader, indicating a wider range of intermolecular contact distances in the dilute solution. Soper and Finney reported in their results for a 1 methanol : 9 waters mixture [13] the presence of water molecules forming a hydration shell around the methyl group at an average distance of 3.6 $\mathring{A}$. With further dilution as in the present case, it is expected that there will be more water molecules in this hydration shell. This will be looked into at a later stage, but if this is indeed the case, then the movement of the first peak in the CC correlations compared to that noted in pure methanol may indicate that the water molecules in the first hydration shell of methanol prevent the methanol molecules from approaching as close as in the case of the pure liquid.

Integrating under this peak, we obtain (table 6.3) an average centres coordination number of essentially 2. This indicates that on average each methanol molecule is in contact with two neighbours. In pure methanol, for the same partial radial distribution function a coordination number of 11 is obtained (see table 5.5). If the methanol and water mixed randomly then for a 1:19 dilution a coordination number of 0.55 is more realistic. Hence there exists preferential association of methanols. The $g_{CC}(r)$ obtained from the present work is quite different from that reported in the simulation study by Okazaki et al [108] for a methanol-water

Correlation	Atomic density ρ	R_{min} Å	R_{max} Å	Coordination number 25°C (atoms)
CC	0.0016	3.0	6.31	2.2 ± 0.4
OO	0.0016	2.0	3.32	0.1 ± 0.01
	0.0016	3.32	8.52	3.8 ± 0.5
OH	0.0016	1.0	2.53	0.06 ± 0.05
HH	0.0016	1.5	3.27	0.2 ± 0.1
CO_w	0.03	2.5	5.28	15.4 ± 0.7
CH_w	0.06	2.0	2.93	1.1 ± 0.2
	0.06	2.93	5.6	36.5 ± 1.1
	0.06	2.0	5.6	37.6 ± 1.1
OO_w	0.03	2.0	3.33	2.7 ± 0.3
	0.03	3.33	5.97	21.2 ± 0.9
OH_w	0.06	1.0	2.45	1.4 ± 0.2
	0.06	2.45	3.85	7.9 ± 0.5
HO_w	0.03	1.0	2.51	0.9 ± 0.2
	0.03	2.51	3.96	4.7 ± 0.4
HH_w	0.06	1.5	3.08	4.5 ± 0.4
O_wO_w	0.03	2.0	3.48	4.8 ± 0.1
	0.03	3.48	5.76	18.4 ± 0.3
O_wH_w	0.06	1.0	2.45	1.9 ± 0.06
H_wH_w	0.06	1.0	3.03	5.2 ± 0.1

Table 6.3: Coordination numbers obtained from the integration of the peaks observed in the partial pair distribution functions of the 1:19 mixture at 25° obtained from the EPSR analysis.

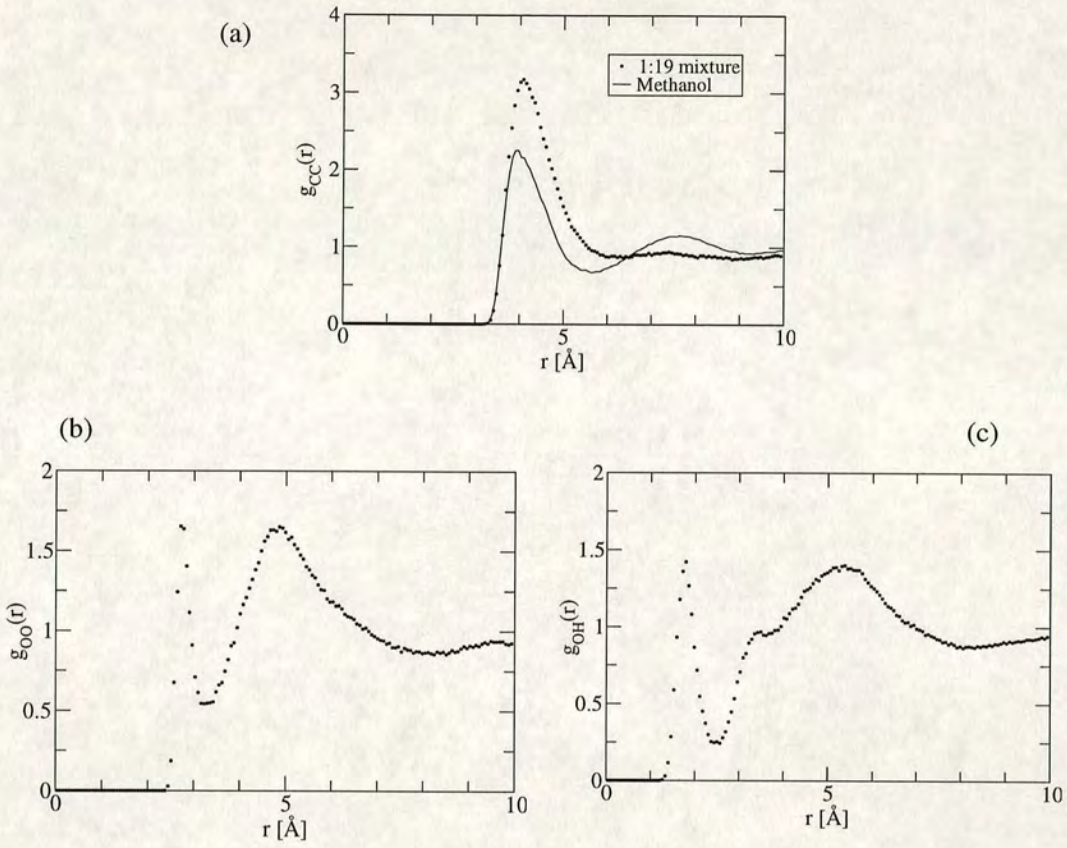

Figure 6.2: (a)CC, (b)OO and (c)OH partial radial distribution functions determined by the EPSR procedure for the 1:19 methanol-water mixture. These functions provide information on methanol-methanol correlations. Also shown in (a) is the same function for pure methanol [82].

mixture at the same concentration (1:19). The first peak position in the $g_{CC}(r)$ obtained by the authors is closer to 3.75 $\AA$. Moreover, Okazaki et al [108] also report the presence of a second coordination shell in the $g_{CC}(r)$ around 6.6 Å which is not as prominent in the present data where the shell is at approximately 7.3 Å . The average first shell coordination number obtained from the $g_{CC}(r)$ by Okazaki et al [108] is around 1 and is lower than the value determined from the $g_{CC}(r)$ in the present study.

However, it is important to note that the width of the first peak in the $g_{CC}(r)$ compared to pure methanol or the 7:3 mixture could be due to the weak constraint introduced by the XX composite partial structure factor in this dilute mixture.

Further, this function does not have a well defined first minimum and integration under the first peak is performed up to a maximum radius value which could be overestimated.

The correlation between methanol oxygens, $g_{OO}(r)$, shown in fig.6.2b shows two distinct peaks, a sharp one at 2.72 $\AA$, with a much broader one centred at about 4.8 $\AA$. This first peak is at a distance that corresponds to hydrogen bonding between the hydroxyl groups of two neighbouring molecules, as does the first peak in $g_{OH}(r)$ shown in fig.6.2c. Integration under these two peaks yields coordination numbers of 0.1 and 0.06 respectively (see table 6.3), indicating that this hydrogen-bonded contact, although present in the correlation function, occurs rarely in the solution: the coordination numbers are only slightly larger than zero. To first order, we therefore conclude that the dominant methanol-methanol contact in this solution is through the methyl head groups, with very little direct hydrogen bonding between methanols. The coordination numbers from these functions are more robust given that the HH and XH composite partial structure factors involved substitutions on the hydroxyl hydrogens of methanol.

Some indication of the possible relative orientations of neighbouring methanol molecules is given by the broad second peak in fig.6.2b centred at 4.8 $\AA$, but with a long high-r tail. Taking two methanol molecules contacting through their head groups and anti parallel to each other, simple calculations (see fig. 6.3, typical bond lengths and van der Waals radii are used) give a shortest oxygen-oxygen distance on neighbouring molecules of around 6.7 $\AA$, a distance on the extreme right of the tail of the second peak. This implies that this head-to-head orientation is not favoured. This is in contrast to the situation in t-butanol, where this head-to-head orientation appears to dominate [61].

6.3.2 Methanol-water intermolecular correlations

To examine the organisation of water molecules in the neighbourhood of a methanol molecule, $g_{COw}(r)$ (fig. 6.4a) is examined. The well defined first peak at 3.61 $\AA$

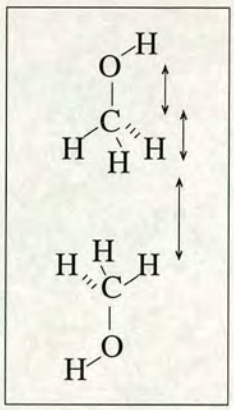

Figure 6.3: Schematic of a possible methyl group orientation in a head to head geometry with a reference methanol molecule. The blue arrows indicate the bond lengths and van der Waals radius of the hydrogen atom used to determine the O-O separation in the present case.

is at essentially the same position as observed earlier in a more limited study of a higher concentration (1:9) mixture [13]. A coordination number of 16 is obtained from $g_{COw}(r)$ (see table 6.3), a figure expectedly higher than the 10 found in the 1:9 study [13]. To extract information on the interaction between water molecules and the methanol hydroxyl group, $g_{OOw}(r)$ is interrogated. This function is shown in fig. 6.4b. The first shell coordination number of 2.7 ± 0.3 implies each alcohol hydroxyl group hydrogen bonds to between 2 and 3 waters. The maximum number of waters that the alcohol hydroxyl can accommodate is 3. Thus, the hydrogen bonding complement is nearly fully maximised. These coordination numbers are slightly higher than those found for t-butanol at 0.06 mole fraction [61]; it may be that the bulkiness of the t-butanol molecule is responsible for the more limited water coordination in that case. The $g_{OHw}(r)$ and $g_{HOw}(r)$ functions shown in 6.4c and 6.4d respectively distinguish between hydrogen bond acceptance and donation of the methanol hydroxyl group. From the coordination numbers in table 6.3, we see as expected that the methanol hydroxyl hydrogen is essentially fully hydrogen bonded to a neighbouring water, while the methanol oxygen accepts slightly less than its nominal full complement of two water molecule hydrogens. These results are consistent with there being very

little direct methanol-methanol hydrogen bonding.

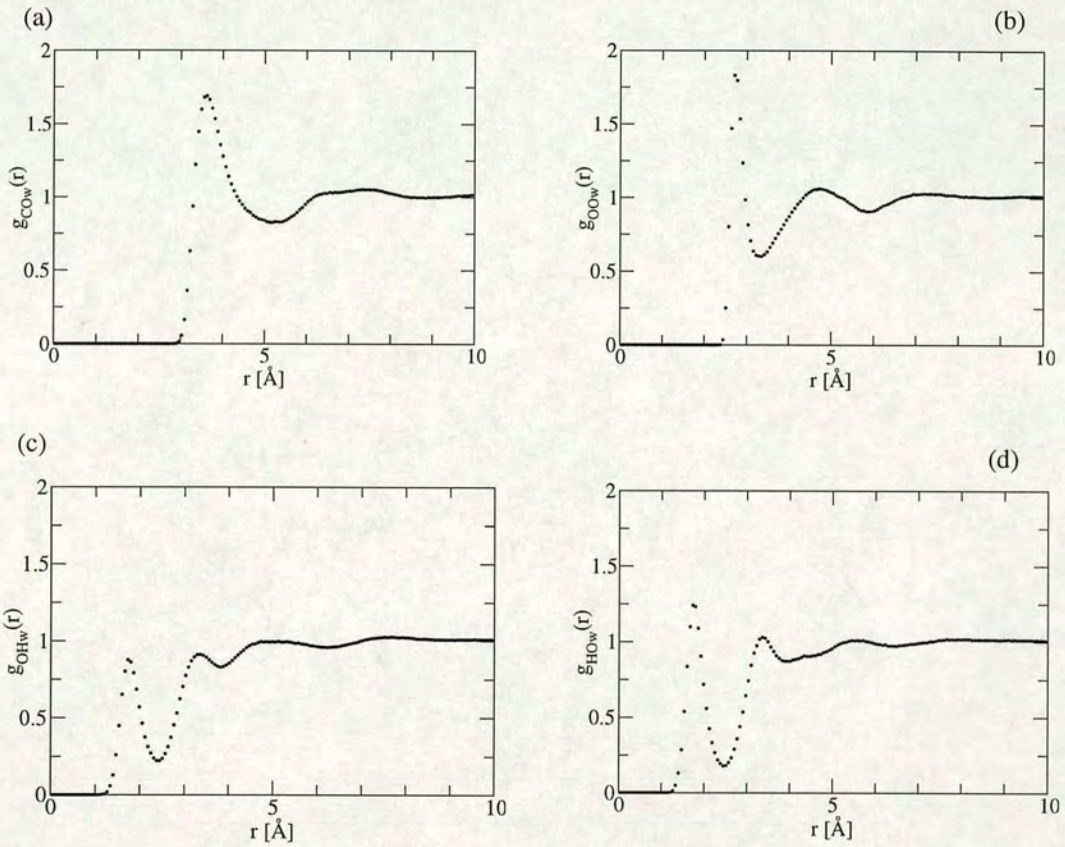

Figure 6.4: (a)COw, (b)OOW, (c)OHw and (d) HOw partial radial distribution functions determined by the EPSR procedure for the 1:19 methanol-water mixture. These functions provide information on methanol-water correlations.

6.3.3 Water intermolecular correlations

One of the most important reasons behind continued efforts in the investigation of this simple system, especially at concentrations where there is sufficient water to hydrate the methanol molecules in loose cages [13] is to determine whether the non-polar methyl head group perturbs the water molecules to some form of more ordered structure [5]. To date no experimental evidence has been found to verify the 'iceberg' hypothesis of Frank and Evans [5]. Rather, in a number of systems [13, 58, 61, 109], the hydrogen-hydrogen correlation function looks

remarkably similar to that in the bulk. However, there has as yet been no specific comparison with bulk water of the hydration structure through the OwOw and OwHw correlations. Although the HwHw correlation is likely to be a sensitive structural measure, we cannot rule out that a significant change might be found in the OwOw and OwHw correlations even in the absence of a difference between the solution and bulk water HwHw functions.

We note first from table 6.3 that the coordination numbers for the water are normal, pointing to a tetrahedral water network which is similar to that found in pure water [99] (see table 5.6).

The three partial correlation functions for the water in this system are shown in fig.6.5. Referring first to the HwHw function, we again see little difference from the bulk water picture, consistent with previously reported results. Turning to the OwHw and OwOw functions, however, we see some small but possibly significant peak shifts. For both OwOw and OwHw, the first intermolecular peak in the solution is shifted *outwards* very slightly compared to the bulk. These may be indicative of perturbations of solvent structure. However, a much larger perturbation is seen in an inward shift of the *second* neighbour OwOw peak by about 5%. Along with an apparent inward shift noted in the second neighbour OwOw coordination shell, there appears to be some increased intensity between the second and third neighbour correlations which is not present in the same function for pure water [99].

Such an effect has not been observed in computer simulations of this system at similar concentrations [102, 108]. A similar effect has however been reported by Bowron *et al* for in their study of a 0.06 mole fraction t-butanol in water mixture, where a shift inwards of the second neighbour water oxygen was also found [61]. In the t-butanol case, the non-polar moiety is much larger, having a stronger hydrophobic character than methanol. It is interesting therefore that this perturbation is also seen in the methanol case, where the non-polar moiety is smaller, and the system therefore perhaps "less hydrophobic". As in the case

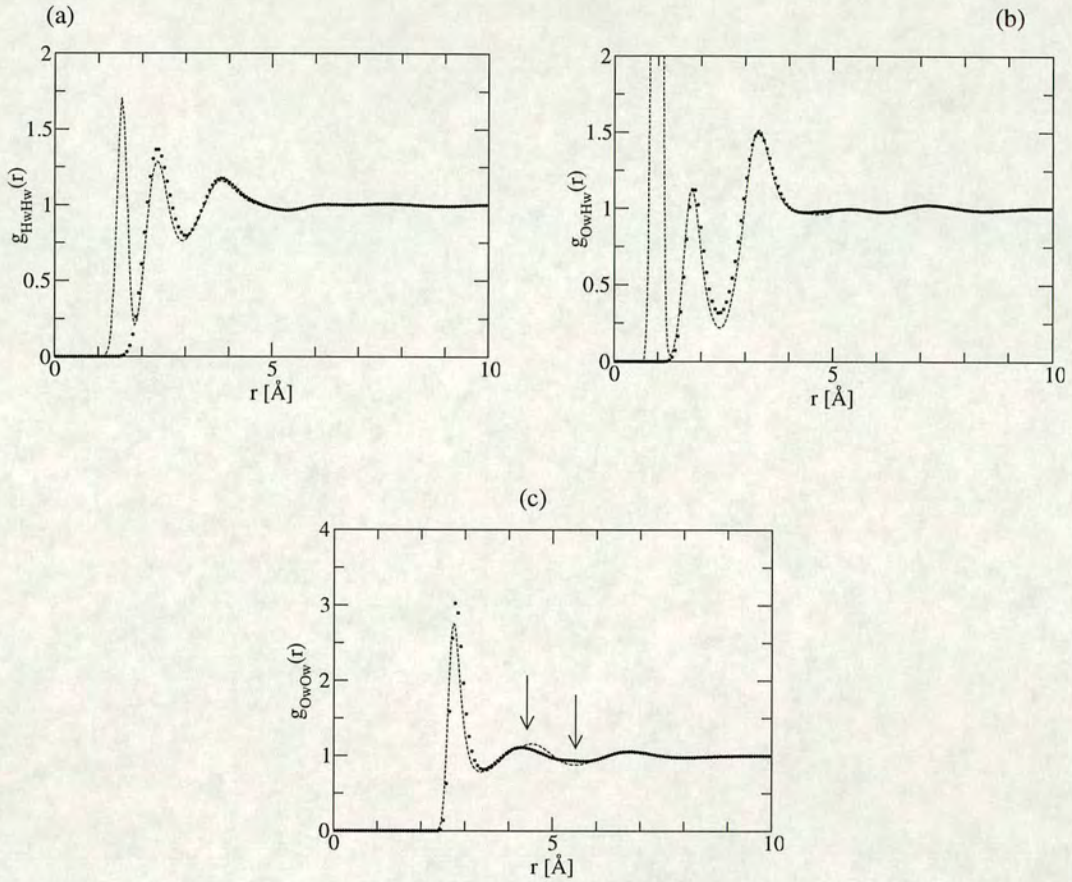

Figure 6.5: (a)HwHw, (b)OwHw and (c)OwOw partial radial distribution functions determined by the EPSR procedure for the 1:19 methanol-water mixture. These functions provide information on water-water hydrogen bond interactions. The corresponding functions for pure water are shown as dashed lines [99]. Intramolecular peaks in the pure water data are not present in the partials from the EPSR analysis.

of t-butanol, it is tempting to suggest this water perturbation may be relevant in the context of the entropic driving force of the hydrophobic interaction. This point is revisited below in the context of the orientational correlations determined in this system.

6.3.4 Orientational distribution functions and spatial density plots

The partial pair correlation functions give orientationally averaged structural information. With the EPSR ensembles available, we can look also at orientational correlation functions. This gives information relating to the way in which molecules interact, and can thus throw more light on the structures and the nature of the intermolecular interactions involved in this model system. The coordinate system used to define these correlations has been shown in fig. 5.10. As in the 7:3 methanol-water study we consider two kinds of orientation functions. First, the spatial density function is defined as the density of neighbouring molecular centres as a function of distance and direction away from a central molecule. The orientational distribution function is plotted along one direction in the spatial density function, and represents the density of neighbouring molecules as a function of their orientation and distance relative to a central molecule. In the figures shown here these densities and correlations have been averaged over the rotation of the molecules about their axes (the O-C bond for methanol and the bisector of the H-O-H angle for water).

6.3.4.1 Solute-Solute Correlations

Fig 6.6 shows the spatial densities of methanol molecules about a reference methanol molecule. A pronounced and largely continuous lobe is noted between $\theta_l = 0°$ and $\pm 90°$. This corresponds to inter methanol interaction via the methyl head group. There is hardly any intensity in the lower hemisphere which is expected since, as discussed above, there are negligibly few inter-methanol hydrogen bonds. To understand how methanol molecules in the first solvation shell of a reference methanol molecule orient, three orientational distribution functions were examined, one at $\theta_l = 0°$, one at $\theta_l = 45°$ and the last one at $\theta_l = 90°$. These are shown in fig. 6.7a, 6.7b and 6.7c respectively. From fig. 6.7a, for an approach at $\theta_l = 0°$, i.e. directly above the methyl group on the reference molecule, we

see strong lobes in the θ_m=$\pm$90° direction. These tell us that the dominant orientation of the O-C vector of methanol molecules in the first solvation shell is edge-wise. This is similar to the conclusion drawn earlier from consideration of the position of the second peak of the OO partial correlation function (fig.6.2b).

This preferential orientation is different from that reported by Bowron *at el* for the preferred approach geometry of the alcohol molecules in a 0.06 mole fraction mixture of tertiary butanol in water. In their report by Bowron *at el* [61], the highest intensity lobe was in the $\theta_m = 180°$ direction in the equivalent of fig. 6.7a, indicating a preference for the head-on (C-O vectors at 180°) rather than side-on (C-O vectors at 90°). The reasons for this difference relate to differences in the structure of the methyl and tertiary butyl groups. Both intermolecular orientations aim to maximise the contact area between the nonpolar alkyl groups.

For an approach angle of $\theta_l = 45°$ (fig. 6.7b), the orientation of the OC vectors is quite mixed with brighter lobes around the angular directions of $\theta_m = 135°$* and $\theta_m = -60°$. A hydroxyl group to methyl group is not favoured at all as noted from the lack of intensity around the $\theta_m = 45°$.

For an approach angle of $\theta_l = 90°$ (fig. 6.7c), the O-C vectors of methanols in the first solvation sample a wide range of angular orientations in a crescent from $\theta_m = 0°$ through $-90°$ to 180°. These orientations correspond to the C-O vectors moving from parallel, through perpendicular, to anti parallel. The lack of intensity in the +90°) direction shows yet again that a polar-apolar contact is not favoured.

Again, it is important to remember that the solute-solute intermolecular correlations are determined from the configurations generated from the EPSR simulations. Hence, given the low concentration of methanol and the fact that there are slight deviations at intermediate Q in the XX composite partial structure factors, these 2D plots may show more disorder than is actually present in the sample.

*The coordinate system is the same as the one used to explain methanol orientations in the previous chapter.

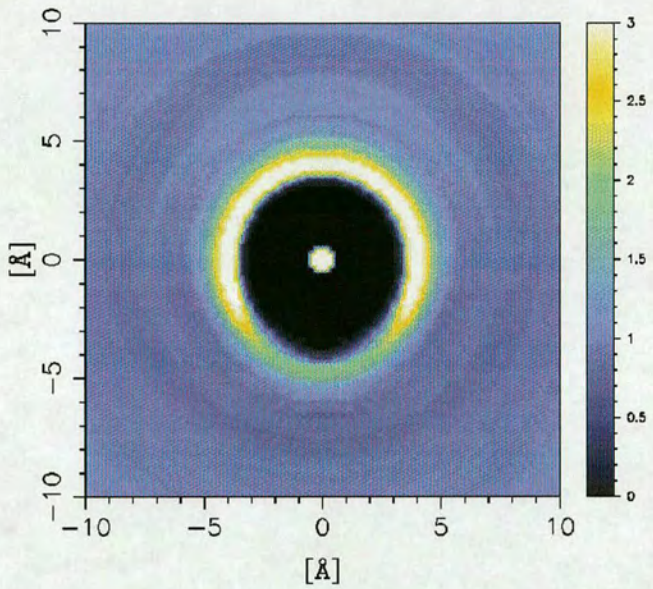

Intermethanol interactions via methyl group

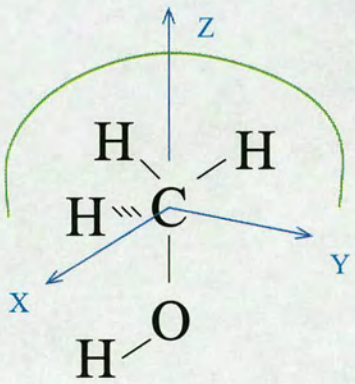

Figure 6.6: (a)Average intermolecular spatial density map of neighbouring methanol molecular centres around a central methanol molecule in the 1:19 methanol-water mixture as a function of (r,θ_1) after averaging over rotations about the O-C axis on both molecules.

6.3.4.2 Solute-Solvent Correlations

The spatial densities of water molecules about a reference methanol are shown in fig. 6.8. The lobes of high density at the 5 o'clock and 7 o'clock positions

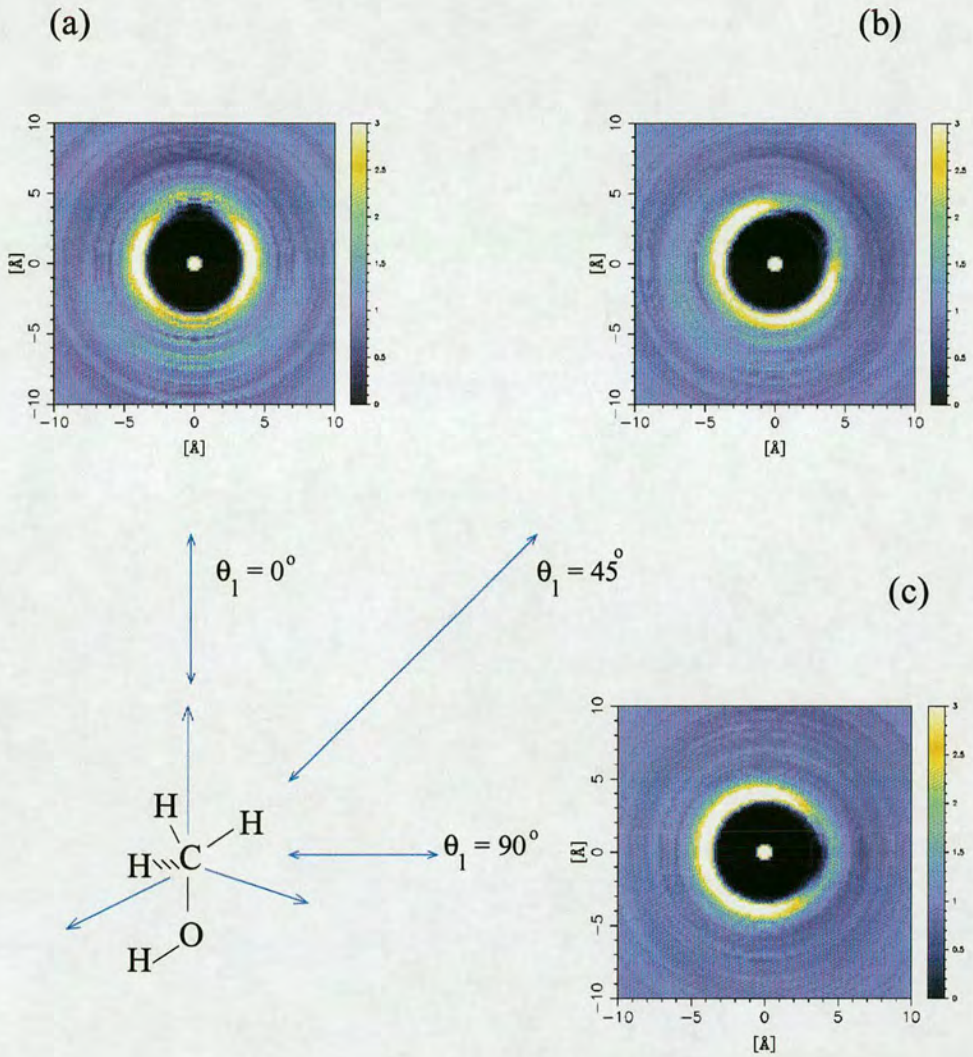

Figure 6.7: (a) Orientational distribution map of the methanol OC vector around a central methanol molecule in the 1:19 methanol-water mixture as a function of (r,θ_m) with $\theta_l = 0°$ after averaging over rotations about the O-C axis on both molecules. (b) same as in frame (a) but with $\theta_l = 45°$; (c) same as in frame(a) but with $\theta_l = 90°$.

indicate water molecules hydrogen bonded to the methanol hydroxyl group. The more diffuse density between the 2 o'clock and 10 o'clock positions are due to water molecules hydrating the methyl group of the reference methanol.

Fig. 6.9 shows the orientations of water dipole moments in the first hydration shell

at $\theta_l = 45°$. The two intense lobes correspond to water molecules in the methyl group hydration shell with their dipole moments preferring to be tangential to an imaginary sphere centred on the methyl carbon. This is the familiar tangential orientation reported first experimentally by Soper and Finney [13], and seen in a number of subsequent experiments on non-polar group hydration [58, 61, 109]. The presence of these hydration shell water molecules suggests a methyl group - methyl group hydrophobic interaction which occurs with the water molecules in their close proximity. This undoubtedly prevents the methyl groups from contacting as closely as their van der Waals interaction would let them (approx 3.8 $\AA$).

6.3.4.3 Solvent-Solvent Correlations

The final spatial density function to be discussed is that of water correlations. This is shown in fig. 6.10a for pure water and in fig. 6.10b for the 1:19 methanol-water mixture. The tetrahedral nature of the first shell is obvious in both cases, which show very similar distributions, confirming the water-water first shell structures are essentially the same. Recalling the discussion earlier, comments on the differences *at the second neighbour level* between bulk water and the methanol-water mixture have been made.

From the spatial density plots two further observations are made. First, the second neighbour lobes in the bulk water case are almost continuous around the ring: there is significantly lower intensity at 45° and at subsequent 90° intervals. In contrast, the lobes for the mixture case are less continuous, with particularly noticeable gaps at ±45°. Again, a similar increased localisation at second neighbour level was noted by Bowron *et al* on a 0.06 mole fraction sample of tertiary-butanol in water [61]. Thus, these results provide further evidence of a second shell perturbation, here in a system that has a much smaller nonpolar head group. It is actually difficult to make direct comparisons of the coordination numbers obtained from the OwOw partial radial distribution function, $g_{OwOw}(r)$

for the mixture and pure water since in the former case the upper limit for the integration of g(r) extends to nearly 5.76 Å where as for pure water this value is closer to 5.58 Å . Thus the coordination numbers reported for the mixture include the weak intensity seen between the second and third coordination shells of $g_{OwOw}(r)$ which was pointed out earlier. At first glance however, there appears to be no significant change in the numbers (see tables 5.6 and 6.3).

The non-zero density beyond the second shell at $\pm 45°$ which gives rise to the weak intensity between the second and third coordination shells of $g_{OwOw}(r)$ could relate to the reduction in intensity in the second neighbour ring at these θ_l values and indicate a further localisation of the water structure. It would be interesting to determine whether this perturbation is noted in future diffraction studies of other solutes in aqueous mixtures.

6.4 Discussion

While the thermodynamic properties of water - methanol mixtures in the dilute concentration region (i.e. where there is enough water to form an extended network like that present in pure water) are remarkably similar to aqueous solutions of non polar solutes [1], solutes like methanol have a polar group (-OH) which aid in the miscibility of the solutes in water. In spite of the presence of the polar group, traditional views argue that the non polar groups of such simple amphiphilic solutes impose a more ordered structure on the surrounding water molecules [5, 45, 46]. This restructuring of water molecules which goes into cavity formation in the water network to accommodate the solute is entropically unfavourable. However recent experimental reports which have examined the HwHw pair correlation function in such aqueous solutions show a negligible perturbation of the solvent in the presence of the solute compared to pure water [13, 58, 61, 109]. Since the present experiment was performed on a 1:19 mixture, all the water molecules in the aqueous solution are involved in the hydration of a methanol molecule since the $g_{COw}(r)$ yielded a first shell coordination number of

around 16. Hence the $g_{OwOw}(r)$ consists of correlations between water molecules in the hydration shell of methanol. The present results show that while the water molecules do form a loose cage around the methyl group, there is no discernible enhancement of water structure in the mixture as compared to pure water in complete agreement with all the previous results. Some mild changes were noted in the OwHw and OwOw pair correlations in the form of the position of the first peak moving outwards slightly.

The hydrophobic interaction dictates the association of methanol molecules in this mixture. Indeed, the methanol molecules show a tendency to preferentially self associate, an association which is driven by the methyl group interaction. On an average, the methyl groups form clusters of around 3 molecules. Recent investigations of alcohol-water mixtures using theoretical approaches concluded that in dilute alcohol - water mixtures small clusters (dimers,trimers) of alcohols can be present [110, 111]. Thus the present results provide experimental evidence to support conclusions from theoretical treatments used to understand the structure of alcohol-water mixtures. A similar cluster size was also observed in a dilute tertiary butanol-water mixture [61]. In the present study the hydrophobic interaction between the methyl groups occurs in the presence of hydration shell water molecules which govern the geometries of the contacting methyl groups. An interesting future direction of analysis would be to interrogate the distribution of these cluster sizes in the methanol and tertiary butanol aqueous systems to understand how cooperative the alkyl group interaction can be in these simple amphiphilic - water systems.

A potentially significant observation from the present data is the perturbation noted in the second coordination shell of the OwOw pair correlations. Since similar effects have been observed in a dilute tertiary butanol - water mixture [61] and a dilute dimethyl sulfoxide - water mixture [112] a common theme emerging from these investigations is that these amphiphilic solutes indeed perturb the water structure but in a way not anticipated from the old views of hydration of non polar groups in dilute aqueous mixtures. It is remarkable that a similar

effect, although of a much larger magnitude, is also observed in structure studies of pure water under high pressures where a collapse of the second shell is observed [7]. Even concentrated aqueous salt solutions show a perturbed water structure at the second neighbour level [8]. Clearly the trends noted so far imply that the water structure responds to perturbation (pressure, amphiphilic solutes, salts) via a structural response which results in an entropic loss to the water through a restriction in its configurational freedom, but at the second neighbour level of the water-water correlations.

An interesting future line of investigation will necessarily involve the determination the *exact* source of this second shell perturbation in the aqueous solutions. Bearing in mind that all solutes studied so far in dilute mixtures with water are mixed solutes (containing both polar and non polar groups) and in light of results reported in high salt concentration aqueous solutions [8], it may be entirely plausible that the mixed solutes perturb the water structure at the second neighbour level due to the presence of the polar group. Indeed, to ascertain whether this conjecture is true, results (structures obtained from the EPSR analysis of the neutron data) from several experiments (methanol, tertiary butanol, dimethyl sulfoxide) need to be examined to extract the water correlation around the polar groups and those around the non polar groups of these solutes. This will perhaps be easier in the latter two solutes since the polar groups (-OH, S=O) are removed from the non polar groups ($(CH_3)_3$, $(CH_3)_2$) spatially. Briefly, such a procedure would involve the separation of water molecules in the first hydration shell of these solutes as either belonging to the polar group environment or the non polar group environment and further determining the OwOw pair correlation function for these two groups over the entire simulation box. This may provide the answer to the above query.

That hydrophobic interactions are operative in these systems (alcohols) is unambiguously established here and elsewhere [61] from the orientational distribution functions. Data for other solutes like acetone and dimethyl sulfoxide is eagerly awaited [113]. It remains to be established whether non polar groups (molecules)

are indeed responsible for the perturbations noted in the most recent neutron data. What is certain however is that the perturbation caused by these solutes results in the water molecules losing orientational freedom. Such water structure perturbation may be extremely important in determining to what extent solute induced structural reorganisation of water is responsible for macromolecular self assembly in aqueous media.

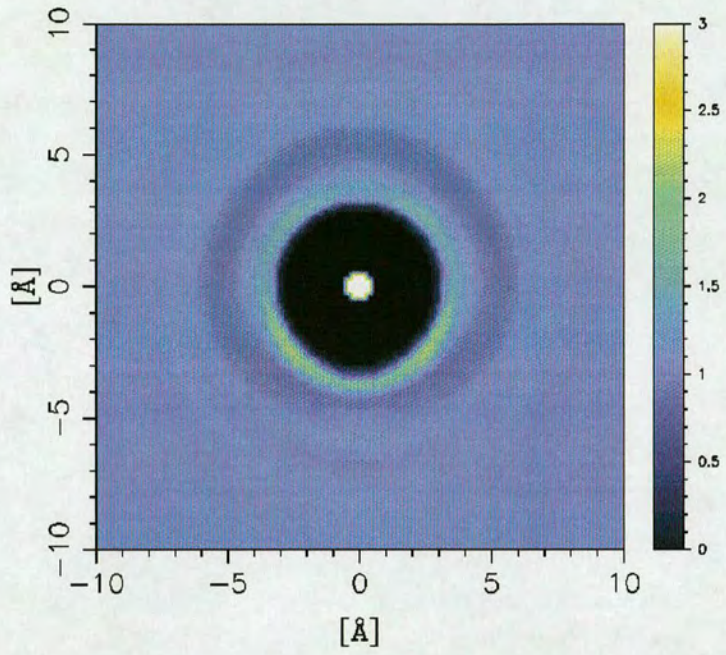

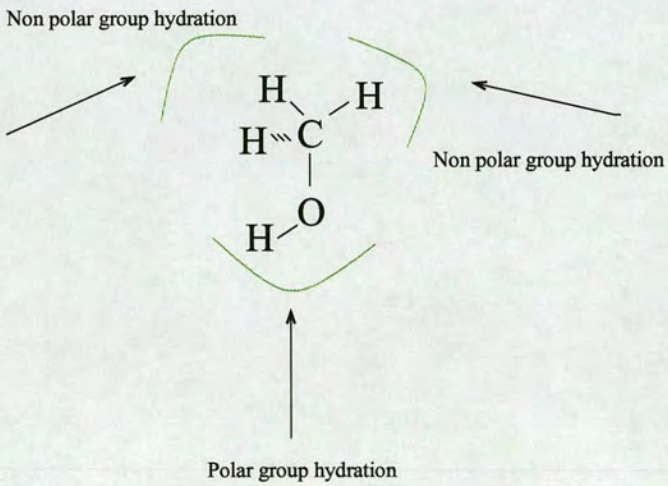

Figure 6.8: Average intermolecular spatial density map of neighbouring water molecular centres around a central methanol molecule in the 1:19 methanol-water mixture as a function of (r,θ_1) after averaging over rotations about the O-C axis of the reference methanol molecule and the water dipole moment. The schematic below the map shows the distribution of the water molecules around both ends of the reference methanol molecule.

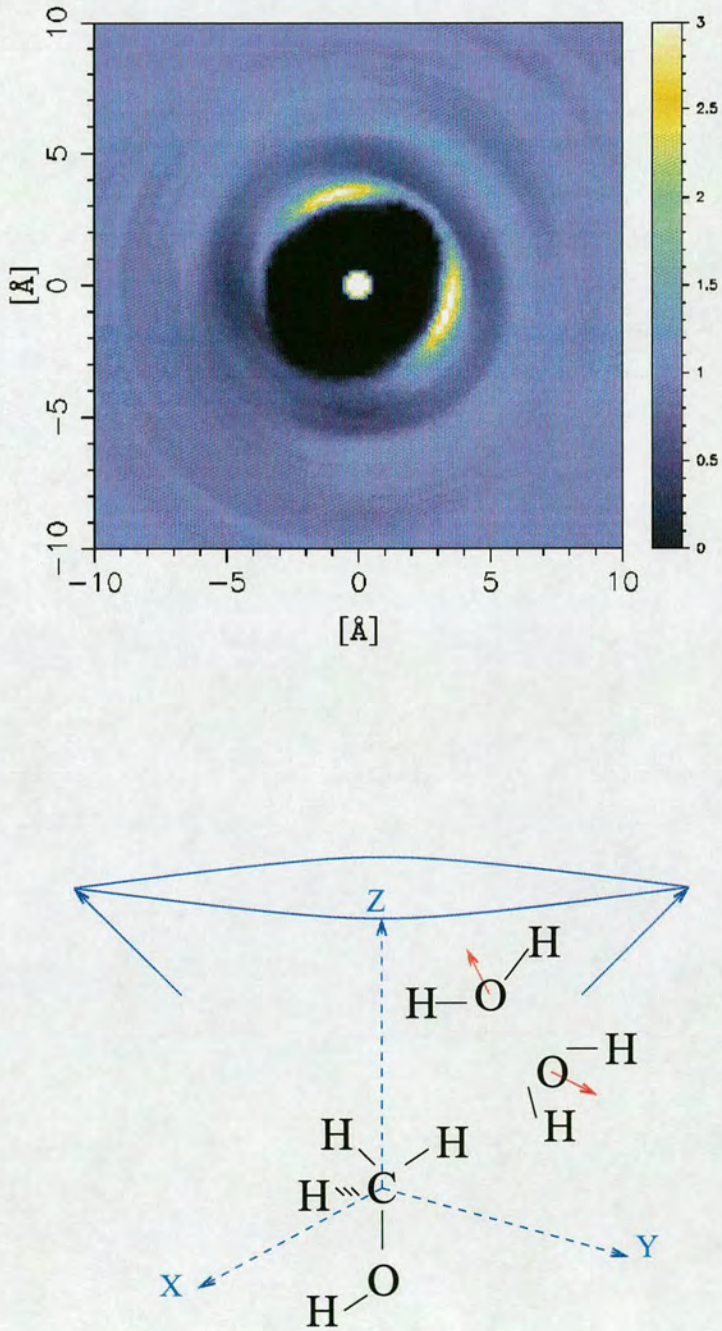

Figure 6.9: Orientational distribution map of the water dipole moment vector around a central methanol molecule in the 1:19 methanol-water mixture as a function of (r,θ_m) with $\theta_l = 45°$ after averaging over rotations about the O-C axis of the reference methanol molecule and the water dipole moment. The schematic below the map shows the *tangential* orientation of the water molecules around the methyl group of the reference methanol as a visual aid to understand the map.

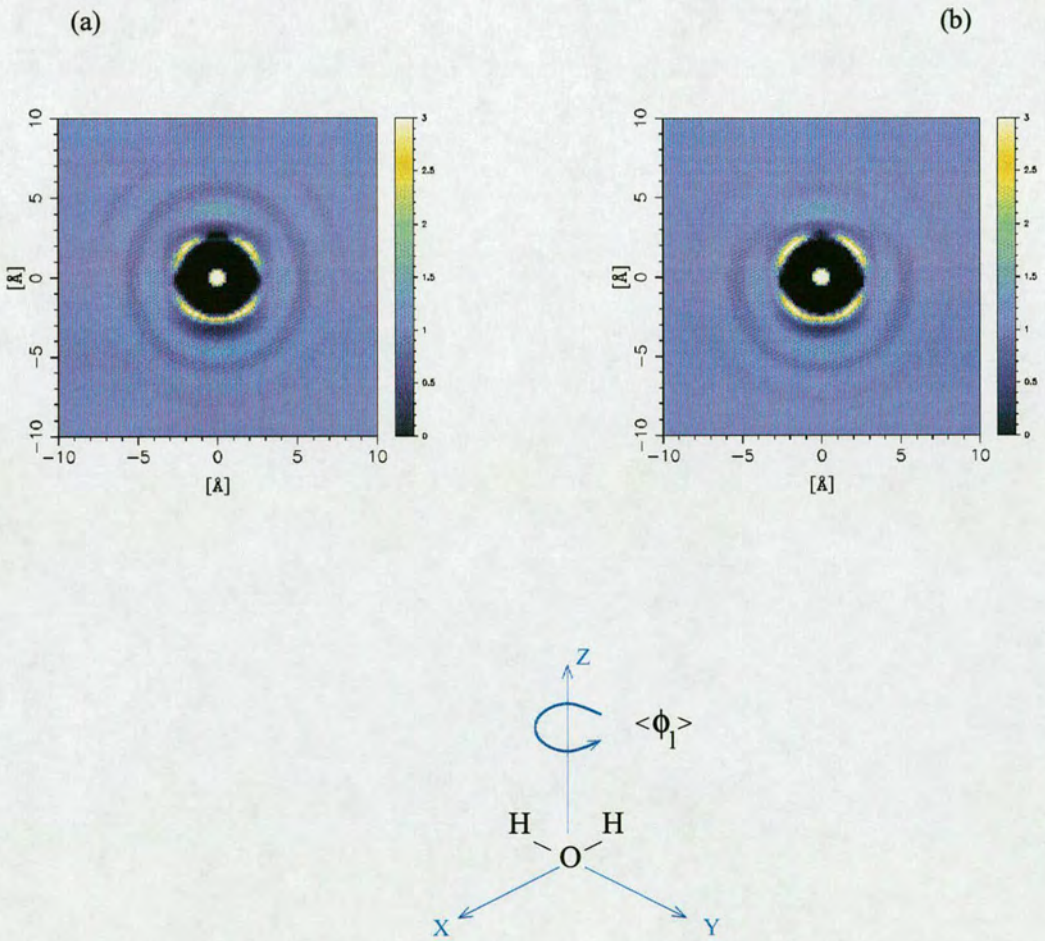

Figure 6.10: (a)Average intermolecular spatial density map of neighbouring water molecular centres around a central water molecule in pure water as a function of (r,θ_1) after averaging over rotations about the water dipole moment on both molecules; (b) Same as in frame (a) but for the 1:19 methanol-water mixture

Chapter 7

Conclusions

Here, a summary of the main conclusions drawn from the work presented in this thesis is accompanied with suggestions for possible avenues that can be explored further in the study of simple model systems of aqueous solutions.

7.1 Conclusions

The most important results from this thesis is that methanol and water do not mix homogeneously. In the concentrated 0.7 mole fraction methanol in water mixture, the water molecules were found to self associate preferentially and anchor strongly to the methanol hydroxyl group. This structural observation is in complete disagreement with all previous work which claimed that the water structure would be completely destroyed and the water molecules would be dispersed randomly in methanol. This preference of the water molecules to self associate results in the chain structure of methanol being broken down. This provides the water molecules with hydrogen bonding sites on the methanol hydroxyl group and shields them from the hydrocarbon rich methyl group environment. Since the hydrogen bonds between the methanol molecules are broken, the methyl groups get significantly more orientational freedom which helps them to form a dense methyl

fluid which isolates the water molecules.

In the dilute 0.05 methanol in water mixture, the methanol molecules are found to retain their tendency to associate via their methyl groups. This is a clear structural signature of the hydrophobic interaction. However, the water molecules are seen to hydrate the methyl group significantly thereby restricting their direct contact. Hence there is a solvent mediated component which acts against the methanol molecules from forming direct contact configurations. Methanol affects the water structure significantly at the level of second neighbours. The orientational freedom of water molecules is arrested in the second shell of water correlations which is also accompanied by a compression of this shell. A new feature is also seen in the water structure as an intensity between the second and third shell coordinations in the extended water network which is absent in pure water. These perturbations are not anything like those predicted by the standard iceberg model. In fact, the methanol molecules seem to perturb the extend network of water in the dilute mixture towards more disorder. Hence, the loss in entropy observed in experimental calorimetric measurements of dilute methanol-water mixtures has different microscopic origins. The observations noted in the present work indicate one source, i.e. the restriction of the orientational freedom of water due to cavity formation to accommodate the solute.

7.2 Directions for Future Work

To begin with, it is suggested that for dilute aqueous solutions, the problem of removal of inelastic scattering from neutron data has to be addressed prior to any data modelling process more carefully. The work presented here indicates that higher order polynomials may improve the inelasticity corrections. Further, it is recommended that the EPSR simulation may be needed to run longer to collect better statistics on the solute correlations.

There are several new avenues to explore given that a fairly detailed picture has

now emerged on the structure of methanol-water mixtures. The first is to perform one experiment at an intermediate concentration, where the water molecules are just beginning to hydrate the methyl groups of the methanol molecules, this would be the onset of solvent mediated methyl group interactions.

Next, the methanol-water system would be a simple system to study the effects of pressure on the hydration of this amphiphile-like molecule. Pressure is being increasingly used as a thermodynamic variable to study self assembly.

It would be immensely useful to study some chemically diverse prototypical mixed solutes like acetone, dimethyl sulfoxide and methylamine using neutron scattering. This would give a molecular level understanding of the hydration of different polar groups and how the presence of the nonpolar groups affects the dominant intermolecular interaction between these solutes in water. Given that the structure of these liquids (acetone, dimethyl sulfoxide) is dominated by dipolar interaction rather than hydrogen bond interaction as in the case of methanol there may or may not be inhomogeneous mixing in these aqueous mixtures. Only key concentrations should be investigated, i.e. spectroscopic (Raman, NMR, Dielectric measurements) techniques should be used to determine which concentrations would be most suitable to observe inhomogeneous mixing. Also, it would be interesting to perform scattering experiments to study the effects of salts on the hydrophobic interaction between mixed solutes.

It will be sometime before complex macromolecular self assembly problems like protein folding are actually solved. Simple model systems will provide the necessary microscopic details of the sensitivity of chemically diverse molecular groups to the presence of water as well as their influence on the structure of water. However, this is only part of the entire jigsaw. We still know very little about the physics that bridges the microscopic and macroscopic length scales in self assembly processes. It is clear that the response of water to the presence of these solutes is important for the process of self assembly. What is not clear however is whether the response of water to the presence of nonpolar species is a local one.

Further, it has only recently been demonstrated that the presence of extended nonpolar regions result in a totally different response of water and a drying effect is predicted from current theoretical investigations.

It appears that answers to questions pertaining to hydration at nanometer length scales will easily be the next step and is bound to stir the scientific community into the realm of the unknown.

List of Figures

List of Tables

Bibliography

[1] F. Franks, *Water: A Comprehensive Treatise, Volume 2* (Plenum Press, New York, U.S.A, 1973).

[2] E. Matteoli and L. Lepori, *Solute-Solute Interactions in Water. II. An Analysis Through the Kirkwood-Buff Integrals for 14 Organic Solutes*, J. Chem. Phys. **80**, 2856 (1984).

[3] C. Tanford, *The Hydrophobic Effect: Formation of Micelles and Biological Membranes* (Krieger Publishing Company, Florida, U.S.A, 1991).

[4] W. Kauzmann, *Some Factors in the Interpretation of Protein Denaturation*, Advan. Protein Chem. **14**, 1 (1959).

[5] H. S. Frank and M. W. Evans, *Entropy in Binary Liquid Mixtures; Partial Molal Entropy in Dilute Solutions; Structure and Thermodynamics in Aqueous Electrolytes*, J. Chem. Phys. **13**, 507 (1945).

[6] B. W. Blokzijl and J. B. F. N. Engberts, *Hydrophobic effects. Opinions and Facts*, Angew. Chem. Int. Ed. Engl **32**, 1545 (1993).

[7] A. K. Soper and M. A. Ricci, *Structures of High-Density and Low-Density Water*, Phys. Rev. Lett. **84**, 2881 (2000).

[8] R. Leberman and A. K. Soper, *Effect of High Salt Concentrations on the Water-Structure*, Nature **378**, 364 (1996).

[9] K. Egashira and N. Nishi, *Low-Frequency Raman Spectroscopy of Ethanol-Water Binary Solution: Evidence for Self-Association of Solute and Solvent Molecules*, J. Phys. Chem. B. **102**, 4054 (1998).

[10] K. Yoshida and T. Yamaguchi, *Low-Frequency Raman Spectroscopy of Aqueous Solutions of Aliphatic Alcohols*, Z. Naturfors. Sect. A-J. Phys. Sci. **56**, 529 (2001).

[11] J. Israelachvili, *Intermolecular and Surface Forces* (Academic Press Limited, San Diego, CA, U.S.A, 1991).

[12] D. Bowron, A. Filipponi, M. A. Roberts and J. L. Finney, *Hydrophobic Hydration and Formation of a Clathrate Hydrate*, Phys. Rev. Lett. **81**, 4164 (1998).

[13] A. K. Soper and J. L. Finney, *Hydration of Methanol in Aqueous Solution*, Phys. Rev. Lett **71**, 4346 (1993).

[14] N. E. Cusack, *The Physics of Structurally Disordered Matter: An Introduction* (IOP Publishing Ltd., Bristol, U.K., 1987).

[15] B. Lee, *The Physical Origins of the Low Solubility of Non Polar Solutes in Water*, Biopolymers **24**, 813 (1985).

[16] R. A. Pierotti, *Aqueous Solutions of Nonpolar Gases*, J. Phys. Chem. **69**, 281 (1965).

[17] B. Lee, *Analysing Solvent Reorganisation and Hydrophobicity*, Methods Enzymol. **259**, 255 (1995).

[18] B. Lee, *Enthalpy-Entropy Compensation in the Thermodynamics of Hydrophobicity*, Biophys. Chem. **51**, 271 (1994).

[19] G. Graziano and G. Barone, *Group Additivity Analysis of the Heat Capacity Changes Associated with the Dissolution into Water of Different Organic Compounds*, J. Am. Chem. Soc. **118**, 1831 (1996).

[20] G. Graziano, *On the Size Dependence of Hydrophobic Hydration*, J. Chem. Soc. -Faraday Trans. **94**, 3345 (1998).

[21] G. Graziano, *Hydration Thermodynamics of Aliphatic Alcohols*, Phys. Chem. Chem. Phys. **1**, 3567 (1999).

[22] P. A. Egelstaff, *An Introduction to the Liquid State* (Oxford University Press, New York, U.S.A, 1992).

[23] T. Lazaridis and M. E. Paulaitis, *Simulation Studies of the Hydration Entropy of Simple, Hydrophobic solutes*, J. Phys. Chem. **98**, 635 (1994).

[24] H. S. Ashbaugh and M. E. Paulaitis, *Entropy of Hydrophobic Hydration: Extension to Hydrocarbon Chains*, J. Phys. Chem. **100**, 1900 (1996).

[25] M. E. Paulaitis, S. Garde and H. S. Ashbaugh, *The Hydrophobic Effect*, Curr. Opin. Coll. Int. Sc. **1**, 376 (1996).

[26] M. E. Paulaitis, *Molecular Thermodynamics of Hydrophobic Effects*, Curr. Opin. Coll. Int. Sc. **2**, 315 (1997).

[27] G. Hummer, S. Garde, A. E. Garcia, A. Pohorile and L. R. Pratt, *An Information Theory Model of Hydrophobic Interactions*, Proc. Natl. Acad. Sci. USA **93**, 8951 (1996).

[28] G. Hummer, S. Garde, A. E. Garcia, M. E. Paulaitis and L. R. Pratt, *Hydrophobic Effects on a Molecular Scale*, J. Phys. Chem. B. **102**, 10469 (1998).

[29] N. T. Skipper, *Computer Simulations of Methane Water Solutions - Evidence for a Temperature Dependent Hydrophobic Attraction*, Chem. Phys. Lett. **207**, 424 (1993).

[30] N. T. Skipper, C. H. Bridgeman, A. D. Buckingham and R. L. Mancera, *Computer Simulation Studies of the Hydration and Aggregation of Simple Hydrophobic Molecules*, Faraday Discuss. **103**, 141 (1996).

[31] S. Ludemann, H. Schreiber, R. Abseher and O. Steinhauser, *Influence of Temperature on Pairwise Hydrophobic Interactions of Methane Particles: A Molecular Dynamics Study of Free Energy*, J. Chem. Phys. **104**, 286 (1996).

[32] R. L. Mancera, A. D. Buckingham and N. T. Skipper, *The Aggregation of Methane in Aqueous Solution*, J. Chem. Soc. Faraday Trans. **93**, 2263 (1997).

[33] R. L. Mancera, *Hydrogen Bonding Behaviour in the Hydrophobic Hydration of Simple Hydrocarbons*, J. Chem. Soc. -Faraday Trans. **92**, 2547 (1996).

[34] K. A. T. Silverstien, A. D. J. Haymet and K. A. Dill, *Strength of Hydrogen Bonds in Liquid Water and Around Non Polar Solutes*, J. Am. Chem. Soc. **122**, 8037 (2000).

[35] J. Hernández-Cobos, A. D. Mackie and L. F. Vega, *The Hydrophobic Hydration of Methane as a Function of Temperature from Histogram Reweighting Monte Carle Simulations*, J. Chem. Phys. **114**, 7527 (2001).

[36] R. D. Mountain and D. Thirumalai, *Hydration for a Series of Hydrocarbons*, Proc. Natl. Acad. Sci. USA **95**, 8436 (1998).

[37] S. R. Durell and A. Wallqvist, *Atomic Scale Analysis of the Solvation Thermodynamics of Hydrophobic Hydration*, Biophys. J. **71**, 1695 (1996).

[38] K. A. Sharp and B. Madan, *Hydrophobic Effect, Water Structure, and Heat Capacity Changes*, J. Phys. Chem. B. **101**, 4343 (1997).

[39] T. Lazaridis, *Solvent Reorganisation Energy and Entropy in Hydrophobic Hydration*, J. Phys. Chem. B. **104**, 4964 (2000).

[40] T. M. Raschke, J. Tsai and M. Levitt, *Quantification of the Hydrophobic Interaction by Simulations of the Aggregation of Small Hydrophobic Solutes in Water*, Proc. Natl. Acad. Sci. USA **98**, 5965 (2001).

[41] J. A. Rank and D. Baker, *A Desolvation Barrier to Hydrophobic Cluster Formation May Contribute to the Rate-Limiting Step in Protein Folding*, Protein Sc. **6**, 347 (1997).

[42] J. A. Rank and D. Baker, *Contributions of Solvent-Solvent Hydrogen Bonding and Van Der Waals interactions to the Attraction Between Methane Molecules in Water*, Biophys. Chem. **71**, 199 (1998).

[43] L. R. Pratt and A. R. Pohorille, *Theory of Hydrophobicity - Transient Cavities in Molecular Liquids*, Proc. Natl. Acad. Sci. USA **89**, 2995 (1992).

[44] B. Madan and B. Lee, *Role of Hydrogen Bonds in Hydrophobicity: The Free Energy of Cavity Formation in Water Models with and without Hydrogen bonds*, Biophys. Chem. **51**, 279 (1994).

[45] S. H. Tanaka, H. I. Yoshihara, A. W. C. Ho, F. W. Lau, P. Westh and Y. Koga, *Excess Partial Molal Enthalpies of Alkane-mono-ols in Aqueous Solutions*, Can. J. Chem. **74**, 713 (1996).

[46] K. Tamura, J. H. Hu, C. Trandum, P. Westh, C. A. Haynes and Y. Koga, *Mixing Scheme of Aqueous Butan-1-ol in the Water-Rich region at 25 Degrees C: Excess Chemical Potential, Partial Molar Enthalpy, Entropy and Volume, Heat Capacity, Compressibility and Thermal Expansivity*, Phys. Chem. Chem. Phys. **2**, 355 (2000).

[47] J. Hernández-CobosJ and I. Ortega-Blake, *Hydrophobic Hydration in Methanol Aqueous Solutions*, J. Chem. Phys. **103**, 9261 (1995).

[48] J. Fidler and P. M. Rodger, *Solvation Structure Around Aqueous Alcohols*, J. Phys. Chem. B. **103**, 7695 (1997).

[49] P. G. Kusalik, D. Bergman and A. Laaksonen, *The Liquid Structure in Liquid Methylamine and Methylamine-water Mixtures*, J. Chem. Phys. **113**, 8036 (2000).

[50] S. Shimizu and H. S. Chan, *Statistical Mechanics of Solvophobic Aggregation: Additive and Cooperative Effects*, J. Chem. Phys. **115**, 3424 (2001).

[51] S. R. Durell, B. R. Brooks and A. Bennaim, *Solvent Induced Forces Between Two Hydrophilic Groups*, J. Phys. Chem. **98**, 2198 (1994).

[52] S. Shimizu and H. S. Chan, *Anti-Cooperativity in Hydrophobic Interactions: A Simulation Study ofSpatial Dependence of Three-Body Effects and Beyond*, J. Chem. Phys. **115**, 1414 (2001).

[53] C. G. Windsor, *Pulsed Neutron Scattering* (Taylor and Francis, London, U.K., 1981).

[54] J. L. Finney and A. K. Soper, *Solvent Structure and Perturbations in Solutions of Chemical and Biological Importance*, Chem. Soc. Rev. **1**, 23 (1994).

[55] A. K. Soper, *The Quest for the Structure of Water and Aqueous Solutions*, J. Phys.: Condens. Matter **9**, 2717 (1997).

[56] A. K. Soper, *Empirical Potential Monte Carlo Simulation of Fluid Strucutre*, Chem. Phys. **202**, 295 (1996).

[57] J. Turner, A. Soper and J. Finney, *Ionic Versus Apolar Behaviour of the Tetramethyl Ammonium Ion in Water*, J. Chem. Phys **102**, 5438 (1995).

[58] J. Turner and A. K. Soper, *The Effect of Apolar SOlutes on Water-Structure - Alcohols and Tetraalkylammonium ions*, J. Chem. Phys. **101**, 6116 (1994).

[59] D. T. Bowron, J. L. Finney and A. K. Soper, *Structural Investigations of Solute-Solute Interactions in Aqueous Solutions of Tertiary Butanol*, J. Phys. Chem. B **102**, 3551 (1998).

[60] J. L. Finney, D. T. Bowron and A. K. Soper, *The Structure of Aqueous Solutions of Tertiary Butanol*, J. Phys.: Condens. Matter **12**, A123 (2000).

[61] D. T. Bowron, A. K. Soper and J. L. Finney, *Temperature Dependence of the Structure of a 0.06 Mole Fraction Tertiary Butanol-Water Solution*, J. Chem. Phys. **114**, 6203 (2001).

[62] A. K. Soper and A. Luzar, *A Neutron Diffraction Study of Dimethyl Sulphoxide - Water Mixtures*, J. Phys. Chem. **100**, 1357 (1996).

[63] A. K. Soper, *The Excluded Volume Effect in Confined Fluids and Liquid Mixtures*, J. Phys.: Condens. Matter **9**, 2399 (1997).

[64] C. A. Koh, R. P. Wisbey, X. Wu, R. E. Westacott and A. K. Soper, *Water Ordering Around Methane During Hydrate Formation*, J. Chem. Phys. **113**, 6390 (2000).

[65] K. Lum, D. Chandler and J. D. Weeks, *Hydrophobicity at Small and Large Length Scales*, J. Phys. Chem. B. **103**, 4570 (1999).

[66] N. T. Southall and K. Dill, *The Mechanism of Hydrophobic Solvation Depends on Solute Radius*, J. Phys. Chem. B. **104**, 1326 (2000).

[67] Y. Cheng and P. Rossky, *Surface Topography Dependence of Biomolecular Hydrophobic Hydration*, Nature **392**, 696 (1998).

[68] E. A. F. M. Barton, *Solubility Data Series Vol 15, Alcohols with water* (Pergamon Press, IUPAC, 1984).

[69] C. Perchard and J. P. Perchard, J. Raman. Spec. **3**, 277 (1975).

[70] G. Kabisch and K. Pollmer, *Hydrogen Bonding in Methanol-Organic Solvent and Methanol-Water Mixtured as Studied by the nu-CO and nu-CH Raman Bands*, J. Mol. Struct **81**, 35 (1982).

[71] T. W. Zerda, H. D. Thomas, M. Bradley and J. Jonas, *High Pressure Isotropic Bandwidths and Frequency Shifts of the C-H and C-O Modes of Liquid Methanol*, J. Chem. Phys. **86**, 3219 (1987).

[72] K. Kamogawa and T. Kitagawa, *Solute Solvent and Solvent Solvent Interactions in Methanol Solutions - Quantitative Separation by Raman Difference Spectroscopy*, J. Phys. Chem. **89**, 1531 (1985).

[73] M. D'Angelo, G. Onori and A. Santucci, *Self-Association of Monohydric Alcohols in Water: Compressibility and Infrared Absorption Measurements*, J. Chem. Phys. **100**, 3107 (1993).

[74] C. V. Raman and K. S. Krishnan, *A New Type of Secondary Radiation*, Nature **121**, 501 (1928).

[75] W. G. Rothschild, *Dynamics of Molecular Liquids* (John Wiley and Sons, U.S.A, 1984).

[76] J. Mchale, *Molecular Spectroscopy* (Prentice Hall, New Jersy, U.S.A, 1999).

[77] P. W. Atkins and R. S. Friedman, *Molecular Quantum Mechanics* (Oxford University Press, New York, U.S.A, 1997).

[78] W. Schindler, P. T. Sharko and J. Jonas, *Raman Study of Pressure Effects on Frequencies and Isotropic Line-Shapes in Liquid Acetone*, J. Chem. Phys. **76**, 3493 (1982).

[79] C. H. Wang and J. Mchale, *Vibrational Resonance Coupling and the Non Coincidence Effect of the Isotropic and Anisotropic Raman Spectral Components in Orientationally Anisometric Molecular Liquids*, J. Chem. Phys. **72**, 4039 (1980).

[80] J. Mchale, *The Influence of Angular Dependent Intermolecular Forces on Vibrational Spectra of Solution Phase Molecules*, J. Chem. Phys. **75**, 30 (1981).

[81] H. Torii and M. Tasumi, *Local Order and Transition Dipole Coupling in Liquid Methanol and Acetone as the Origin of the Raman Noncoincidence Effect*, J. Chem. Phys. **99**, 8459 (1993).

[82] T. Yamaguchi, K. Hidaka and A. K. Soper, *Erratum: The Structure of Methanol Revisited: a Neutron Diffraction Experiment at -80°C and +25°C*, Mol. Phys. **97**, 603 (1999).

[83] K. Kamogawa and T. Kitagawa, *Evidence for Direct Intermolecular Interactions as an Origin of the Hydration Shifts of the C-H Stretching Vibrations - 1,4-dioxane Water-System*, Chem. Phys. Lett **179**, 271 (1991).

[84] C. J. Gruenloh, G. M. Florio, J. R. Carney, F. C. Hagemeister and T. S. Zwier, *C-H Stretch Modes as a Probe of H-bonding in Methanol-Containing Clusters*, J. Phys. Chem. A. **103**, 496 (1999).

[85] T. Sato, A. Chiba and R. Nozaki, *Hydrophobic Hydration and Molecular Association in Methanol-Water Mixtures Studied by Microwave Dielectric Analysis*, J. Chem. Phys. **112**, 2924 (2000).

[86] K. Nakanishi, *Partial Molal Volumes of Butyl Alcohols and of Related Compounds in Aqueous Solution*, Bull. Chem. Soc. Japan **33**, 793 (1993).

[87] S. Dixit, W. C. K. Poon and J. Crain, *Hydration of Methanol in Aqueous Solutions: a Raman Spectroscopic Study*, J. Phys.: Cond. Matt. **12**, L323 (2000).

[88] P. M. Chaikin and T. C. Lubensky, *Principles of Condensed Matter Physics* (Cambridge University Press, New York, U.S.A, 1995).

[89] B. H. Bransden and C. J. Joachain, *Introduction to Quantum Mechanics* (Longman Scientific and Technical, U.K, 1989).

[90] L. V. Hove, *Correlations in Space and Time and Born Approximation Scattering in Systems of Interacting Particles*, Phys. Rev. **95**, 249 (1954).

[91] A. K. Soper, W. S. Howells and A. C. Hannon, *ATLAS-Anlysis of Time of Flight Diffraction Data from Liquids and Amorphous Samples* (Rutherford Appleton Laboratory Report RAL 89-046, U.K., 1989).

[92] A. K. Soper and A. Luzar, *A Neutron Diffraction Study of Dimethyl Sulphoxide - Water Mixtures*, J. Chem. Phys **97**, 1320 (1992).

[93] J. E. Enderby and G. W. Neilson, *Water: A Comprehensive Treatise, edited by F. Franks* (Plenum, New York, U.S.A, 1979).

[94] C. G. Gray and K. E. Gubbins, *Theory of Molecular Fluids, Volume 1: Fundamentals* (Clarendon Press, Oxford, U.K., 1984).

[95] A. K. Soper, *Determination of the Orientational Pair Correlation Function of a Molecular Liquid from Diffraction Data*, J. Molec. Liquids **78**, 179 (1998).

[96] M. P. Allen and D. J. Tildesley, *Computer Simulation of Liquids* (Oxford University Press, Oxford, U.K., 1987).

[97] H. J. C. Berendsen, J. R. Grigera and T. P. Straatsma, *The Missing Term in Efefctive Pair Potentials*, J. Phys. Chem. **91**, 6269 (1987).

[98] M. Haughney, M. Ferrario and I. R. MacDonald, *Molecular-Dynamics Simulation of Liquid Methanol*, J. Phys. Chem. **91**, 4934 (1987).

[99] A. K. Soper, *The Radial distribution functions of Water and Ice from 220 to 673 K and at Pressures up to 400 Mpa*, Chem. Phys. **258**, 121 (2000).

[100] T. Yamaguchi, K. Hidaka and A. K. Soper, *The Structure of Methanol Revisited: a Neutron Diffraction Experiment at -80°C and +25°C*, Mol. Phys. **96**, 1159 (1998).

[101] G. Palinkas, E. Hawlicka and K. Heinzinger, *Molecular Dynamics Simulations of Water-Methanol Mixtures*, Chem. Phys. **158**, 65 (1991).

[102] A. Laaksonen, P. G. Kusalik and I. M. Svishchev, *Three-Dimensional Structure in Water-Methanol Mixtures*, J. Phys. Chem. A. **101**, 5910 (1997).

[103] H. Tanaka and K. E. Gubbins, *Structure and Thermodynamic Properties of Water-Water Mixtures: Role of the Water-Water Interaction*, J. Chem. Phys. **97**, 2626 (1992).

[104] M. Ferrario, M. Haughney, I. R. MacDonald and M. L. Klein, *Molecular Dynamics Simulations of Aqueous Mixtures: Methanol, Acetone and Ammonia*, J. Chem. Phys. **93**, 5156 (1990).

[105] S. Dixit, J. Crain, W. C. K. Poon, J. L. Finney and A. K. Soper, *Molecular Scale Immiscibility Observed in a Concentrated Alcohol-Water Solution*, Under Peer Review (2001).

[106] A. Wakisaka, S. Komatsu and Y. Usui, *Solute-Solvent and Solvent-Solvent interactions Evaluated through Clusters Isolated from Solutions: Preferential Solvation in Water-Alcohol Mistures*, J. Molec. Liquids **93**, 5156 (1990).

[107] A. K. Soper and R. N. Silver, *Hydrogen-Hydrogen Pair Correlation Function in Liquid Water*, Phys. Rev. Lett. **49**, 471 (1982).

[108] S. Okazaki, H. Touhara and K. Nakanishi, *Computer Experiments of Aqueous Solutions.V. Monte Carlo Calculation on the Hydrophobic Interaction in 5 Mol % Methanol Solution*, J. Chem. Phys. **81**, 890 (1984).

[109] J. Turner, A. K. Soper and J. L. Finney, *Water Structure in Aqueous-Solutions of Tetramethylammonium Chloride*, Mol. Phys. **77**, 411 (1992).

[110] I. Shulgin and E. Ruckenstein, *Kirkwood-Buff Integrals in Aqueous Alcohol Systems: Aggregation, Correlation Volume, and Local Composition*, J. Phys. Chem. B. **103**, 872 (1999).

[111] I. Shulgin and E. Ruckenstein, *Kirkwood-Buff Integrals in Aqueous Alcohol Systems: Comparison Between Thermodynamic Calculations and X-Ray Scattering Experiments*, J. Phys. Chem. B. **103**, 2496 (1999).

[112] A. K. Soper, *Probing the Structure of Water Around Biological Molecules: Concepts, Constructs and Consequences*, Physica B **276**, 12 (2001).

[113] A. K. Soper, *Private Communication* .

J. Phys.: Condens. Matter **12** (2000) L323–L328. Printed in the UK PII: S0953-8984(00)13406-X

LETTER TO THE EDITOR

Hydration of methanol in aqueous solutions: a Raman spectroscopic study

S Dixit, W C K Poon and J Crain†

Department of Physics and Astronomy, The University of Edinburgh, Mayfield Road, Edinburgh EH9 3JZ, UK

Received 19 April 2000

Abstract. High-resolution Raman spectroscopy was used to study methanol–water mixtures over the whole concentration range. We report a highly non-linear dependence of the carbon–oxygen and carbon–hydrogen stretching frequencies with composition. The difference between the polarized and depolarized frequencies of the carbon–oxygen stretching mode (non-coincidence effect) was also measured. Taken together, the data suggest a global picture of the progressive hydration of methanol: water first breaks up the molecular chains which exist in pure methanol, and then completely hydrates the hydroxyl groups before solvating the hydrophobic methyl groups.

1. Introduction

The importance of hydrogen-bonded liquids in physics, chemistry, biology and technology has kept them at the focus of experimental and theoretical attention for many decades. As prototype hydrogen-bonding molecules, water and methanol (CH_3OH, MeOH) both hold special status. MeOH has another claim to be at the focus of attention—it is one of the simplest amphiphile-like molecules. An *amphiphile* [1] is a bipolar molecule with solvent-loving and solvent-hating moieties, and they self-assemble to form superstructures (micelles, bilayers etc) in highly polar or highly non-polar solvents. Understanding the behaviour of amphiphiles is a central aim of soft-condensed-matter physics. Amphiphiles are also widespread in the chemical industry, e.g. as detergents, and are central to biology, most notably making up cell membranes. MeOH is the simplest amphiphile-like molecule capable of hydrogen bonding. The shortness of its alkyl chain means that MeOH probably does not show conventional self-assembly behaviour. Nevertheless, its clearly bipolar nature means that it can act as the starting point for a fundamental understanding of the solvation of amphiphiles.

There is a considerable literature on MeOH–water mixtures. A popular method of study is computer simulations (e.g. [2–6]). These are aimed at determining the detailed hydrogen-bond structure, but so far have produced conflicting results, partly because of the extreme sensitivity to the model potentials used as inputs. To deal with this problem, the empirical potential structure refinement method was invented in which the potentials themselves are refined against scattering data [7]. Its use on neutron scattering data from an $x = 0.1$ MeOH–water mixture [8] (where x is the mole fraction of methanol) and from neat methanol [9] has produced a picture of the local positional as well as orientational correlations with unprecedented detail.

† Present address: IBM Corporation Research Division, Lab S-73, 1623-14 Shimotsuruma, Yamato, Kanagawa, Japan.

0953-8984/00/210323+06$30.00

Simulations and neutron scattering investigations are both time-consuming methods, and have only been used on a very limited number of concentrations, mostly at high dilution ($x \lesssim 0.1$). Spectroscopy, however, has high throughput, and can easily cover the whole composition range ($0 < x \leqslant 1$). In particular, Raman spectroscopy has been used to monitor the carbon–hydrogen ($\nu_{CH} \approx 2836\ cm^{-1}$ at $x = 1$) and carbon–oxygen ($\nu_{CO} \approx 1036\ cm^{-1}$ at $x = 1$) stretching frequencies. Kabisch and Pollmer [10] found a non-linear dependence of ν_{CO} on x, and interpreted this (in the light of their data on other solute–solvent pairs) in terms of the participation of the MeOH hydroxyl group in donating and accepting hydrogen bonds. Kamogawa and Kitagawa [11] claimed that the shifts in ν_{CH} with x were too small to observe directly with any accuracy, and used an intensity-difference method to give, again, a non-linear dependence, interpreted in terms of intermolecular interactions. Zerda *et al* [12] reported, in a study otherwise devoted to high-pressure effects, that ν_{CO} is a *linear* function of x, contradicting Kabisch and Pollmer [10]. More recently, Kamogawa and Kitagawa reported *both* ν_{CH} and ν_{CO} [13], but did not comment on their correlation. None of these authors use the spectroscopic data to give a *global* picture of the progressive hydration of methanol, concentrating instead on the particulars of hydrogen bonding in special regimes (mostly at small x). Moreover, all of these studies predate two significant recent advances: the neutron scattering data already mentioned [8,9], and an infrared study of ν_{CH} in various MeOH complexes in the gas phase [14].

Below, we report a detailed study of ν_{CH} and ν_{CO} as functions of x. A closely spaced sequence of data points at $x \to 1$ and $x \to 0$ shows that ν_{CH} and ν_{CO} saturate at these two regimes respectively. We correlate the data from the hydrophobic and hydrophilic moieties, and show that they give a consistent overall picture of the progressive hydration of MeOH as x decreases. Our interpretation is corroborated by a measurement of the non-coincidence effect in ν_{CO} (the difference in frequency between the polarized and depolarized components of the mode), by recent neutron scattering data [8] and by the work of Gruenloh *et al* [14]. However, the suggestion that ν_{CH} reflects the hydrogen-bond environment of the hydroxyl group [14] is shown to be incomplete, at least for condensed phases.

2. Experimental procedure

MeOH from Sigma was used as purchased. Deionized water was boiled and passed through a 0.2 Millipore filter. Mixtures were used within 72 hours of being sealed in sample tubes. Raman spectra were excited at room temperature (290 ± 2 K) using 400 mW of the 514.5 nm line of an Ar^+ laser, and analysed at 90° using a Coderg T800 triple-axis spectrometer to 1.2 cm^{-1} resolution. To study the environment of the hydrophilic and hydrophobic ends of the molecule, we monitored ν_{CO} and ν_{CH} respectively†. The incident laser light was always polarized perpendicular to the scattering plane. The scattered light polarized parallel (VV) or perpendicular (VH) to the incident radiation was monitored for ν_{CO}. Only VV scattering was monitored for ν_{CH}. A neon emission line was used as an internal frequency standard. Peak frequencies were determined by inspection and the quoted error bars reflect the uncertainties in estimating the positions of peak maxima.

3. Results and discussion

Measured values of ν_{CO} in VV and VH polarizations and ν_{CH} in VV polarization are shown in figures 1 and 2. The x-dependence of ν_{CO} clearly separates into three regimes. Above

† The OH-stretch bands in MeOH overlap those in water and hence are not useful for studying the hydrophilic moiety of the former.

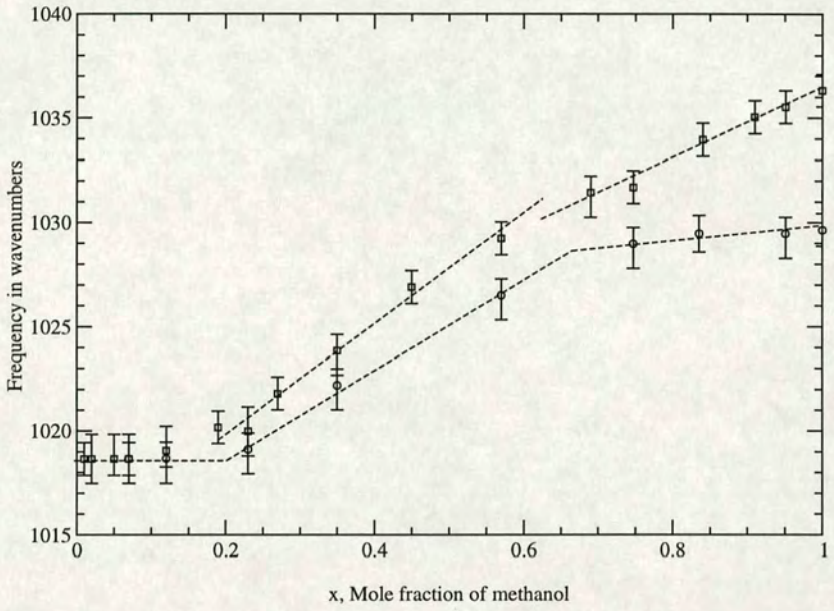

Figure 1. Variation of the C–O symmetric stretch frequencies (□: VV; ○: VH) of methanol as a function of concentration in water. Lines are guides to the eye.

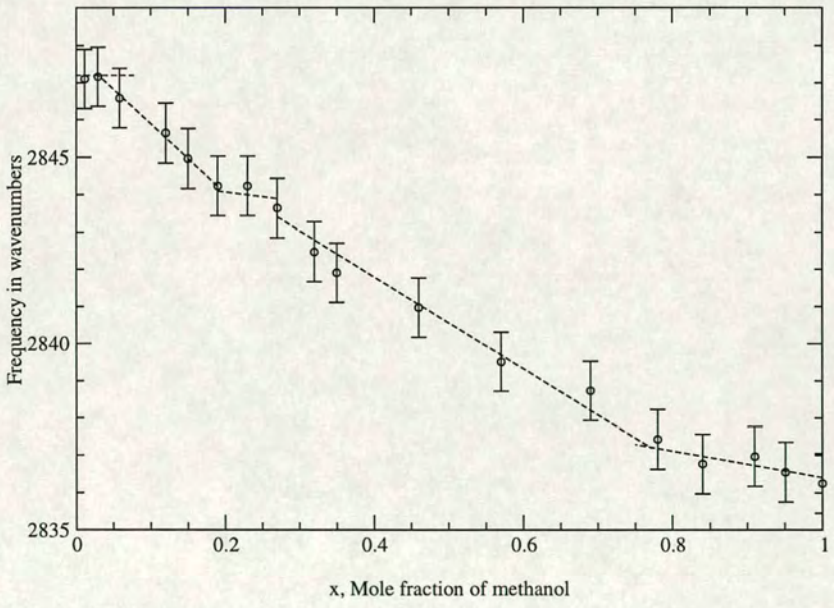

Figure 2. Variation of the C–H stretch frequency (VV) as a function of methanol concentration in water. Lines are guides to the eye

$x \sim 0.7$, $\nu_{CO}^{(VH)}$ is approximately constant while $\nu_{CO}^{(VV)}$ red-shifts at ~ 2 cm^{-1} per 0.1 decrease in x. Below $x \sim 0.7$, $\nu_{CO}^{(VH)}$ starts to red-shift, and the rate of red-shifting of $\nu_{CO}^{(VV)}$ increases by nearly 50%. Finally, below $x \sim 0.25$, there is no difference between $\nu_{CO}^{(VV)}$ and $\nu_{CO}^{(VH)}$ within

experimental error, and both remain constant down to $x = 0$. The x-dependence of ν_{CH} is consistent with this picture. ν_{CH} is nearly constant down to $x \sim 0.7$, whereupon significant blue-shift begins. The blue-shift somewhat saturates at $x \sim 0.25$, but starts to rise again below $x \sim 0.15$ until $x \sim 0.05$, below which it again saturates.

We propose that these trends can be interpreted as follows. It has long been suggested that molecules in pure MeOH (i.e. $x = 1$) hydrogen bond with each other to form chains. A recent scattering and simulation study [9] confirms this, giving an average chain length of five or so molecules at 25 °C; see figure 3(a). The existence of these chains implies non-zero average orientational correlation between molecules, which is reflected in the measured non-coincidence effect, $\nu_{CO}^{(VV)} - \nu_{CO}^{(VH)} \neq 0$ [15, 16]. We suggest that in the first hydration regime, $1 > x \gtrsim 0.7$, water molecules participate in hydrogen bonding to chain ends [10]; see figure 3(b). Chain-end hydration in this concentration regime has also been suggested very recently by Sato *et al* [17] on the basis of reorientation relaxation time measurements using dielectric spectroscopy. The fact that $\nu_{CO}^{(VV)}$ red-shifts suggests that the chain-end methanols act preferentially as H-bond acceptors† [10]. The reason for this preference is unclear.

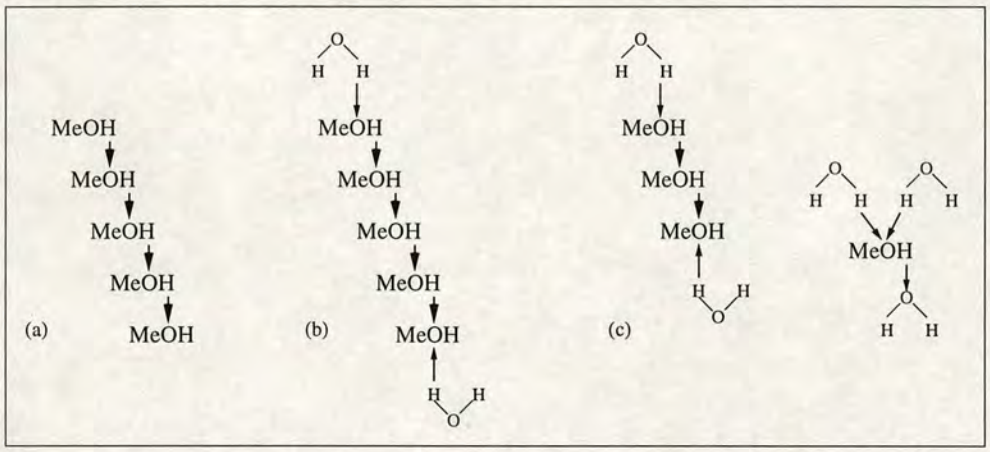

Figure 3. A schematic picture of progressive methanol hydration. (a) An average chain in pure methanol. (b) Water molecules donating hydrogen bonds to chain ends. The proposed mode of hydration in the regime $1 \gtrsim x \gtrsim 0.7$. (c) Water molecules breaking chains; on the right is a single MeOH molecule with 'AAD' hydrogen bonds round its hydroxyl group. The proposed hydration mechanism for $0.7 \gtrsim x \gtrsim 0.25$.

Given that the two ends of a chain can accept up to three hydrogen bonds, we can estimate that this effect saturates (for chains of average length five) at $x \sim 5/(3+5) \gtrsim 0.6$, which is not far from the crossover at $x \sim 0.7$ to the second regime of behaviour. Once the chain ends are saturated, further hydration proceeds by the water molecules progressively breaking up chains of MeOH and solvating the molecules individually; see figure 3(c). Recently Gruenloh *et al* [14] have measured ν_{CH} in MeOH in which the hydroxyl group is hydrogen bonded to other species in the gas phase. They found that ν_{CH} is sensitive to the *configuration* of hydrogen bonds at the polar moiety, but not to the kind of complexing species giving rise to a particular hydrogen-bond configuration. A single MeOH molecule can maximally accept two and donate one hydrogen bond; see figure 3(c). For such an 'AAD' configuration, Gruenloh *et al* always found ν_{CH} blue-shifting, as indeed we observe in MeOH in the regime $0.7 \gtrsim x \gtrsim 0.15$. We mention in passing that in the previous concentration regime, $1 > x \gtrsim 0.7$, ν_{CH} is essentially

† The oxygen atom on an *acceptor* molecule forms a hydrogen bond with a hydrogen atom on a *donor* molecule.

constant, indicating that there is as yet no significant 'AAD' hydrogen bonding, supporting our earlier conclusion of chain-end hydration.

When all direct MeOH–MeOH hydrogen bonds are broken by this process, we expect little or no average alignment of intermolecular dipoles, i.e. the non-coincidence effect should decrease to zero. This we do observe at $x \sim 0.25$, which corresponds to three waters per MeOH, $1/(1+3) = 0.25$. Moreover, at $x \sim 0.25$, the blue-shift in ν_{CH} appears to saturate, suggesting that the hydrogen-bond configuration round the hydroxyl groups in MeOH has stabilized.

Blue-shift in ν_{CH} starts again at $x \sim 0.15$. By this stage, the primary 'AAD' hydration shell of the hydroxyl group is associated with a further three or so water molecules. When this process of hydroxyl solvation is complete, further increase in water content takes the form of water molecules forming structure round the methyl groups. This we propose as the hydration process below $x \sim 0.15$. Indeed, very recent neutron scattering and simulation work by Finney and Soper [8] reports a more or less complete shell of water molecules surrounding each MeOH at $x = 0.1$. Interestingly, even though the average hydrogen-bonding configuration of the hydroxyl group is not expected to change in this regime, ν_{CH} continues to blue-shift. The conclusion of Gruenloh *et al* [14] from gas-phase work, that ν_{CH} in MeOH is sensitive to the hydrogen-bond configuration at the polar moiety, therefore needs supplementing in the condensed phase, where ν_{CH} clearly also responds to the immediate environment of the non-polar moiety.

At very low concentration, $x \lesssim 0.05$, ν_{CH} again saturates. This may be taken as evidence that the primary hydration around methyl groups is complete. This suggestion has also been made very recently on the basis of dielectric spectroscopy relaxation data [17]. Note that the saturation of ν_{CH} was *not* observed by Kamogawa and Kitagawa [11]; but these authors used a highly complex procedure to analyse their 'Raman difference spectra', so direct comparison is not straightforward.

Before summarizing the global picture of MeOH hydration to emerge from our findings, we return to a feature of our data on which we have not yet commented. In the regime $1 > x \gtrsim 0.7$, $\nu_{CO}^{(VH)}$ remains constant while $\nu_{CO}^{(VV)}$ red-shifts. Perhaps surprisingly, this behaviour is almost identical to that observed in pure MeOH under pressure from 1 bar to 4 kbar [12]. Detailed modelling of the non-coincidence effect in pure MeOH based on the model of McHale [18] has been carried out by Torii and Tasumi [15]. They suggest that the initial increase in density on application of pressure is largely absorbed by closer packing of methyl groups, leaving the hydrogen-bonding structure at the methyl moieties (and therefore the chain structure) little affected. That there is little change in the chain structure is consistent with our interpretation of what happens in the regime $1 > x \gtrsim 0.7$; see figure 3(b). Furthermore, thermodynamic measurements on MeOH–water mixtures have yielded a *decrease* in the MeOH partial molar volume for all concentrations down to $x \sim 0.1$ [19]. The partial molar volume at $x \sim 0.7$ is equivalent to an effective MeOH density of $\rho \sim 0.8$ g cm^{-3}. This is equivalent to pure bulk MeOH at ~0.5 kbar [20]. It is therefore at least plausible that the behaviour of the non-coincidence effect in ν_{CO} in the concentration range $1 > x \gtrsim 0.7$ basically reflects an increase in MeOH packing density due to the presence of water, and is an example of a 'solvation pressure' effect [21].

4. Summary and conclusions

The behaviour of ν_{CO} and ν_{CH} in MeOH–water mixtures suggests three regimes of hydration. At $1 > x \gtrsim 0.7$, the addition of water leaves the chain structure of pure MeOH substantially

intact; hydration takes place at the chain ends, where the MeOH molecules act principally as H-bond acceptors. For intermediate concentrations, $0.7 \gtrsim x \gtrsim 0.25$, water progressively breaks up MeOH chains; individually molecules become hydrated, accepting two and donating one H bond with water. Below $x \sim 0.15$, when the hydroxyl groups are completely surrounded by water, hydration of the methyl groups take place, resulting in their complete primary solvation by $x \sim 0.05$. The naive picture of water hydrating an amphiphile-like molecule, namely, that it solvates the polar moiety before the non-polar moiety, is therefore seen to be essentially correct.

Corroboration for our proposed picture has come from a number of sources, including dielectric spectroscopy, thermodynamic measurements [22] and neutron scattering and simulations. Further use of the last two techniques, in the form of the empirical potential structure refinement method, at key concentrations ($x \sim 0.7$ and ~ 0.05) should provide direct confirmation. Work in this direction is under way. The comparison of the effect of dilution with water and hydrostatic pressure is intriguing. High-pressure spectroscopic data on MeOH–water mixtures will be published elsewhere, where the comparison will be taken further. We conclude with a general remark. This work shows how careful spectroscopy at high frequency and concentration resolutions can be a powerful tool in the study of liquid mixtures. In particular, it provides a guide to the choice of parameters for studies using more time-consuming techniques, such as direct structural investigations using scattering and simulation methods.

It is a pleasure to thank Professor John Finney and Dr Alan Soper for illuminating discussions throughout this project. Hugh Vass provided valuable technical assistance. SD is funded by the University of Edinburgh and an ORS award. Some ancillary equipment for the work was purchased under EPSRC grant GR/M91402.

References

[1] Evans D F and Wennerstrom H 1994 *The Colloidal Domain: Where Physics, Chemistry, Biology and Technology Meet* (Weinheim: VCH)
[2] Okazaki S, Touhara H and Nakanishi K 1984 *J. Chem. Phys.* **81** 890
[3] Palinkas G, Hawlicka E and Heinzinger K 1991 *Chem. Phys.* **158** 65
[4] Hernandez J C and Blake I O 1995 *J. Chem. Phys.* **103** 9261
[5] Laaksonen A, Kusalik P G and Svishchev I M 1997 *J. Phys. Chem.* A **101** 5910
[6] Jorgensen W L and Madura J D 1983 *J. Am. Chem. Soc.* **105** 1407
[7] Soper A K 1996 *Chem. Phys.* **202** 295
[8] Finney J L and Soper A K 1993 *Phys. Rev. Lett.* **71** 4346
[9] Yamaguchi T, Hidaka K and Soper A K 1999 *Mol. Phys.* **96** 1159
[10] Kabisch G and Pollmer K 1982 *J. Mol. Struct.* **81** 35
[11] Kamogawa K and Kitagawa T 1985 *J. Phys. Chem.* **89** 1531
[12] Zerda T W, Thomas H D, Bradley M and Jonas J 1987 *J. Chem. Phys.* **86** 3219
[13] Kamogawa K and Kitagawa T 1991 *Chem. Phys. Lett.* **179** 271
[14] Gruenloh C J, Florio G M, Carney J R, Hagemeister F C and Zwier T S 1999 *J. Phys. Chem.* A **103** 496
[15] Torii H and Tasumi M 1993 *J. Chem. Phys.* **99** 8459
[16] Torii H 1999 *J. Phys. Chem.* A **103** 2843
[17] Sato T, Chiba A and Nozaki R 2000 *J. Chem. Phys.* **112** 2924
[18] McHale J L 1981 *J. Chem. Phys.* **75** 30
[19] Nakanishi K 1960 *Bull. Chem. Soc. Japan* **33** 793
[20] Jonas J and Akai J A 1973 *J. Chem. Phys.* **58** 4030
[21] Wood J R, Frogley M D, Meurs E R, Prins A D, Peijs T, Dunstan D J and Wagner H D 1999 *J. Phys. Chem.* B **103** 10 388
[22] Tanaka S H, Yoshihara H I, Ho A W-C, Lau F W, Westh P and Koga Y 1996 *Can. J. Chem.* **74** 713